PhD

PROGRAM IN TRANSLATIONAL

AND MOLECULAR MEDICINE

DIMET

UNIVERSITY OF MILANO-BICOCCA

SCHOOL OF MEDICINE AND FACULTY OF SCIENCE

A Brugada Syndrome mutation (S216L) and its modulation by H558R polymorphism: standard and dynamic characterization

Stefano Federico Marangoni

Coordinator: Prof. Andrea Biondi

Tutor: Prof. Antonio Zaza

XXIII CYCLE

ACADEMIC YEAR

2009-2010

Table of Contents

Chapter 1: General Introduction

The Brugada Syndrome: definition

Brugada syndrome has been firstly described in 1992 by Pedro and Joseph Brugada[1] as a new clinical and electrocardiographic syndrome. It was defined by the presence of "*right bundle branch block, normal QT interval and persistent ST segment elevation in precordial leads V_1 to V_2–V_3 not explainable by electrolyte disturbances, ischemia or structural heart disease*". As a consequence of these alterations, patients showed a higher susceptibility to malignant ventricular arrhythmias and consequent sudden cardiac death (SCD)[1]. Later on, it has been estimated that BS affects at least 5/10000 people, with a much smaller prevalence in Europe or North America than in Asian countries[2;3], moreover it is considered the cause of 4% to 12% of SCD; this percentage rises up to 20% if considering SCD occurring in structurally normal hearts[4].

Brugada syndrome ECG patterns

The Brugada syndrome is characterized by an ST-segment elevation in the right precordial leads (V1-V3) of a standard 12-leads electrocardiogram (ECG) and a high incidence of sudden death in patients with structurally normal hearts, generally manifests during adulthood. Usually the Brugada sign is more evident in the lead V2, especially in the third intercostals space ($V2_{IC3}$) (Fig. 1.1).

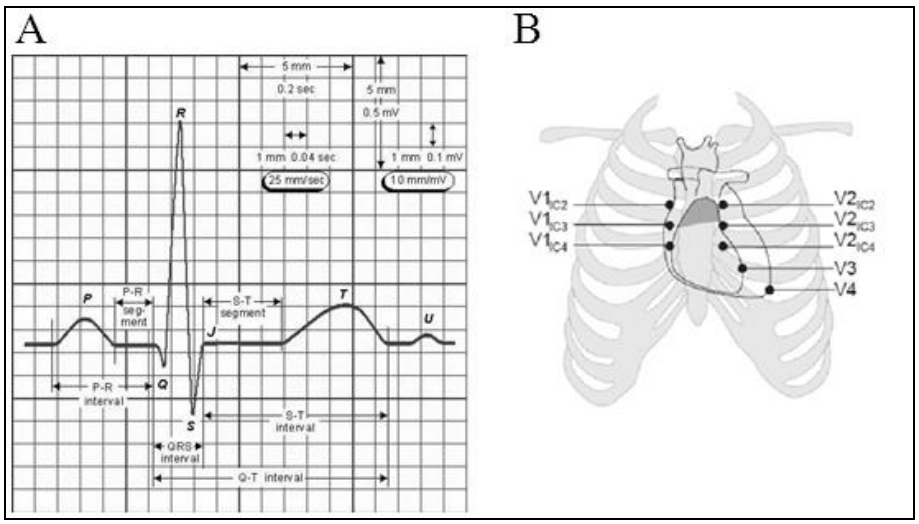

Figure 1.1. A, ECG parameters (lead I); **B**, Position of precordial leads in a standard 12-leads ECG.[5]

Three types of repolarization patterns in the right precordial leads are recognized[6] (Fig. 1.2). Type 1 ST-segment elevation is characterized by a coved ST-segment elevation ≥2 mm (0.2 mV) followed by a negative T wave. Type 2 ST-segment elevation has a saddleback appearance with a high take-off ST-segment elevation of ≥2 mm followed by a trough displaying ≥1 mm ST elevation followed by either a positive or biphasic T wave. Type 3 ST-segment elevation has either a saddleback or coved appearance with an ST-segment elevation of <1 mm.

Another electrocardiographic feature often associated with Brugada syndrome is right bundle brunch block. Signs of conduction defects are often found at many levels: QRS widening[7], electrical axis deviation[1;8;9], and PQ prolongation, presumably reflecting a conduction delay[1;6;8;10;11]. Moreover sinus node dysfunction is

reported[12]. In contrast, QTc duration is generally within the normal range[6;10] but it may be occasionally prolonged[1].

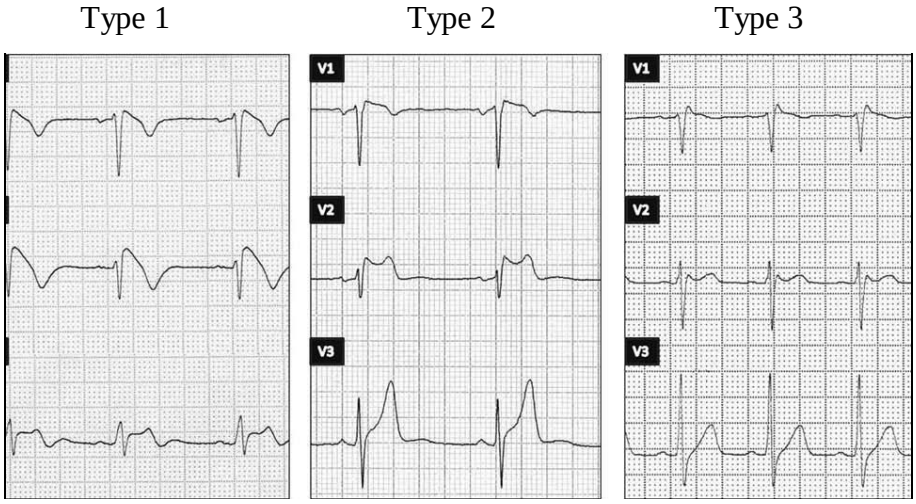

Figure 1.2. Possible electrocardiographic patterns Brugada syndrome patients. Type I only is diagnostic of the syndrome.[13]

Diagnostic criteria

Type 1 ST-segment elevation is diagnostic of Brugada syndrome, whereas Type 2 and 3 should not be considered diagnostic. Brugada syndrome is definitively diagnosed when a Type 1 ST-segment elevation (Brugada ECG) is observed in more than one right precordial lead (V1-V3), and in conjunction with arrhythmic event in the proband or in family history[4;6]. Diagnosis of Brugada syndrome is also considered positive when a Type 2 or Type 3 ST-segment elevation is observed in more than one right precordial lead under baseline conditions and can be converted to the diagnostic Type 1 pattern during a drug test (i.e. exposure to sodium channel blocker, see also "Diagnostic test, drugs and treatment of Brugada syndrome").

Drug-induced conversion of Type 3 to Type 2 ST-segment elevation is considered inconclusive for diagnosis of Brugada syndrome.

Epidemiology

The average age at the time of initial diagnosis of Brugada syndrome is 40 ± 22. The youngest patient diagnosed with the syndrome is 2 days of age, and the oldest is 84 years[14]. Because the ECG is so dynamic and often concealed, it is difficult to estimate the true prevalence of the disease in the general population[15]. The prevalence of the Brugada syndrome is estimated at 1–5 per 10000 inhabitants worldwide. The frequency is lower in western countries and higher (≥5 per 10000) in Southeast Asia, especially in Thailand and the Philippines where Brugada syndrome is considered to be the major cause of sudden death in young individuals[16;17].

Although the number of genetic mutations responsible for the Brugada syndrome is equally distributed between the sexes, the clinical phenotype is 8 to 10 times more prevalent in males than in females[18].

Genetic factors underlying Brugada syndrome

Brugada syndrome is inherited via an autosomal dominant mode of transmission. The first gene to be linked to the Brugada syndrome was *SCN5A*, the gene encoding for the α-subunit of the cardiac sodium channel[19]. Since 1998[19], it has been established that 15–30% of Brugada syndrome cases can be attributed to mutations in *SCN5A*[10]. A further 11–12% of Brugada syndrome cases can be attributed to *CACNA1C* and *CACNB2*[20]. Minor contributions to Brugada syndrome cases are made from mutations in other genes (*GPD1L*, *SCN1B*,

KCNE3 and *SCN3B*). All these genes encode proteins involved, directly or indirectly, in the execution of the cardiac action potential (AP) (Fig. 1.3).

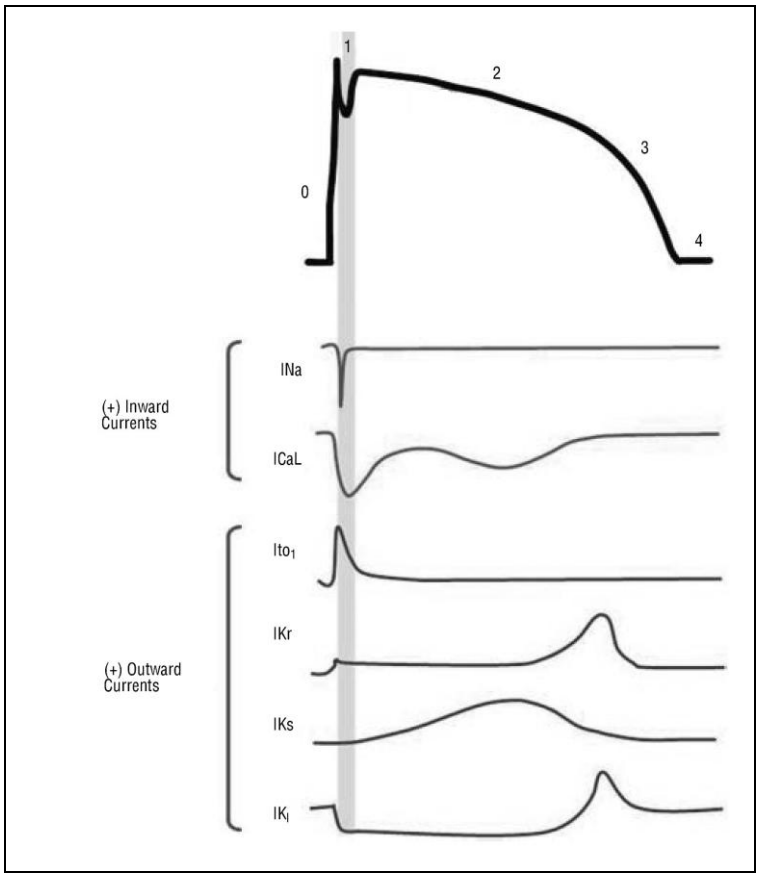

Figure 1.3. Schematic representation of principal ionic currents driving cardiac action potential. The grey field underlie a phase considered crucial in Brugada syndrome (see also "Proposed electrophysiological mechanisms").[13]

A second way to classify Brugada syndrome types has been proposed, in addition to the ECG pattern-based one. This classification is based on the mutation-affected genes. Although the

"type 1" is always associated with SCN5A gene mutation, a consensus on the order to give to the other types (from 2 to N) is not yet reached. Below, a description of the genes associated with Brugada syndrome is reported, basing on the function of the encoded proteins.

Sodium current

The gene *SCN5A* has been associated with Brugada syndrome. This gene encodes the pore-forming α-subunit of the cardiac sodium channel ($Na_v1.5$) conducting the depolarizing sodium inward current, I_{Na}[21]. Mutations in *SCN5A* were initially found in four families with long-QT syndrome linked to chromosome 3[22]. Since then, a number of mutations in all domains of *SCN5A* have been associated with many arrhythmogenic pathologies as long-QT syndrome[23-25], cardiac conduction disease[26-29], atrial fibrillation[30;31] and dilated cardiomyopathy[32]. *SCN5A* mutations are also found in the clinical sudden infant and adult death syndromes[33-35].

In the late 1990s, *SCN5A* was associated with Brugada syndrome when mutations were identified in a number of families with idiopathic ventricular fibrillation[19]. With time, Brugada syndrome has been associated with almost 100 different mutations in *SCN5A*. The functional characteristics of some of the *SCN5A* mutations associated with Brugada syndrome have been usually analyzed in mammalian cell lines and mouse models[36;37]. In most cases, *SCN5A* mutations found in Brugada syndrome patients are loss-of-function types, that is, leading to reduced I_{Na} current, through several mechanisms such as decreased expression of the gene or changes in voltage- and time-dependence of I_{Na} activation, inactivation or reactivation[38].

Mixed phenotypes, where *SCN5A* mutations are associated with a combination of hereditary arrhythmias and structural heart disease, have also been described[31;32;39]. Some mutations also differently affects various aspects of sodium channel gating, thus leading to a mix of loss-of- and gain-of-function properties. This is the case of 1795insD mutation, whose carriers show a Type 1 Brugada ECG pattern and concomitant slightly prolonged PR and QRS duration (suggesting a mild conduction disorder) and a strongly prolonged QT interval (sign of a long-QT syndrome phenotype)[40]. These ECG features were given by a drastic decrease of the transient component of I_{Na}[40], which drives AP phase 0 depolarization and impulse conduction, and a concomitant marked increase of its persistent component (I_{NaL})[41]. I_{NaL} has a crucial role during AP plateau, thus its increase causes a delayed repolarization which leads to long-QT syndrome.

It has been demonstrated that the electrophysiological phenotype of *SCN5A* mutations is temperature dependent[42], and this may explain why Brugada syndrome can be precipitated by fever, particularly in children[43;44].

The gene *SCN1B* encodes the β1-subunit of the cardiac sodium channel[45]. The β-subunits have several functions, including interaction with ankyrin-B and -G. In the heart the biophysical function of the β1-subunits (and β1b splicing variant) is to modify the function of $Na_v1.5$, by increasing the I_{Na} (+69% and +76%, respectively)[45]. When the mutations (E87Q; W179X) were transiently expressed in CHO cells cotransfected with the *SCN5A*, it was found that the mutated forms of *SCN1B* were not able to increase I_{Na}[45].

The β3-subunit of the cardiac sodium channel is encoded by the *SCN3B* gene. In the heart the function of the β3-subunit is to modify the function of $Na_v1.5$, by increasing the I_{Na}, as for the β1 subunit, albeit with another kinetics[46]. A mutation in *SCN3B* was found associated with Brugada syndrome[47]. When the mutation, L10P, was expressed in TSA201 cells together with *SCN5A* and *SCN1B*, the mutation was found to result in defective trafficking of $Na_v1.5$ and reduced I_{Na}[47].

Calcium current

Defects in the *CACNA1C* gene, which encodes a number of isoforms of the pore-forming α1-subunit of the long-lasting (L-type) voltage gated calcium channel ($Ca_v1.2$)[48], cause Brugada syndrome. The $Ca_v1.2$ channel is activated upon depolarization of the cardiomyocyte, and is responsible for the depolarizing influx of calcium, the L-type calcium current (I_{CaL}). I_{CaL} inactivates very slowly, thus it is of major significance for maintaining the plateau phase of the AP. Furthermore, it is the most important source of intracellular calcium and it represents the coupling between excitation and contraction by inducing release of calcium from the sarcoplasmic reticulum. The association between *CACNA1C* and Brugada syndrome was established by the finding of two missense mutations in *CACNA1C* (A39V; G490R)[49]. When expressed with other $Ca_v1.2$ subunits in CHO cells, a clearly reduced I_{CaL} was found in both cases[49]. Thus, in these cases, the mechanism of Brugada syndrome was independent of *SCN5A* and it was the result of decreased depolarizing current during AP.

CACNB2 codes for the β2-subunit ($Ca_v\beta2$) of $Ca_v1.2$[50], which modifies gating, increasing the I_{CaL}, and has been associated with Brugada syndrome[51]. $Ca_v\beta2$ functions as a chaperone for the α-subunit of $Ca_v1.2$, ensuring its transport to the plasma membrane[52]. It is the dominantly expressed $Ca_v1.2$ β-subunit in the heart. When the mutation was expressed in CHO cells together with other components of the $Ca_v1.2$ channel, I_{CaL} was markedly reduced, in absence of trafficking defects[49].

Later on, many other mutations in *CACNA1C* and in other genes encoding for calcium channel subunits (*CACNB2B*; *CACNA2D1*) were described in Brugada syndrome patients[53].

Potassium currents

Brugada syndrome is caused by mutations in *KCNE3* (R99H)[54]. This gene encodes for one of five homologous ancillary β-subunits (KCNE peptides) of voltage-gated potassium ion channels[55;56]. The KCNE peptides modulate several potassium currents in the heart [56-62], including I_{Ks}[63], I_{Kr}[57], and I_{to}[54]. When the mutated *KCNE3* was coexpressed in CHO cells with Kv4.3, the α-subunit of the I_{to} channel, an increase in the I_{to}, as well as an accelerated inactivation of the current, was found[54]. As the KCNE peptides are ‘‘promiscuous’’ in their choice of interacting α-subunit[57], it cannot be said for certain that this is the mechanism of the association between the R99H mutation and Brugada syndrome.

Other gene(s)

Mutations associated with Brugada syndrome were also described in a gene which does not encode for an ion channel-forming

protein. This is the case of the *GPD1L* gene (E83K; I24V; R273C), which encodes glycerol-3-phosphate dehydrogenase 1-like protein (G3PD1L)[64]. Although the protein is predicted to contain a NAD^+-binding site and a dehydrogenase catalytic site[64], its function has not been established. The link with Brugada syndrome was established through linkage analysis[65], followed by candidate gene analysis[64]. The mutations were coexpressed with *SCN5A* in HEK cells and neonatal cardiomyocytes, and found to reduce the I_{Na} current and/or surface expression of $Na_v1.5$[64;66].

Genotype-phenotype relation

In a comparison between the ECG morphology of *SCN5A* mutation carriers versus patients where mutations in *SCN5A* had been excluded, it was found that *SCN5A* mutation carriers had significantly longer PQ intervals on the ECG and prolonged His-to-ventricle time during electrical programmed stimulation. No significant differences were found in QT or QRS duration and the magnitude of ST segment elevation[11]. No significant difference with respect to prognosis have been found between *SCN5A*-positive Brugada syndrome patients and non-*SCN5A* carriers[67]. The patients with mutations involving calcium channel express a phenotype that is essentially a combination of Brugada and short-QT syndrome, due to early repolarization, as expected by reduction of inward current during AP plateau[49].

Arrhythmia initiation and mechanism

In many cases, arrhythmia initiation is bradycardia-related[68]. This may contribute to the higher incidence of sudden death at night in

individuals with the syndrome and may account for the success of pacing in controlling the arrhythmia in isolated cases of the syndrome[69]. However, not all patients die at night and not all the cases are controlled with rapid ventricular pacing. It has been reported that loss-of-function *SCN5A* mutations resulting in Brugada syndrome are distinguished by profound bradyarrhythmias[70]. Pertinent to this observation is the report of the expression of the cardiac sodium channel gene, *SCN5A*, in intracardiac ganglia[71]. This interesting finding suggests that loss-of-function mutations in *SCN5A* may not only create the dangerous substrate in ventricular myocardium, but may also increase vagal activity in intracardiac ganglia, thus facilitating the development of arrhythmias in patients with the Brugada syndrome. Febrile state is often associate with Brugada syndrome[72]. This observation is mechanistically supported by the finding that mutation-induced loss-of-function of the sodium channel could be temperature-dependent[44].

General mechanisms of arrhythmias include reentry, early afterdepolarizations (EADs), delayed afterdepolarizations (DADs), and abnormal automaticity. Reentry is regarded as the dominant mechanism in Brugada syndrome, based on: conduction slowing, easy ventricular tachycardia/fibrillation induction during electrophysiologic study (EPS), and the polymorphic nature of the arrhythmias. Although polymorphic tachycardia and tachycardia onset during slow heart rates are also compatible with EADs, EADs typically require QT prolongation, which is usually not present in Brugada syndrome. Furthermore, efficacy of quinidine in preventing tachyarrhythmias[73;74], while also causing QT prolongation, argues

against a causative role of EADs. DADs are even less likely: DADs typically occur during calcium overload (e.g. during fast heart rates). Attenuation of ST elevations by catecholamines[75] provides further evidence against DADs, as catecholamines generally increase calcium overload and facilitate DADs[76]. Abnormal automaticity does not usually present as a polymorphic tachycardia and exhibits a warm-up phenomenon, rather than the abrupt tachyarrhythmia onset seen in Brugada syndrome.

Proposed electrophysiological mechanisms

The pathophysiological mechanism of Brugada syndrome remains a matter of debate[5;14]. This is partially because Brugada syndrome, similarly to other inheritable arrhythmia syndromes, is characterized by a large variability in clinical and molecular phenotype among patients, although there seems to be a consensus on a right ventricular origin and the positive association between the Type 1 ECG and arrhythmias. Although the actual mechanisms still remain uncertain, two leading hypotheses have been proposed. The "repolarization hypothesis" was initiated by studies in canine wedge preparations[77]. This hypothesis relies on transmural dispersion of repolarization between the right ventricular endocardium and epicardium, especially in the outflow tract. In contrast, the "depolarization hypothesis" relies on right ventricular conduction slowing and involvement of mild structural abnormalities[5].

The repolarization hypothesis

This model was developed by to explain Brugada syndrome, basing on the study of arterially perfused right ventricular wedge

preparations of dogs[77;78]. Repolarization hypothesis revolves around an imbalance between inward and outward currents during AP phase 1 (AP notch). The unequal expression of the transient outward potassium current (I_{to}) between epicardium and endocardium[79;80] provides basis for AP heterogeneity in this phase, rendering epicardium more susceptible to the effects of reduced depolarizing force (e.g. a mutation-induced loss of I_{Na}). Moreover, this difference between right ventricular walls is also supported by the lower functional expression of I_{Na} in the epicardium[81].

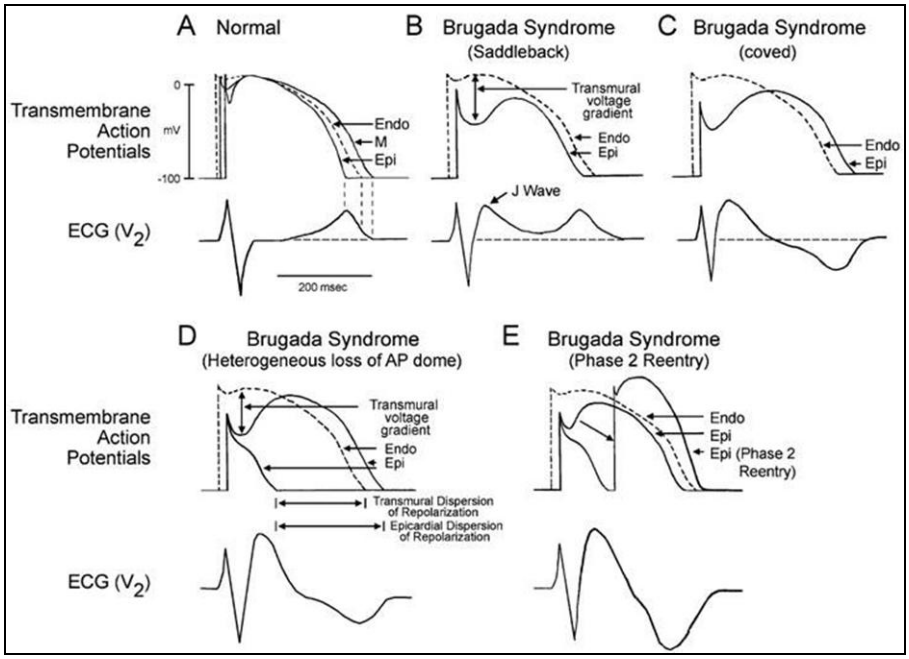

Figure 1.4. Repolarization disorder model. The imsbalance between inward depolarizing current (I_{Na}) and outward repolarizing one (I_{to}) generates the electrocardiograohic features of Brugada syndrome and arrhythmogenic events (phase 2 Reentry).[82]

Fig. 1.4 schematizes in detail the repolarization hypothesis. The presence of a I_{to}-mediated spike and dome morphology or notch in the ventricular epicardium, but not endocardium, of larger mammals creates a transmural voltage gradient responsible for the inscription of the electrocardiographic J wave (Osborn wave)[83]. Under normal conditions, the J wave is relatively small, in large part reflecting the left ventricular AP notch, since that of the right ventricular epicardium is usually buried in the QRS. The ST segment is isoelectric because of the absence of transmural voltage gradients at the level of the AP plateau (Fig. 1.4A). Accentuation of the right ventricular notch under pathophysiological conditions is attended by exaggeration of transmural voltage gradients and thus exaggeration of J point elevation and the appearance of a saddleback configuration of the repolarization waves (Fig. 1.4B). The development of a prominent J wave can also be construed as ST segment elevation. Under these conditions, the T wave remains positive because epicardial repolarization precedes repolarization of the cells in the M and endocardial regions. Further accentuation of the notch may be accompanied by prolongation of the epicardial AP such that the direction of repolarization across the right ventricular wall and transmural voltage gradients are reversed, thus leading to the development of a coved-type of ST segment elevation and inversion of the T wave (Fig. 1.4C), typically observed in the ECG of Brugada patients.

Although the typical Brugada morphology is present in Fig. 1.4B and C, the substrate for reentry is not. A further shift in the balance of current, leading to loss of the AP dome at some epicardial

sites, would manifest in the ECG as an additional ST segment elevation (Fig. 1.4D). The loss of the AP dome in epicardium but not endocardium results in the development of a marked transmural dispersion of repolarization and refractoriness, responsible for the development of a vulnerable window during which a premature impulse or extrasystole can induce a reentrant arrhythmia. Since loss of the AP dome in the epicardium is generally not spatially uniform, a striking epicardial dispersion of repolarization develops (Fig. 1.4D).

Conduction of the AP dome from sites where it is maintained to sites where it is lost causes local reexcitation via a phase 2 reentry mechanism, leading to the development of a closely coupled extrasystole, capable of triggering circus movement reentry (Fig. 1.4E and 1.5)[77;84]. The phase 2 reentrant beat fuses with the negative T wave of the basic response. Because the extrasystole originates in the epicardium the QRS is largely comprised of a Q wave, which serves to accentuate the negative deflection of the inverted T wave, thus giving the ECG a more symmetrical appearance. This morphology is often observed in the clinic preceding the onset of polymorphic ventricular tachycardia. Phase 2 reentry has been shown to trigger circus movement reentry in isolated sheets of the right ventricular epicardium[84] as well as in the intact wall of the canine right ventricle[83].

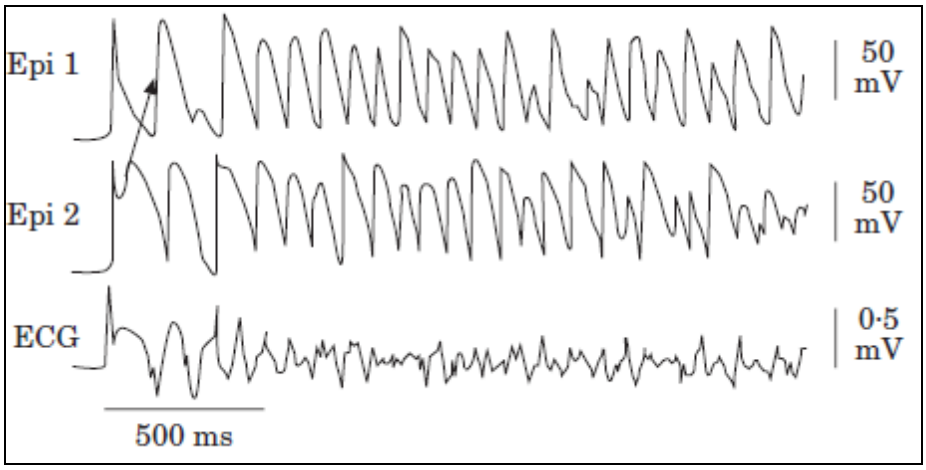

Figure 1.5. Ventricular tachyarrhythmia provoked by phase 2 reentry.[82]

***The depolarization* hypothesis**

An alternative explanation for the ECG signature in Brugada syndrome, which does not invoke fundamentally different AP shapes, is based on conduction delay in right ventricular outflow tract (RVOT) (Fig. 1.6). The RVOT AP (Fig. 1.6B, top) is delayed with respect to the rest of right ventricle (RV) (Fig. 1.6B, bottom). During the hatched phase of the cardiac cycle in Fig. 1.6D, the membrane potential in RV is more positive than in the outflow tract, thus acting as a source, and driving intercellular current to RVOT, which acts as a sink (Fig. 1.6C, a). To ensure a closed-loop circuit, current passes back from RVOT to RV in the extracellular space (Fig. 1.6C, c), and an ECG electrode positioned over the RVOT (V2) inscribes a positive signal, as it records the limb of this closed-circuit which travels towards it (Fig. 1.6C, b). Thus, this electrode inscribes ST elevation during this phase of the cardiac cycle (Fig. 1.6D, bottom, bold line). Reciprocal events are recorded in the left precordial leads[85]. Here,

current flowing from the extracellular space into RV (Fig. 1.6C, d) causes ST depression. In the next phase of the cardiac cycle (following the upstroke (Fig. 1.6F, hatched phase) of the delayed AP in RVOT), the potential gradients between RV and RVOT are reversed, as membrane potentials are now more positive in RVOT than RV. Thus, RVOT now acts as the source, driving the closed-loop circuit in the opposite direction (Fig. 1.6E), with current now passing away from lead V2 (Fig. 1.6E, d), thus resulting in the negative T wave (Fig. 1.6F, bottom, bold line). Note that in Fig. 1.5D and F, the delayed AP of RVOT is abbreviated in comparison to RV one, as electrotonic interaction between RV and RVOT (which is present when RV and RVOT are electrically well-coupled) accelerates repolarization of RVOT AP because the mass of RV strongly exceeding that of RVOT[86].

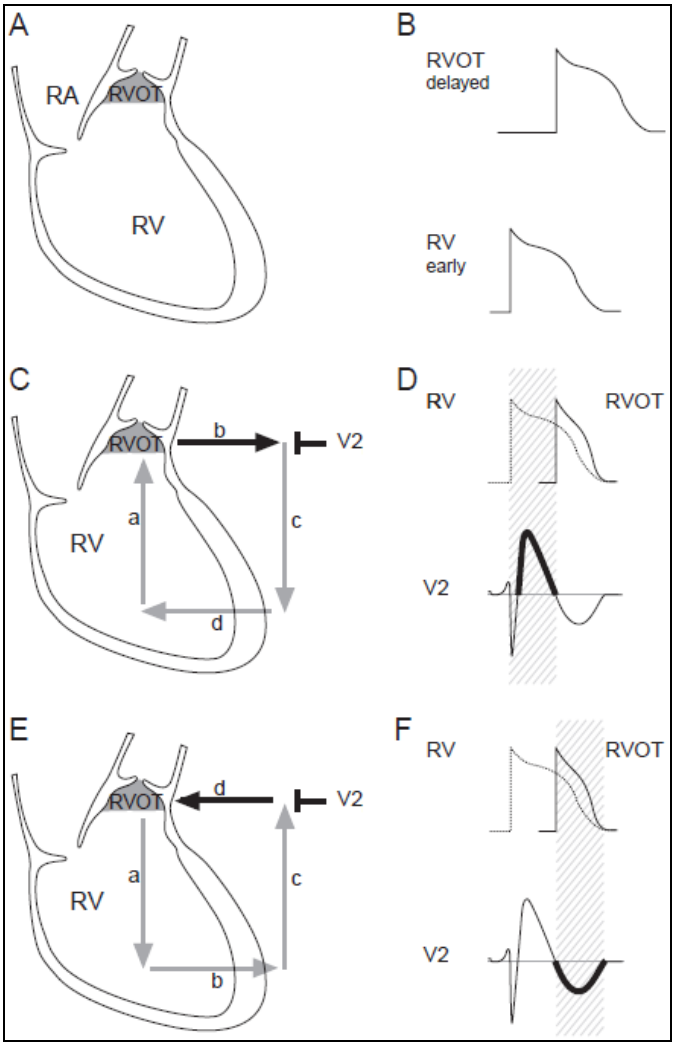

Figure 1.6. Depolarization disorder model. The conduction delay in RVOT generate current loops responsible for Brugada ECG pattern.[5]

This qualitative model of ST elevation in Brugada syndrome derives from the mechanism believed to cause ST-segment elevation in regional transmural ischemia, where large differences in membrane potential exist between ischemic and nonischemic zones[87]. Similar to regional ischemia, where premature beats which trigger reentrant

tachyarrhythmias originate in the border zone between areas with disparate membrane potentials, the first beat of the ventricular tachyarrhythmia in Brugada syndrome may originate in the border zone between early and delayed depolarizations[87].

Repolarization vs depolarization hypothesis

The repolarization hypothesis (RH) or the depolarization one (DH) differentially explained many features of Brugada syndrome.

The presence of the ECG changes in right, but not left, precordial leads is justified by larger I_{to} expression in right than left ventricular epicardium[88] by RH, whereas the finding of a conduction delay in RVOT[89] and its embryological origin, which is different from left ventricular one[90], are invoked by DH. The outflow tract derives from the same group of cells that compose the atrioventricular region, thus possessing slow, I_{CaL}-mediated conduction properties[91;92]. RH or DH ascribe the large prevalence of the syndrome in males to the sexual differences in I_{to}[18] or I_{CaL}[93] expression, respectively.

Autonomic modulation strongly affects ST-segment elevations in Brugada syndrome[68;94-96]. Indeed, parasympathetic stimulation increases ST-segment elevation and an augmented vagal tone usually precedes ventricular fibrillation episodes[68]. Accordingly, opposing effects of sympathetic stimulation were reported, as isoproterenol reduced ST-segment elevation and prevented ventricular tachycardia/fibrillation inducibility[75;94]. Interestingly, abnormal norepinephrine recycling was identified in Brugada syndrome[97] indicating that abnormal autonomic innervations may cause ST-segment elevation. Both RH and DH ascribe this autonomic regulation to the vagal-induced reduction of I_{CaL}. I_{CaL} is crucial to sustain AP

plateau[98] or the RVOT conduction, from the RH or the DH point of view. Parasympathetic activity also reduces heart frequency. The observations that long RR intervals[99;100] augment ST-segment elevations and that ventricular tachycardia/fibrillation occurs at night were used as support for the repolarization disorder hypothesis. These observations were ascribed to slow gating kinetics of I_{to}, which increase this current at slow heart rates[80]. Accordingly, pacing provided an effective therapy against bradycardia-related ventricular arrhythmia onset in Brugada syndrome patients[101]. Yet, ST-segment elevations may also increase at fast heart rates[9;41;102;103].

Many *in vitro* studies provide additional support to RH by demonstrating that I_{Na} blockers[104;105] and $I_{K\text{-}ATP}$ openers[106] worsen transmural dispersion generating a spike-and-dome AP wave in the epicardium of RV wedge preparation, also generating a phase 2 reentry mechanism. By contrary, I_{to} blockers ameliorate transmural dispersion[88;107]. However, to support DH, these findings were only partially confirmed by another investigation on isolated RV preparation[108]. Removal of transmural gradient of I_{to} by 4-aminopyridine (I_{to} blocker), restored the AP dome and electrical homogeneity in the canine wedge preparation[77;82], consistent with the clinical efficacy of quinidine in normalizing the ECG pattern[94;109] and preventing spontaneous or induced arrhythmias[73;110]. RH ascribed this phenomena to I_{to} blocking properties of quinine, although DH considered this effects due to its anticholinergic action[111;112] and to blockade of delayed rectifier potassium channel[113;114] which suppress reentrant arrhythmias by prolonging AP duration.

In vivo studies (both open- or closed-chest)[115-117] are ambivalent. Indeed, spike-and-dome AP shapes were recorded, even though loss of the dome was never observed and RVOT was always involved in the experiments.

Ventricular late potentials reflect delayed and fragmented ventricular conduction and are strong predictors of ventricular arrhythmias[118]. Late potentials have been shown to be highly prevalent in Brugada syndrome[68;99;103;118-120], thus supporting DH; furthermore, they usually coincide with spontaneous ST-segment elevation in right precordial leads (V1–V3)[68]. Moreover, flecainide, a sodium channel blocker, elicits late potentials along with ST-segment elevations[99]. Nevertheless some studies failed to document delayed potentials of RV[94].

DH was also supported by the idea that the large transmural dispersion required by RH is unlikely in a tissue with normal electrical coupling. The presence of non-excitable tissue (e.g. fibrosis) and/or mild structural defects, not observable under routine analysis, provides an argument in favor of a slow-conduction explanation of Brugada syndrome. Electron beam tomography scan studies revealed RV enlargement, abundant adipose tissue[121] and RV wall motion abnormalities[122]. The link between structural and functional derangements was further tightened by another electron beam tomography scan study, in which wall motion abnormalities were exacerbated/provoked with a pharmacological challenge[123]. Using cardiac magnetic resonance imaging, a sensitive tool for detection of RV structural abnormalities[124], significant RVOT enlargement was found in Brugada syndrome patients[125]. Moreover, the explanted heart

of a Brugada syndrome patient with a *SCN5A* mutation substantial structural derangements (fatty replacement and intense fibrosis) in the RVOT, while LV was normal[126]. This study found no spike-and-dome AP shapes in RV epicardium, but prominent conduction slowing, arguing in favor of the DH[126].

A cause-effect relation between functional and structural derangements has been also suggested basing on the finding that *SCN5A* loss-of-function mutations can provoke severe degenerative changes in the specialized conduction system[26]. Moreover, transgenic mice with *SCN5A* haploinsufficiency developed cardiac fibrosis as they aged[127].

Modulating factors of Brugada syndrome

A number of factors modulate the electrocardiographic and arrhythmic manifestations of Brugada syndrome and ST-segment elevation is often dynamic. Brugada ECG may often be concealed, but can be unmasked or modulated by many drugs including sodium channel blockers, vagotonic agents, α-adrenergic agonists, β-adrenergic blockers, tricyclic or tetracyclic antidepressants, first generation antihistaminic (dimenhydrinate), a combination of glucose and insulin, hyperkalemia, hypokalemia, hypercalcaemia, and by alcohol and cocaine toxicity[94;128-137]. These agents may also induce acquired forms of Brugada syndrome. A list of drugs interacting with the syndrome and a guidance about their administration has been recently formulated[138] (see also "Diagnostic test, drugs and treatment of Brugada syndrome").

Arrhythmia and sudden death in Brugada syndrome usually occur at rest and at night. Circadian variation of sympathovagal balance, hormones, and other metabolic factors are likely to contribute to this circadian pattern. Bradycardia, due to altered sympathovagal balance or other factors, may contribute to arrhythmia initiation[68;69;95]. A presynaptic sympathetic dysfunction has also been proposed to play a role in arrhythmogenesis[139]. Hypokalemia, known to unmask Brugada syndrome in asymptomatic patients[129], has been implicated as a contributing cause for the high prevalence of sudden death in the Northeastern region of Thailand where potassium deficiency is endemic due to low level in food[129;139].

An association between a large meal of carbohydrates ingested and sudden death has been observed[139]. Consistent with this observation, it was found that glucose and insulin could unmask the Brugada ECG[134]. Another possibility is that sudden death in these patients is due to the increased vagal tone produced by the stomach distention[118].

SCN5A mutation functional defects have been shown to be accentuated at higher temperature[18], providing a mechanism to explain the several case reports where a febrile illness revealed the Brugada ECG and precipitate ventricular arrhythmia[43;140-142].

Although the genetic mutation responsible for the Brugada syndrome is equally distributed between sexes, the clinical phenotype is largely more prevalent in males than in females[18]. Indeed, about 80% of all published patients with Brugada syndrome, or asymptomatic individuals with a Brugada ECG, are male[143]. The basis for this sex-related distinction are still not completely elucidated.

Different explanation to gender-based prevalence is provided by repolarization hypothesis or by depolarization one. The former involved the prominent I_{to} expression in males[18] and the consequent accentuated AP notch and facilitation to loss of the AP dome; whereas the latter ascribed this difference to the lower expression of I_{CaL}[93] which would lead to conduction delay in the right ventricular outflow tract. To justify the higher prevalence of the syndrome in males, a role of hormones, especially testosterone, has been also proposed[144] and supported by some reported effects on various ionic currents[145;146]. The hypothesis of an involvement of sex hormones is also supported by the apparent absence of gender-based differences before 16 years of age[147].

Risk stratification

A great deal of focus and debate has centered around the issue of risk stratification of patients. It is generally accepted that Brugada syndrome patients presenting with aborted sudden death are at high risk for recurrence and that they should be protected by an implantable cardioverter defibrillator (ICD). There is also little argument that patients presenting with syncope, particularly those with a spontaneous Type 1 ECG, are at higher risk. By contrast, risk stratification of asymptomatic patients diagnosed with the disease has met with considerable debate[148-151]. Several invasive and non-invasive parameters have been proposed for identification of patients at risk of sudden death, including the presence of spontaneous Type 1 ST-segment elevation, the characteristics of the S wave[7], the presence of late potentials[12], and inducibility of ventricular tachycardia/fibrillation

using programmed electrical stimulation (PES). All the major registry studies agree that Brugada syndrome patients at higher risk for the development of subsequent events are those presenting with a spontaneous Type 1 (diagnostic) ST-segment elevation or Brugada ECG and/or those with a previous arrhythmic event[149].

The registries also agree that PES inducibility is greatest among patients with previous ventricular tachycardia/fibrillation or syncope, moreover approximately one-third of asymptomatic patients are inducible. Nevertheless, although the results of the divergent groups are gradually coming together, a consensus on the positive predictive value of the procedure has been not yet reached. Some studies failed to reveal an association between inducibility of ventricular tachycardia/fibrillation in asymptomatic patients and higher risk[149;152]. On the other hand, it has been reported that the risk for developing ventricular tachycardia/fibrillation is much greater in patients who were inducible during PES, independently of presence of Type 1 ST-segment elevation and/or symptomatology[15]. These discrepancies may be due to differences in patient characteristics and the use of multiple testing centers with non-standardized or non-comparable stimulation protocols[153]. Some studies on both humans and animal models suggested that PES applied to the epicardium may provide a more accurate assessment of risk than the current approach in which stimuli are applied to the endocardial surface[14;154].

Transmural dispersion of repolarization (TDR) within the ventricular myocardium has been suggested to underlie arrhythmogenesis in a number of syndromes, including Brugada, short- and long-QT syndromes[155]. Thus, the time interval between

peak and end of the T wave, reflecting transmural dispersion[156-158], has been proposed to be helpful in forecasting risk for the development of life-threatening arrhythmias[156;158-161]. Supports to this idea have been provided in many studies on several pathophysiological conditions[156;158-162], including Brugada syndrome[11;163], thus suggesting that these parameters may be useful in risk stratification of patients.

As discussed above ("Modulating factors of Brugada syndrome"), Brugada syndrome prevalence is largely higher in males[18]. The actual mechanism underling this phenomenon is still matter of debate, nevertheless it is widely accepted that male population is at higher risk than female one.

Race-related differences in Brugada syndrome prevalence are largely accepted (see also "Epidemiology"). In addition to food (see also "Modulating factors of Brugada syndrome"), it has been proposed a genetic base to explain endemic presence of Brugada syndrome in Asian[164]. A reduction of *SCN5A* expression through a lower activity of its promoter has been observed as a consequence of a haplotype variant consisting of 6 polymorphisms in near-complete linkage disequilibrium. This haplotype occurred at an allele frequency of 22% in Asian subjects and was absent in whites and blacks. The results of this study demonstrate that sodium channel transcription in the human heart may vary considerably among individuals and races, suggesting that some ethnic group could be associated with higher risk of arrhythmias.

The ethnic-specific frequency of many *SCN5A* polymorphisms (both common and rare) has been investigated because some of them are suspected to modulate sodium channel expression and/or function,

although the mechanisms of these modulations are still extremely uncertain[23;165]. Thus, the study of the role of polymorphisms in increasing susceptibility to arrhythmias would be of interest to develop a genetic background-based risk stratification.

The role of the common $Na_v1.5$ polymorphism H558R is still a matter of debate. A higher frequency of the H558R polymorphism has been observed in patients affected by atrial fibrillation[166], and in subjects with a long (non pathologic) QT interval[167]. Similar results have been obtained analysing Brugada syndrome patients. This finding led some author to postulate a negative role of H558R interpreting its presence as a risk factor[168]. By contrary, the observation that the higher frequency was restricted to *SCN5A* mutation-based patients and the analysis of some ECG parameters in this population, suggested that H558R could be a protective factor, maintained by positive selection in a high risk population[169]. This point of view is supported by some functional studies carried out on heterologous expression systems, which demonstrate a positive effects of rescuing gating and folding/trafficking defects induced by various mutations have been described[170-172]. Nevertheless, a reduced conductance in a constitutive sodium channel splicing variant due to H558R presence was also reported[173]. Although the effects of H558R interaction with different mutations are probably unpredictable, the observation that a single genetic variant may compensate diverse abnormalities, caused by different mutations, is intriguing and the unknown underlying mechanism, which seems to be a gain-of-function, deserves to be investigated.

Diagnostic test, drugs and treatment of Brugada syndrome

Given that the ECG pattern of patients with Brugada syndrome varies over time and even can be temporarily normal, the use of drug challenge tests has grown in recent years. Sodium channel blockers are the most often used drugs, mainly because they are effective, easily available, and have rapid activity[132]. Brugada syndrome is confirmed if, after testing, a Type 1 ECG pattern appears or is accentuated (Fig. 1.2). Although both ajmaline and flecainide challenge test are widely used, the former seems to be better[174-176]. This clinical evidence are also supported by patch-clamp studies which verified that flecainide, in addition to blocking the sodium channel, decreases I_{to}, thus reducing its effectiveness as compared to ajmaline[176].

Due to the limited value of the standard electrocardiogram, even when facilitated by drug challenge, new strategies have been proposed to help clinicians in the diagnosis of Brugada syndrome. It has been demonstrated that positioning the right precordial leads in higher intercostal spaces (third and even second intercostal space) increases sensitivity in relation to the baseline electrocardiogram and after administration of sodium channel blockers[177]. This strategy demonstrated to facilitate identification of patients at risk who would not have been otherwise identified[178].

Many other drugs have been reported to induce the Type 1 ECG pattern and/or arrhythmias in patients with Brugada Syndrome. Although the most appropriate treatment of the syndrome is still under discussion[149;179], avoidance of potentially proarrhythmic drugs and treatment of fever[180;181] are generally accepted to be an important part

of prophylactic treatment. To this aim, a list of drugs interacting with Brugada syndrome and a guidance for their administration have been recently formulated[138]. Drugs have been classified in four categories: *a*) drugs to be avoided, *b*) drugs preferably avoided, *c*) potential antiarrhytmic drugs and *d*) diagnostic drugs. Both the formers were suggested to be avoided; the third category contained drugs with therapeutic properties for Brugada syndrome patients (see below); in the latter, in addition to ajmaline and flecainide, pilsicainid and procainamide were identified as useful drugs for diagnostic challenge test.

An ICD is the only treatment with demonstrated efficacy in Brugada syndrome. The current indications for ICD follow the recommendations of the II International Consensus[182], where, in general, ICD implantation has been recommended for all patients who have already had symptoms and for asymptomatic patients in whom the EPS induces ventricular arrhythmias, especially if they present a spontaneous Type 1 ECG pattern. In the asymptomatic patients, without a family history of arrhythmias or sudden death and whose Type 1 ECG pattern is only documented after drug challenge test, periodic follow-up has been recommended without the need of an EPS for risk stratification[182]. It has been shown that the rate of inappropriate shocks during an ICD therapy was considerable (20% to 36%[183;184]). The leading causes of inappropriate therapy were reported to be, sinus tachycardia, supraventricular arrhythmias, T-wave oversensing and lead failure[183;184]. Thus, and because the ICD is not universally applicable therapy, in recent years a special effort has been

dedicated to search for possible drug options for the treatment of Brugada syndrome.

With the aim of reducing the ion current imbalance during AP phase 1 and/or sustaining the AP dome, the strategies of pharmacologically reduce I_{to} or increase I_{CaL} have been proposed. Unfortunately many potentially useful drugs are not cardiac-specific, thus their administration is almost impossible. Nevertheless, it has been demonstrated that quinidine, an antiarrhythmic agent that blocks I_{to}, reduces the incidence of induced arrhythmias in patients with Brugada syndrome[73], and it has been used successfully in specific clinical situations, such as the treatment of arrhythmia storms[110]. Furthermore, its usefulness has been demonstrated as adjunctive therapy to ICD in patients with multiple shocks[74] or as a therapeutic alternative to ICD in children at risk of arrhythmias[147]. In turn, betamimetic drugs, such as isoproterenol, that increase I_{CaL}, have been used with positive results[185]. Finally, the administration of a phosphodiesterase III inhibitor (i.e. cilostazol) which decreases I_{to} and increases I_{CaL}, has emerged as a promising therapy, although results are still inconsistent[186].

The cardiac voltage-gated sodium channel

Structure

The main physiological role of sodium current is to mediate the impulse propagation in excitable tissues. Indeed, during an action potential, sodium channels first activate, allowing the sodium ion flux (i.e. sodium current) which drives the upstroke, and then inactivate, facilitating repolarization to the resting potential mediated by outward currents. The channel purified from mammalian brain consists of the large, pore-forming α-subunit (more than 250 kDa) associated with smaller modulatory β-subunits (30 to 40 kDa) (Fig. 1.7).

Although α-subunit is sufficient for conduction, interaction with the extracellular domain of β-subunit modulates voltage-dependency and kinetics, mainly resulting in a large increase of sodium current flowing trough the channel[187;188]. The α-subunit consists of four domains (D1-D4), each with six transmembrane α-helical segments (S1-S6), of which S4 bears several positive charges originating from arginine or lysine residues. The four domains wrap around a central pore such that the P-loops between S5 and S6 form part of the pore lining. Several isoforms of both α- and β-subunits are expressed in mammals. In the cardiac tissue *SCN5A* gene encodes for the largely most expressed α-subunit ($Na_v1.5$), whereas the prevalent β-subunit is the β1, encoded by *SCN1B* gene.

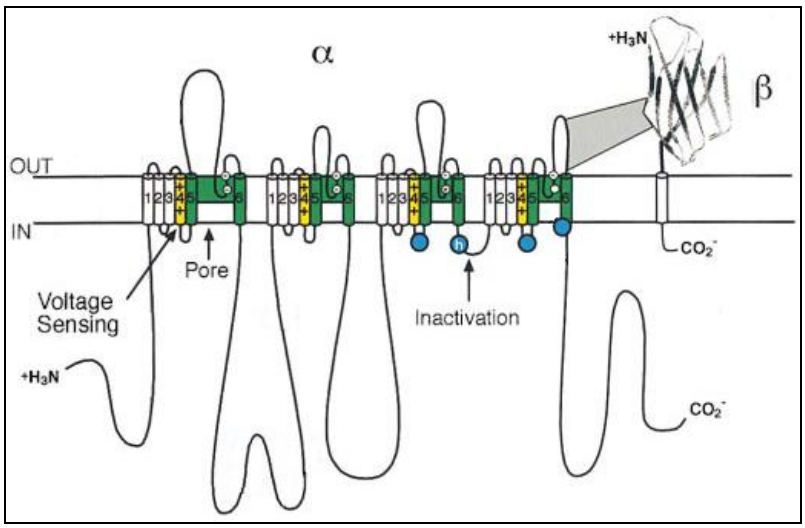

Figure 1.7. Sodium channel structure. **Green**, pore-lining segments; **white circles**, the outer and inner rings of amino residues that form the ion selectivity filter; **yellow**, S4 voltage sensors; **h** in blue circle, inactivation particle in the inactivation gate loop; **blue** circles, sites implicated in forming the inactivation gate receptor.[189]

Details of molecular mechanisms of many sodium channel functions are still not completely demonstrated, nevertheless some of the speculative or empirical models which were proposed, have gained further supports with time, thus reaching a widely acceptance.

Selectivity

Voltage clamp studies provided both the demonstration of selectivity of the channel for sodium ions and a model of the action of tetrodotoxin and saxitoxin as plugs of the selectivity filter, in the outer pore of sodium channels[190]. Mutational analysis identified firstly a glutamate (at position 387) in the membrane-reentrant loop in domain I (between S5 and S6, P-loop) as a crucial residue for tetrodotoxin and

saxitoxin binding[191]. Subsequent studies revealed a pair of important amino acid residues, mostly negatively charged, in analogous positions in all four domains (Fig. 1.7)[192]. These amino acid residues were postulated to form outer and inner rings that serve as the receptor site for tetrodotoxin and saxitoxin and as the selectivity filter in the outer pore of sodium channels (Fig. 1.8A). This view derives strong support from the finding that selectivity of sodium and calcium channels can be inverted by exchanging the amino acid residues in the inner ring[193]. Other mutations in this ring of four amino acid residues have been reported to have strong effects on selectivity for organic and inorganic monovalent cations, in agreement with the idea that they form the selectivity filter[194;195]. The ability of ion channels to discriminate among monovalent cations is supposed to be based on the differences in dimensions of the ion itself and of its waters of hydration[190]. Thus, on one hand, sodium channel allows the flowing of sodium ions because they are smaller then potassium ones; on the other, potassium channel pores are too small for the large waters of hydration of sodium ions. Once in the pore, sodium ions lose their waters of hydration and are weakly and transiently bound by the negative charged residues of the rings of the selectivity filters (Fig. 1.8B). The weakly nature of this electrostatic bond allows the electrochemical gradient to drive the flux of ions, thus generating the sodium current.

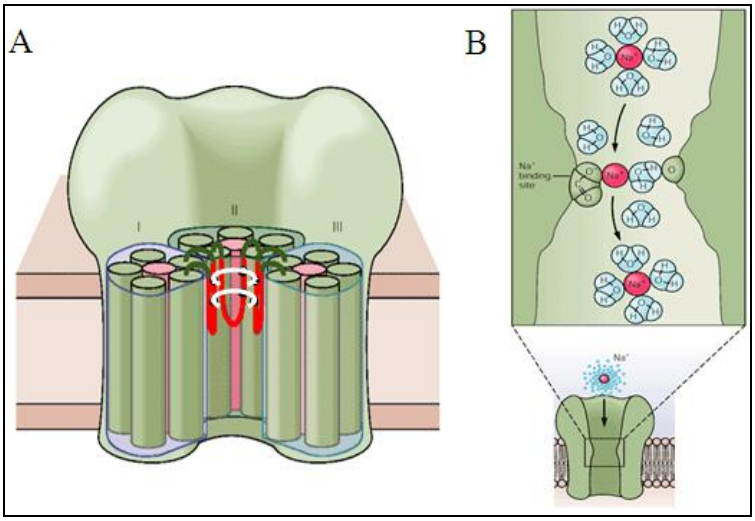

Figure 1.8. Sodium channel selectivity. **A**, 3D structure. **Pink segments**, S4 voltage sensors; **red lines**, P-loops; **white rings**, selectivity filter. **B**, Mechanism of sodium ion flowing.[196]

Activation

The voltage dependence of activation of the sodium channel derives from the outward movement of gating charges in response to changes in the membrane electric field[197;198]. It has been demonstrated that about 12 electronic charges in the sodium channel protein move across the membrane electric field during activation[199]. The S4 transmembrane segments contain repeated motifs of a positively charged (gating charges) amino acid residue followed by two hydrophobic residues, potentially creating a cylindrical α-helix with a spiral ribbon of positive charge around it. The negative internal transmembrane electrical field would exert a strong force on these positive charges arrayed across the plasma membrane, pulling them into the cell in a cocked position (Fig. 1.9A and 1.10B). It has been proposed that these positively charged amino acid residues may be

stabilized in the transmembrane environment by forming ion pairs with negatively charged residues in adjacent transmembrane segments[200]. Depolarization of the membrane was proposed to release the S4 segments to move outward, initiating a conformational change that opens the pore (Fig. 1.9B, 1.10B and C). All the four S4 segments are required to move to make the channel conductive (open state) (Fig. 1.9B, 1.10C and D). The first empirically inferred hypothesis of the activation mechanism[198] has been later on supported when channel sequence and predicted structure were described[201]. The final confirmation and widely acceptance has been reached with some mutagenesis and covalent modification studies which demonstrated that cysteine residues, in place of positively charged residues of S4 segments, became progressively more accessible to reaction with extracellular reagents and less accessible to reaction with intracellular reagents as the membrane was depolarized[202;203].

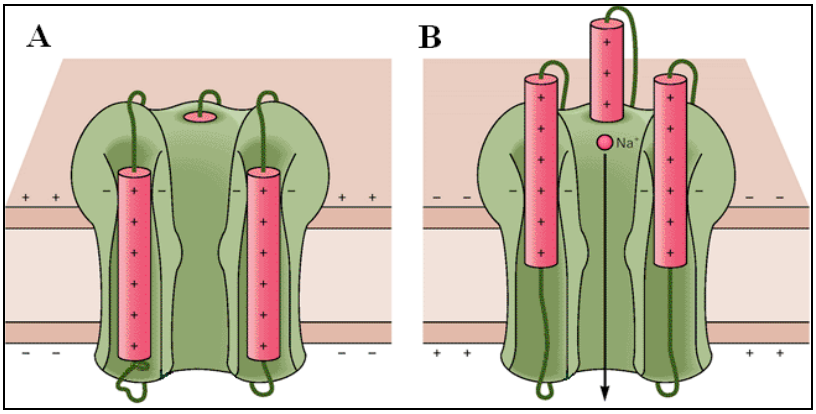

Figure 1.9. Sodium channel activation mechanism. **Left,** hyperpolarized membrane potential maintain S4 segments in a cocked position; **Right**, depolarization induced S4 segments outward movement and consequent channel activation.[196]

The conformational change course of channel, allowing the sodium current flowing within the cell, is graphically simplified in Fig. 1.10. Some aspects shown in the figure are discussed below.

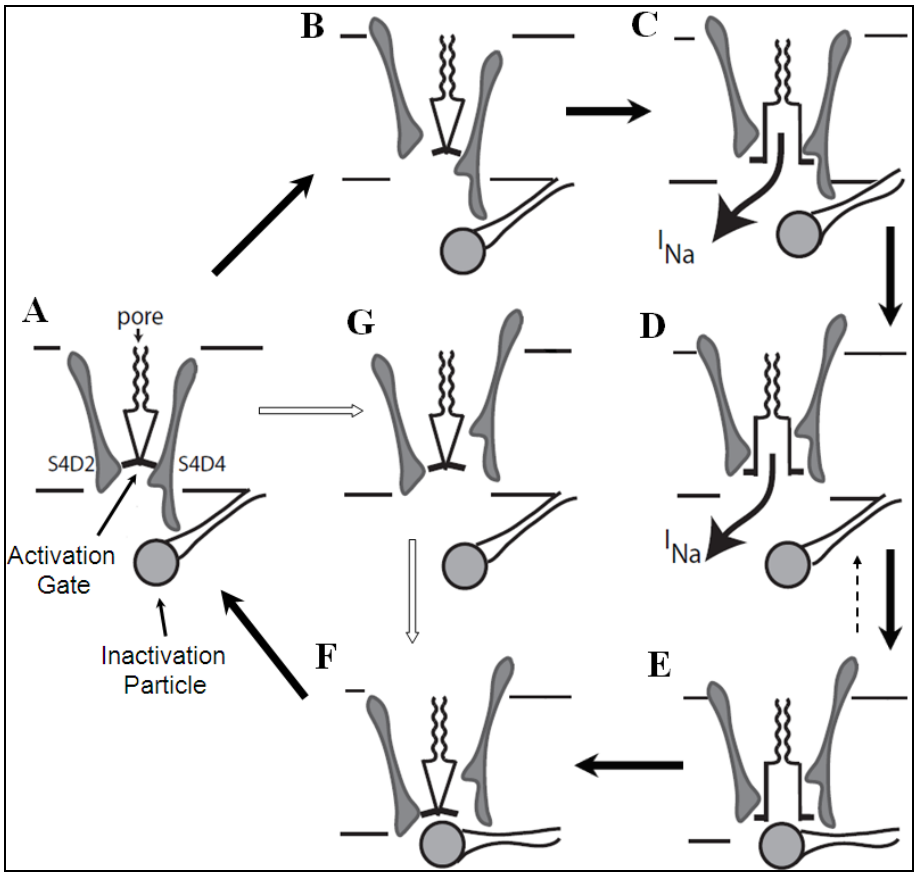

Figure 1.10. Conformational change course. To simplify, only S4 segments of domain II and IV are represented. **Bold arrows** show the classical course of conformational changes; **open arrows** represent the close-state inactivation mechanism; **thin dashed arrow** shows the proposed mechanism for persistent current.[204]

Inactivation

Sodium channels inactivate, becoming non-conductive, within a few milliseconds of opening. The main physiologic effect of the inactivation is the refractoriness of excitable tissues. Indeed, to allow the reopening of the channels it is necessary to remove inactivation. This process of recovery from inactivation takes place only with a few milliseconds of repolarization of the membrane[198].

Basing on its sensitivity to intracellular proteases, inactivation was thought to be mediated by an intracellular gate that binds to the intracellular mouth of the pore and was modeled as a ball tethered to the intracellular surface of the channel by a flexible chain[197] (Fig. 1.10). Further antibody binding studies identified both the highly conserved intracellular loop connecting domains III and IV, responsible for inactivation, and its receptor site within the pore[205;206]. Later on, these studies have been confirmed by the identification of a hydrophobic triad of residues (isoleucine, phenylalanine and methionine) with a key role for inactivation[207]. Similar scanning mutagenesis experiments have revealed multiple amino acid residues that may form the inactivation gate receptor within and near the intracellular mouth of the pore[208-213] (Fig. 1.7). These findings demonstrated the mechanism of sodium channel inactivation in which multiple peptide segments form a complex inactivation gate receptor into which the inactivation gate closes to occlude the inner pore (graphically represented in Fig. 1.10E and F).

Inactivation process was firstly viewed as voltage-dependent[198]. Later works showed that inactivation gate does not have a voltage sensor, but it derives most of its voltage dependence from coupling to

the activation process[214;215]; thus, inactivation occurrence depends on the availability of inactivation receptor site, consequent to S4 segments transmembrane movement (Fig. 1.10D and E).

Further studies on the sodium channel inactivation revealed some features which were not considered above. One of these properties is the close-state inactivation, actually the inactivation of the channel without its full activation[216;217]. Taking together both studies on gating currents and channel structure, a model to account for close-state inactivation has been proposed[204] (dashed arrow course in Fig. 1.10). The model suggested that opening the activation gate requires S4 segment movement in domains I-III, with partial activation of the S4 segment of domain IV. By contrast, close-state inactivation would require only S4 segment activation of domains III and IV, which are not sufficient to open the activation gate. Close-state inactivation takes place during slow depolarizations. Thus it would have its major physiological relevance during the passive electrotonic depolarization of membrane which occurs before action potential onset. The close-state inactivation model, provide also an explanation for the observed voltage dependency of recovery from inactivation, as a consequence of its relation with S4 segments of domain III and IV[204].

A different inactivating process has been also described and named slow inactivation. Slow inactivation take places during very long depolarizations (seconds), with strong differences among channel isoforms[218]. It is a separate process that does not involve the linker segment between domain III and IV[219]. A hypothesis to explain slow inactivation is that it results from a structural rearrangement of the

pore, even though mutational studies aimed to test this hypothesis provided controversial results[220;221]. However, the involvement of conformational changes in other channel segments has been proposed[218;222;223]. Thus, although it is accepted that slow inactivation might involve a significant conformational change, the actual mechanism that prevents ionic flow is still unknown[219].

An even slower process termed ultra-slow inactivation has been also observed[224]. Although ultra-slow inactivation is also distinct from fast inactivation, it has been shown to be inhibited by binding of the fast inactivation particle, possibly because of allosteric modulation[225]. This finding demonstrated that there are interactions among the different inactivation events.

Persistent sodium current

Even during sustained depolarizations, a very small portion of sodium current can be recorded[226]. This component of sodium current, with very slow or negligible inactivation has been named persistent (or late) sodium current, by contrast with the transient component which occurs in the very first milliseconds of depolarization. Persistent sodium current results from channel reopening during sustained depolarization by two different modes, burst openings and scattered late openings (Fig. 1.11). The burst opening mode undergoes slow but complete voltage-dependent inactivation and quickly deactivates upon repolarization. On the other hand, scattered late openings inactivate very slowly and may include a non-inactivating component, which supports, in terms of macroscopic current, a truly steady-state or "background" sodium current[227]. These behaviors were interpreted as a sort of instability of the inactivated state of the

channel[228]; moreover, the sustained nature of persistent sodium current is supposedly due to direct transitions between the inactivated and open states of the channel[228](Fig. 1.10, dashed arrow from E to D). Sodium current persistent component produced by the cardiac channel isoform is usually smaller than 1% (0.2% to 0.5%,[35;41]) of the transient one. Nevertheless, since it flows during phase 2 of the action potential, where net transmembrane current is extremely small, it plays a crucial role in maintaining the plateau phase and in determining the action potential duration[229].

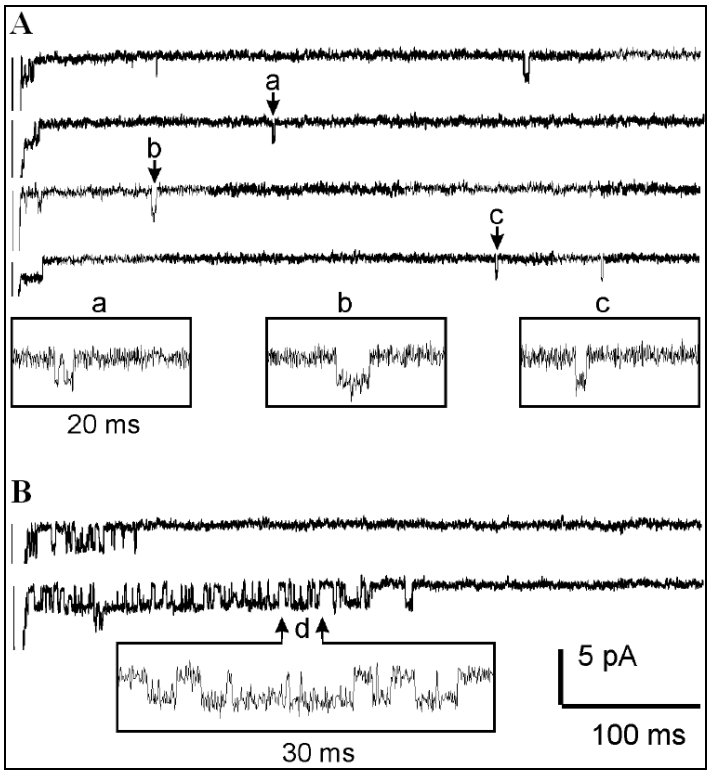

Figure 1.11. Persistent sodium current. Single channel recordings showing the scattered late (**A**) and the burst (**B**) component of persistent sodium current.[228]

Sodium current equation

Hodgkin and Huxley in 1952 quantitatively described sodium current and provided an empirical mathematical model to account for its non-ohmic features[198]. They postulated the presence of four voltage-dependent processes; three of them led sequentially to the channel activation whereas the fourth to its inactivation. At the end of their work they implemented the Ohm equation ($I = G \cdot \Delta V$) as following:

$$\boldsymbol{I_{Na} = G_{Na} \cdot m^3 \cdot h \cdot (E - E_{rev})}$$

where $\boldsymbol{I_{Na}}$ is the sodium current, $\boldsymbol{G_{Na}}$ sodium channel conductance, $\boldsymbol{m^3}$ account for the three activation processes, $\boldsymbol{h}$ account for the inactivation one, $\boldsymbol{E}$ is the actual membrane potential and $\boldsymbol{E_{rev}}$ is the reversal potential for the ion (thus $\boldsymbol{E-E_{rev}}$ represents the driving force). The *m* and *h* factors change between 0 to 1, as a function of membrane voltage and time, in an opposite way. This original model could be perfected, since it considers activation and inactivation processes as fully independent and not couplet each other; moreover, it takes account only of three identical activation processes in spite of the four S4 segments, differentially charged and thus differentially dependent from membrane voltage[204]; finally, it views I_{Na} in every moment as a function which merely depends on membrane potential (voltage-dependency) and time (kinetic properties), with no regard for the state of each molecular process in the former moment during dynamic voltage changes. The latter required a very elaborate and completely different modeling (i.e. markovian model).

Nevertheless, the Hodgkin-Huxley model easily account for the large majority of voltage- and time-dependent properties of sodium current; moreover, every further feature (e.g. slow inactivation or persistent current) which would be considered requires only simple implementations. For these reasons this model is sill widely used.

Scope of the thesis

This work is aimed to electrophysiologically characterize the effects of the mutation S216L in the α-subunit of the cardiac sodium channel and how the common polymorphism H558R modulates these effects, in order to explain the Brugada syndrome phenotype of a proband carrying this genotype.

Moreover, since many times the physiological role of classical steady-state voltage-clamp findings remains uncertain, this work has carried out the first quantitative dynamic voltage-clamp analysis applied to this kind of study, in order to investigate the actual relevance of the mutation effects in the cellular electrophysiological activity.

Reference List of Chapter 1

1. Brugada P, Brugada J. Right bundle branch block, persistent ST segment elevation and sudden cardiac death: a distinct clinical and electrocardiographic syndrome. A multicenter report. *J Am Coll Cardiol*. 1992;20:1391-1396.
2. Hermida JS, Lemoine JL, Aoun FB, Jarry G, Rey JL, Quiret JC. Prevalence of the brugada syndrome in an apparently healthy population. *Am J Cardiol*. 2000;86:91-94.
3. Miyasaka Y, Tsuji H, Yamada K, Tokunaga S, Saito D, Imuro Y, Matsumoto N, Iwasaka T. Prevalence and mortality of the Brugada-type electrocardiogram in one city in Japan. *J Am Coll Cardiol*. 2001;38:771-774.
4. Antzelevitch C, Brugada P, Borggrefe M, Brugada J, Brugada R, Corrado D, Gussak I, LeMarec H, Nademanee K, Perez Riera AR, Shimizu W, Schulze-Bahr E, Tan H, Wilde A. Brugada syndrome: report of the second consensus conference. *Heart Rhythm*. 2005;2:429-440.
5. Meregalli PG, Wilde AA, Tan HL. Pathophysiological mechanisms of Brugada syndrome: depolarization disorder, repolarization disorder, or more? *Cardiovasc Res*. 2005;67:367-378.
6. Wilde AA, Antzelevitch C, Borggrefe M, Brugada J, Brugada R, Brugada P, Corrado D, Hauer RN, Kass RS, Nademanee K, Priori SG, Towbin JA. Proposed diagnostic criteria for the Brugada syndrome. *Eur Heart J*. 2002;23:1648-1654.
7. Atarashi H, Ogawa S. New ECG criteria for high-risk Brugada syndrome. *Circ J*. 2003;67:8-10.
8. Atarashi H, Ogawa S, Harumi K, Sugimoto T, Inoue H, Murayama M, Toyama J, Hayakawa H. Three-year follow-up of patients with

right bundle branch block and ST segment elevation in the right precordial leads: Japanese Registry of Brugada Syndrome. Idiopathic Ventricular Fibrillation Investigators. *J Am Coll Cardiol*. 2001;37:1916-1920.

9. Tada H, Nogami A, Shimizu W, Naito S, Nakatsugawa M, Oshima S, Taniguchi K. ST segment and T wave alternans in a patient with Brugada syndrome. *Pacing Clin Electrophysiol*. 2000;23:413-415.
10. Alings M, Wilde A. "Brugada" syndrome: clinical data and suggested pathophysiological mechanism. *Circulation*. 1999;99:666-673.
11. Smits JP, Eckardt L, Probst V, Bezzina CR, Schott JJ, Remme CA, Haverkamp W, Breithardt G, Escande D, Schulze-Bahr E, LeMarec H, Wilde AA. Genotype-phenotype relationship in Brugada syndrome: electrocardiographic features differentiate SCN5A-related patients from non-SCN5A-related patients. *J Am Coll Cardiol*. 2002;40:350-356.
12. Morita H, Takenaka-Morita S, Fukushima-Kusano K, Kobayashi M, Nagase S, Kakishita M, Nakamura K, Emori T, Matsubara H, Ohe T. Risk stratification for asymptomatic patients with Brugada syndrome. *Circ J*. 2003;67:312-316.
13. Benito B, Brugada J, Brugada R, Brugada P. Brugada syndrome. *Rev Esp Cardiol*. 2009;62:1297-1315.
14. Antzelevitch C. Brugada syndrome. *Pacing Clin Electrophysiol*. 2006;29:1130-1159.
15. Brugada J, Brugada R, Brugada P. Determinants of sudden cardiac death in individuals with the electrocardiographic pattern of Brugada syndrome and no previous cardiac arrest. *Circulation*. 2003;108:3092-3096.
16. Nademanee K. Sudden unexplained death syndrome in Southeast Asia. *Am J Cardiol*. 1997;79:10-11.

17. Vatta M, Dumaine R, Varghese G, Richard TA, Shimizu W, Aihara N, Nademanee K, Brugada R, Brugada J, Veerakul G, Li H, Bowles NE, Brugada P, Antzelevitch C, Towbin JA. Genetic and biophysical basis of sudden unexplained nocturnal death syndrome (SUNDS), a disease allelic to Brugada syndrome. *Hum Mol Genet*. 2002;11:337-345.
18. Di Diego JM, Cordeiro JM, Goodrow RJ, Fish JM, Zygmunt AC, Perez GJ, Scornik FS, Antzelevitch C. Ionic and cellular basis for the predominance of the Brugada syndrome phenotype in males. *Circulation*. 2002;106:2004-2011.
19. Chen Q, Kirsch GE, Zhang D, Brugada R, Brugada J, Brugada P, Potenza D, Moya A, Borggrefe M, Breithardt G, Ortiz-Lopez R, Wang Z, Antzelevitch C, O'Brien RE, Schulze-Bahr E, Keating MT, Towbin JA, Wang Q. Genetic basis and molecular mechanism for idiopathic ventricular fibrillation. *Nature*. 1998;392:293-296.
20. Antzelevitch C, Nof E. Brugada syndrome: recent advances and controversies. *Curr Cardiol Rep*. 2008;10:376-383.
21. Gellens ME, George AL, Jr., Chen LQ, Chahine M, Horn R, Barchi RL, Kallen RG. Primary structure and functional expression of the human cardiac tetrodotoxin-insensitive voltage-dependent sodium channel. *Proc Natl Acad Sci U S A*. 1992;89:554-558.
22. Wang Q, Shen J, Li Z, Timothy K, Vincent GM, Priori SG, Schwartz PJ, Keating MT. Cardiac sodium channel mutations in patients with long QT syndrome, an inherited cardiac arrhythmia. *Hum Mol Genet*. 1995;4:1603-1607.
23. Ackerman MJ, Splawski I, Makielski JC, Tester DJ, Will ML, Timothy KW, Keating MT, Jones G, Chadha M, Burrow CR, Stephens JC, Xu C, Judson R, Curran ME. Spectrum and prevalence of cardiac sodium channel variants among black, white, Asian, and Hispanic individuals: implications for arrhythmogenic susceptibility

and Brugada/long QT syndrome genetic testing. *Heart Rhythm*. 2004;1:600-607.

24. Hofman-Bang J, Behr ER, Hedley P, Tfelt-Hansen J, Kanters JK, Haunsoe S, McKenna WJ, Christiansen M. High-efficiency multiplex capillary electrophoresis single strand conformation polymorphism (multi-CE-SSCP) mutation screening of SCN5A: a rapid genetic approach to cardiac arrhythmia. *Clin Genet*. 2006;69:504-511.
25. Napolitano C, Priori SG, Schwartz PJ, Bloise R, Ronchetti E, Nastoli J, Bottelli G, Cerrone M, Leonardi S. Genetic testing in the long QT syndrome: development and validation of an efficient approach to genotyping in clinical practice. *JAMA*. 2005;294:2975-2980.
26. Bezzina CR, Rook MB, Groenewegen WA, Herfst LJ, van der Wal AC, Lam J, Jongsma HJ, Wilde AA, Mannens MM. Compound heterozygosity for mutations (W156X and R225W) in SCN5A associated with severe cardiac conduction disturbances and degenerative changes in the conduction system. *Circ Res*. 2003;92:159-168.
27. Laitinen-Forsblom PJ, Makynen P, Makynen H, Yli-Mayry S, Virtanen V, Kontula K, Aalto-Setala K. SCN5A mutation associated with cardiac conduction defect and atrial arrhythmias. *J Cardiovasc Electrophysiol*. 2006;17:480-485.
28. Petitprez S, Jespersen T, Pruvot E, Keller DI, Corbaz C, Schlapfer J, Abriel H, Kucera JP. Analyses of a novel SCN5A mutation (C1850S): conduction vs. repolarization disorder hypotheses in the Brugada syndrome. *Cardiovasc Res*. 2008;78:494-504.
29. Probst V, Allouis M, Sacher F, Pattier S, Babuty D, Mabo P, Mansourati J, Victor J, Nguyen JM, Schott JJ, Boisseau P, Escande D, Le Marec H. Progressive cardiac conduction defect is the

prevailing phenotype in carriers of a Brugada syndrome SCN5A mutation. *J Cardiovasc Electrophysiol*. 2006;17:270-275.

30. Darbar D, Kannankeril PJ, Donahue BS, Kucera G, Stubblefield T, Haines JL, George AL, Jr., Roden DM. Cardiac sodium channel (SCN5A) variants associated with atrial fibrillation. *Circulation*. 2008;117:1927-1935.
31. Makita N, Behr E, Shimizu W, Horie M, Sunami A, Crotti L, Schulze-Bahr E, Fukuhara S, Mochizuki N, Makiyama T, Itoh H, Christiansen M, McKeown P, Miyamoto K, Kamakura S, Tsutsui H, Schwartz PJ, George AL, Jr., Roden DM. The E1784K mutation in SCN5A is associated with mixed clinical phenotype of type 3 long QT syndrome. *J Clin Invest*. 2008;118:2219-2229.
32. Olson TM, Michels VV, Ballew JD, Reyna SP, Karst ML, Herron KJ, Horton SC, Rodeheffer RJ, Anderson JL. Sodium channel mutations and susceptibility to heart failure and atrial fibrillation. *JAMA*. 2005;293:447-454.
33. Arnestad M, Crotti L, Rognum TO, Insolia R, Pedrazzini M, Ferrandi C, Vege A, Wang DW, Rhodes TE, George AL, Jr., Schwartz PJ. Prevalence of long-QT syndrome gene variants in sudden infant death syndrome. *Circulation*. 2007;115:361-367.
34. Behr ER, Dalageorgou C, Christiansen M, Syrris P, Hughes S, Tome Esteban MT, Rowland E, Jeffery S, McKenna WJ. Sudden arrhythmic death syndrome: familial evaluation identifies inheritable heart disease in the majority of families. *Eur Heart J*. 2008;29:1670-1680.
35. Wang DW, Desai RR, Crotti L, Arnestad M, Insolia R, Pedrazzini M, Ferrandi C, Vege A, Rognum T, Schwartz PJ, George AL, Jr. Cardiac sodium channel dysfunction in sudden infant death syndrome. *Circulation*. 2007;115:368-376.

36. Nuyens D, Stengl M, Dugarmaa S, Rossenbacker T, Compernolle V, Rudy Y, Smits JF, Flameng W, Clancy CE, Moons L, Vos MA, Dewerchin M, Benndorf K, Collen D, Carmeliet E, Carmeliet P. Abrupt rate accelerations or premature beats cause life-threatening arrhythmias in mice with long-QT3 syndrome. *Nat Med*. 2001;7:1021-1027.
37. Papadatos GA, Wallerstein PM, Head CE, Ratcliff R, Brady PA, Benndorf K, Saumarez RC, Trezise AE, Huang CL, Vandenberg JI, Colledge WH, Grace AA. Slowed conduction and ventricular tachycardia after targeted disruption of the cardiac sodium channel gene Scn5a. *Proc Natl Acad Sci U S A*. 2002;99:6210-6215.
38. Antzelevitch C. Brugada syndrome, report of the Second Consensus Conference (vol 2, pg 429, 2005). *Heart Rhythm*. 2005;2:905.
39. Rossenbacker T, Carroll SJ, Liu H, Kuiperi C, de Ravel TJ, Devriendt K, Carmeliet P, Kass RS, Heidbuchel H. Novel pore mutation in SCN5A manifests as a spectrum of phenotypes ranging from atrial flutter, conduction disease, and Brugada syndrome to sudden cardiac death. *Heart Rhythm*. 2004;1:610-615.
40. Bezzina C, Veldkamp MW, van den Berg MP, Postma AV, Rook MB, Viersma JW, Van Langen IM, Tan-Sindhunata G, Bink-Boelkens MT, Der Hout AH, Mannens MM, Wilde AA. A single Na(+) channel mutation causing both long-QT and Brugada syndromes. *Circ Res*. 1999;85:1206-1213.
41. Veldkamp MW, Viswanathan PC, Bezzina C, Baartscheer A, Wilde AA, Balser JR. Two distinct congenital arrhythmias evoked by a multidysfunctional Na(+) channel. *Circ Res*. 2000;86:E91-E97.
42. Rivolta I, Abriel H, Tateyama M, Liu H, Memmi M, Vardas P, Napolitano C, Priori SG, Kass RS. Inherited Brugada and long QT-3 syndrome mutations of a single residue of the cardiac sodium

channel confer distinct channel and clinical phenotypes. *J Biol Chem*. 2001;276:30623-30630.

43. Antzelevitch C, Brugada R. Fever and Brugada syndrome. *Pacing Clin Electrophysiol*. 2002;25:1537-1539.
44. Dumaine R, Towbin JA, Brugada P, Vatta M, Nesterenko DV, Nesterenko VV, Brugada J, Brugada R, Antzelevitch C. Ionic mechanisms responsible for the electrocardiographic phenotype of the Brugada syndrome are temperature dependent. *Circ Res*. 1999;85:803-809.
45. Watanabe H, Koopmann TT, Le Scouarnec S, Yang T, Ingram CR, Schott JJ, Demolombe S, Probst V, Anselme F, Escande D, Wiesfeld AC, Pfeufer A, Kaab S, Wichmann HE, Hasdemir C, Aizawa Y, Wilde AA, Roden DM, Bezzina CR. Sodium channel beta1 subunit mutations associated with Brugada syndrome and cardiac conduction disease in humans. *J Clin Invest*. 2008;118:2260-2268.
46. Morgan K, Stevens EB, Shah B, Cox PJ, Dixon AK, Lee K, Pinnock RD, Hughes J, Richardson PJ, Mizuguchi K, Jackson AP. beta 3: an additional auxiliary subunit of the voltage-sensitive sodium channel that modulates channel gating with distinct kinetics. *Proc Natl Acad Sci U S A*. 2000;97:2308-2313.
47. Hu D, Barajas-Martinez H, Burashnikov E, Springer M, Wu Y, Varro A, Pfeiffer R, Koopmann TT, Cordeiro JM, Guerchicoff A, Pollevick GD, Antzelevitch C. A mutation in the beta 3 subunit of the cardiac sodium channel associated with Brugada ECG phenotype. *Circ Cardiovasc Genet*. 2009;2:270-278.
48. Takimoto K, Li D, Nerbonne JM, Levitan ES. Distribution, splicing and glucocorticoid-induced expression of cardiac alpha 1C and alpha 1D voltage-gated Ca2+ channel mRNAs. *J Mol Cell Cardiol*. 1997;29:3035-3042.

49. Antzelevitch C, Pollevick GD, Cordeiro JM, Casis O, Sanguinetti MC, Aizawa Y, Guerchicoff A, Pfeiffer R, Oliva A, Wollnik B, Gelber P, Bonaros EP, Jr., Burashnikov E, Wu Y, Sargent JD, Schickel S, Oberheiden R, Bhatia A, Hsu LF, Haissaguerre M, Schimpf R, Borggrefe M, Wolpert C. Loss-of-function mutations in the cardiac calcium channel underlie a new clinical entity characterized by ST-segment elevation, short QT intervals, and sudden cardiac death. *Circulation*. 2007;115:442-449.
50. Van Petegem F, Clark KA, Chatelain FC, Minor DL, Jr. Structure of a complex between a voltage-gated calcium channel beta-subunit and an alpha-subunit domain. *Nature*. 2004;429:671-675.
51. Catterall WA, Perez-Reyes E, Snutch TP, Striessnig J. International Union of Pharmacology. XLVIII. Nomenclature and structure-function relationships of voltage-gated calcium channels. *Pharmacol Rev*. 2005;57:411-425.
52. Cornet V, Bichet D, Sandoz G, Marty I, Brocard J, Bourinet E, Mori Y, Villaz M, De Waard M. Multiple determinants in voltage-dependent P/Q calcium channels control their retention in the endoplasmic reticulum. *Eur J Neurosci*. 2002;16:883-895.
53. Burashnikov E, Pfeiffer R, Barajas-Martinez H, Delpon E, Hu D, Desai M, Borggrefe M, Haissaguerre M, Kanter R, Pollevick GD, Guerchicoff A, Laino R, Marieb M, Nademanee K, Nam GB, Robles R, Schimpf R, Stapleton DH, Viskin S, Winters S, Wolpert C, Zimmern S, Veltmann C, Antzelevitch C. Mutations in the Cardiac L-Type Calcium Channel Associated with Inherited J Wave Syndromes and Sudden Cardiac Death. *Heart Rhythm*. 2010.
54. Delpon E, Cordeiro JM, Nunez L, Thomsen PE, Guerchicoff A, Pollevick GD, Wu Y, Kanters JK, Larsen CT, Hofman-Bang J, Burashnikov E, Christiansen M, Antzelevitch C. Functional effects

of KCNE3 mutation and its role in the development of Brugada syndrome. *Circ Arrhythm Electrophysiol*. 2008;1:209-218.

55. Abbott GW, Butler MH, Bendahhou S, Dalakas MC, Ptacek LJ, Goldstein SA. MiRP2 forms potassium channels in skeletal muscle with Kv3.4 and is associated with periodic paralysis. *Cell*. 2001;104:217-231.
56. McCrossan ZA, Lewis A, Panaghie G, Jordan PN, Christini DJ, Lerner DJ, Abbott GW. MinK-related peptide 2 modulates Kv2.1 and Kv3.1 potassium channels in mammalian brain. *J Neurosci*. 2003;23:8077-8091.
57. Abbott GW, Goldstein SA. Disease-associated mutations in KCNE potassium channel subunits (MiRPs) reveal promiscuous disruption of multiple currents and conservation of mechanism. *FASEB J*. 2002;16:390-400.
58. Abbott GW, Sesti F, Splawski I, Buck ME, Lehmann MH, Timothy KW, Keating MT, Goldstein SA. MiRP1 forms IKr potassium channels with HERG and is associated with cardiac arrhythmia. *Cell*. 1999;97:175-187.
59. Grunnet M, Rasmussen HB, Hay-Schmidt A, Rosenstierne M, Klaerke DA, Olesen SP, Jespersen T. KCNE4 is an inhibitory subunit to Kv1.1 and Kv1.3 potassium channels. *Biophys J*. 2003;85:1525-1537.
60. Lewis A, McCrossan ZA, Abbott GW. MinK, MiRP1, and MiRP2 diversify Kv3.1 and Kv3.2 potassium channel gating. *J Biol Chem*. 2004;279:7884-7892.
61. Yu H, Wu J, Potapova I, Wymore RT, Holmes B, Zuckerman J, Pan Z, Wang H, Shi W, Robinson RB, El Maghrabi MR, Benjamin W, Dixon J, McKinnon D, Cohen IS, Wymore R. MinK-related peptide 1: A beta subunit for the HCN ion channel subunit family enhances expression and speeds activation. *Circ Res*. 2001;88:E84-E87.

62. Zhang M, Jiang M, Tseng GN. minK-related peptide 1 associates with Kv4.2 and modulates its gating function: potential role as beta subunit of cardiac transient outward channel? *Circ Res*. 2001;88:1012-1019.
63. Bendahhou S, Marionneau C, Haurogne K, Larroque MM, Derand R, Szuts V, Escande D, Demolombe S, Barhanin J. In vitro molecular interactions and distribution of KCNE family with KCNQ1 in the human heart. *Cardiovasc Res*. 2005;67:529-538.
64. London B, Michalec M, Mehdi H, Zhu X, Kerchner L, Sanyal S, Viswanathan PC, Pfahnl AE, Shang LL, Madhusudanan M, Baty CJ, Lagana S, Aleong R, Gutmann R, Ackerman MJ, McNamara DM, Weiss R, Dudley SC, Jr. Mutation in glycerol-3-phosphate dehydrogenase 1 like gene (GPD1-L) decreases cardiac Na+ current and causes inherited arrhythmias. *Circulation*. 2007;116:2260-2268.
65. Weiss R, Barmada MM, Nguyen T, Seibel JS, Cavlovich D, Kornblit CA, Angelilli A, Villanueva F, McNamara DM, London B. Clinical and molecular heterogeneity in the Brugada syndrome: a novel gene locus on chromosome 3. *Circulation*. 2002;105:707-713.
66. Van Norstrand DW, Valdivia CR, Tester DJ, Ueda K, London B, Makielski JC, Ackerman MJ. Molecular and functional characterization of novel glycerol-3-phosphate dehydrogenase 1 like gene (GPD1-L) mutations in sudden infant death syndrome. *Circulation*. 2007;116:2253-2259.
67. Priori SG, Napolitano C, Vicentini A. Inherited arrhythmia syndromes: applying the molecular biology and genetic to the clinical management. *J Interv Card Electrophysiol*. 2003;9:93-101.
68. Kasanuki H, Ohnishi S, Ohtuka M, Matsuda N, Nirei T, Isogai R, Shoda M, Toyoshima Y, Hosoda S. Idiopathic ventricular fibrillation induced with vagal activity in patients without obvious heart disease. *Circulation*. 1997;95:2277-2285.

69. Proclemer A, Facchin D, Feruglio GA, Nucifora R. [Recurrent ventricular fibrillation, right bundle-branch block and persistent ST segment elevation in V1-V3: a new arrhythmia syndrome? A clinical case report]. *G Ital Cardiol*. 1993;23:1211-1218.
70. Makiyama T, Akao M, Tsuji K, Doi T, Ohno S, Takenaka K, Kobori A, Ninomiya T, Yoshida H, Takano M, Makita N, Yanagisawa F, Higashi Y, Takeyama Y, Kita T, Horie M. High risk for bradyarrhythmic complications in patients with Brugada syndrome caused by SCN5A gene mutations. *J Am Coll Cardiol*. 2005;46:2100-2106.
71. Scornik FS, Desai M, Brugada R, Guerchicoff A, Pollevick GD, Antzelevitch C, Perez GJ. Functional expression of "cardiac-type" Nav1.5 sodium channel in canine intracardiac ganglia. *Heart Rhythm*. 2006;3:842-850.
72. Junttila MJ, Gonzalez M, Lizotte E, Benito B, Vernooy K, Sarkozy A, Huikuri HV, Brugada P, Brugada J, Brugada R. Induced Brugada-type electrocardiogram, a sign for imminent malignant arrhythmias. *Circulation*. 2008;117:1890-1893.
73. Belhassen B, Glick A, Viskin S. Efficacy of quinidine in high-risk patients with Brugada syndrome. *Circulation*. 2004;110:1731-1737.
74. Hermida JS, Denjoy I, Clerc J, Extramiana F, Jarry G, Milliez P, Guicheney P, Di Fusco S, Rey JL, Cauchemez B, Leenhardt A. Hydroquinidine therapy in Brugada syndrome. *J Am Coll Cardiol*. 2004;43:1853-1860.
75. Tanaka H, Kinoshita O, Uchikawa S, Kasai H, Nakamura M, Izawa A, Yokoseki O, Kitabayashi H, Takahashi W, Yazaki Y, Watanabe N, Imamura H, Kubo K. Successful prevention of recurrent ventricular fibrillation by intravenous isoproterenol in a patient with Brugada syndrome. *Pacing Clin Electrophysiol*. 2001;24:1293-1294.

76. Marban E, Robinson SW, Wier WG. Mechanisms of arrhythmogenic delayed and early afterdepolarizations in ferret ventricular muscle. *J Clin Invest*. 1986;78:1185-1192.
77. Yan GX, Antzelevitch C. Cellular basis for the Brugada syndrome and other mechanisms of arrhythmogenesis associated with ST-segment elevation. *Circulation*. 1999;100:1660-1666.
78. Antzelevitch C. Late potentials and the Brugada syndrome. *J Am Coll Cardiol*. 2002;39:1996-1999.
79. Gussak I, Antzelevitch C. Early repolarization syndrome: clinical characteristics and possible cellular and ionic mechanisms. *J Electrocardiol*. 2000;33:299-309.
80. Nabauer M, Beuckelmann DJ, Uberfuhr P, Steinbeck G. Regional differences in current density and rate-dependent properties of the transient outward current in subepicardial and subendocardial myocytes of human left ventricle. *Circulation.* 1996;93:168-177.
81. Cordeiro JM, Mazza M, Goodrow R, Ulahannan N, Antzelevitch C, Di Diego JM. Functionally distinct sodium channels in ventricular epicardial and endocardial cells contribute to a greater sensitivity of the epicardium to electrical depression. *Am J Physiol Heart Circ Physiol*. 2008;295:H154-H162.
82. Antzelevitch C. The Brugada syndrome: ionic basis and arrhythmia mechanisms. *J Cardiovasc Electrophysiol*. 2001;12:268-272.
83. Yan GX, Antzelevitch C. Cellular basis for the electrocardiographic J wave. *Circulation*. 1996;93:372-379.
84. Lukas A, Antzelevitch C. Phase 2 reentry as a mechanism of initiation of circus movement reentry in canine epicardium exposed to simulated ischemia. *Cardiovasc Res*. 1996;32:593-603.
85. Bruns HJ, Eckardt L, Vahlhaus C, Schulze-Bahr E, Haverkamp W, Borggrefe M, Breithardt G, Wichter T. Body surface potential mapping in patients with Brugada syndrome: right precordial ST

segment variations and reverse changes in left precordial leads. *Cardiovasc Res*. 2002;54:58-66.

86. Conrath CE, Wilders R, Coronel R, de Bakker JM, Taggart P, de Groot JR, Opthof T. Intercellular coupling through gap junctions masks M cells in the human heart. *Cardiovasc Res*. 2004;62:407-414.
87. Janse MJ, Kleber AG. Electrophysiological changes and ventricular arrhythmias in the early phase of regional myocardial ischemia. *Circ Res*. 1981;49:1069-1081.
88. Di Diego JM, Sun ZQ, Antzelevitch C. I(to) and action potential notch are smaller in left vs. right canine ventricular epicardium. *Am J Physiol*. 1996;271:H548-H561.
89. Izumida N, Asano Y, Doi S, Wakimoto H, Fukamizu S, Kimura T, Ueyama T, Sakurada H, Kawano S, Sawanobori T, Hiraoka M. Changes in body surface potential distributions induced by isoproterenol and Na channel blockers in patients with the Brugada syndrome. *Int J Cardiol*. 2004;95:261-268.
90. Zaffran S, Kelly RG, Meilhac SM, Buckingham ME, Brown NA. Right ventricular myocardium derives from the anterior heart field. *Circ Res*. 2004;95:261-268.
91. de Jong F, Opthof T, Wilde AA, Janse MJ, Charles R, Lamers WH, Moorman AF. Persisting zones of slow impulse conduction in developing chicken hearts. *Circ Res*. 1992;71:240-250.
92. Moorman AF, Schumacher CA, de Boer PA, Hagoort J, Bezstarosti K, van den Hoff MJ, Wagenaar GT, Lamers JM, Wuytack F, Christoffels VM, Fiolet JW. Presence of functional sarcoplasmic reticulum in the developing heart and its confinement to chamber myocardium. *Dev Biol*. 2000;223:279-290.
93. Pham TV, Robinson RB, Danilo P, Jr., Rosen MR. Effects of gonadal steroids on gender-related differences in transmural

dispersion of L-type calcium current. *Cardiovasc Res*. 2002;53:752-762.

94. Miyazaki T, Mitamura H, Miyoshi S, Soejima K, Aizawa Y, Ogawa S. Autonomic and antiarrhythmic drug modulation of ST segment elevation in patients with Brugada syndrome. *J Am Coll Cardiol*. 1996;27:1061-1070.
95. Mizumaki K, Fujiki A, Tsuneda T, Sakabe M, Nishida K, Sugao M, Inoue H. Vagal activity modulates spontaneous augmentation of ST elevation in the daily life of patients with Brugada syndrome. *J Cardiovasc Electrophysiol*. 2004;15:667-673.
96. Noda T, Shimizu W, Taguchi A, Satomi K, Suyama K, Kurita T, Aihara N, Kamakura S. ST-segment elevation and ventricular fibrillation without coronary spasm by intracoronary injection of acetylcholine and/or ergonovine maleate in patients with Brugada syndrome. *J Am Coll Cardiol*. 2002;40:1841-1847.
97. Kies P, Wichter T, Schafers M, Paul M, Schafers KP, Eckardt L, Stegger L, Schulze-Bahr E, Rimoldi O, Breithardt G, Schober O, Camici PG. Abnormal myocardial presynaptic norepinephrine recycling in patients with Brugada syndrome. *Circulation*. 2004;110:3017-3022.
98. Litovsky SH, Antzelevitch C. Differences in the electrophysiological response of canine ventricular subendocardium and subepicardium to acetylcholine and isoproterenol. A direct effect of acetylcholine in ventricular myocardium. *Circ Res*. 1990;67:615-627.
99. Fujiki A, Usui M, Nagasawa H, Mizumaki K, Hayashi H, Inoue H. ST segment elevation in the right precordial leads induced with class IC antiarrhythmic drugs: insight into the mechanism of Brugada syndrome. *J Cardiovasc Electrophysiol*. 1999;10:214-218.

100. Matsuo K, Shimizu W, Kurita T, Inagaki M, Aihara N, Kamakura S. Dynamic changes of 12-lead electrocardiograms in a patient with Brugada syndrome. *J Cardiovasc Electrophysiol*. 1998;9:508-512.
101. Lee KL, Lau CP, Tse HF, Wan SH, Fan K. Prevention of ventricular fibrillation by pacing in a man with Brugada syndrome. *J Cardiovasc Electrophysiol*. 2000;11:935-937.
102. Krishnan SC, Josephson ME. ST segment elevation induced by class IC antiarrhythmic agents: underlying electrophysiologic mechanisms and insights into drug-induced proarrhythmia. *J Cardiovasc Electrophysiol*. 1998;9:1167-1172.
103. Ohkubo K, Watanabe I, Okumura Y, Yamada T, Masaki R, Kofune T, Oshikawa N, Kasamaki Y, Saito S, Ozawa Y, Kanmatsuse K. Intravenous administration of class I antiarrhythmic drug induced T wave alternans in an asymptomatic Brugada syndrome patient. *Pacing Clin Electrophysiol*. 2003;26:1900-1903.
104. Krishnan SC, Antzelevitch C. Sodium channel block produces opposite electrophysiological effects in canine ventricular epicardium and endocardium. *Circ Res*. 1991;69:277-291.
105. Krishnan SC, Antzelevitch C. Flecainide-induced arrhythmia in canine ventricular epicardium. Phase 2 reentry? *Circulation*. 1993;87:562-572.
106. Di Diego JM, Antzelevitch C. Pinacidil-induced electrical heterogeneity and extrasystolic activity in canine ventricular tissues. Does activation of ATP-regulated potassium current promote phase 2 reentry? *Circulation*. 1993;88:1177-1189.
107. Liu DW, Gintant GA, Antzelevitch C. Ionic bases for electrophysiological distinctions among epicardial, midmyocardial, and endocardial myocytes from the free wall of the canine left ventricle. *Circ Res*. 1993;72:671-687.

108. Kimura M, Kobayashi T, Owada S, Ashikaga K, Higuma T, Sasaki S, Iwasa A, Motomura S, Okumura K. Mechanism of ST elevation and ventricular arrhythmias in an experimental Brugada syndrome model. *Circulation*. 2004;109:125-131.
109. Alings M, Dekker L, Sadee A, Wilde A. Quinidine induced electrocardiographic normalization in two patients with Brugada syndrome. *Pacing Clin Electrophysiol*. 2001;24:1420-1422.
110. Mok NS, Chan NY, Chiu AC. Successful use of quinidine in treatment of electrical storm in Brugada syndrome. *Pacing Clin Electrophysiol*. 2004;27:821-823.
111. Falk RH. Proarrhythmia in patients treated for atrial fibrillation or flutter. *Ann Intern Med*. 1992;117:141-150.
112. Josephson ME, Seides SF, Batsford WP, Weisfogel GM, Akhtar M, Caracta AR, Lau SH, Damato AN. The electrophysiological effects of intramuscular guinidine on the atrioventricular conducting system in man. *Am Heart J*. 1974;87:55-64.
113. Carmeliet E. Use-dependent block of the delayed K+ current in rabbit ventricular myocytes. *Cardiovasc Drugs Ther*. 1993;7 Suppl 3:599-604.
114. Iost N, Virag L, Varro A, Papp JG. Comparison of the effect of class IA antiarrhythmic drugs on transmembrane potassium currents in rabbit ventricular myocytes. *J Cardiovasc Pharmacol Ther*. 2003;8:31-41.
115. Kurita T, Shimizu W, Inagaki M, Suyama K, Taguchi A, Satomi K, Aihara N, Kamakura S, Kobayashi J, Kosakai Y. The electrophysiologic mechanism of ST-segment elevation in Brugada syndrome. *J Am Coll Cardiol*. 2002;40:330-334.
116. Nishida K, Fujiki A, Mizumaki K, Sakabe M, Sugao M, Tsuneda T, Inoue H. Canine model of Brugada syndrome using regional

epicardial cooling of the right ventricular outflow tract. *J Cardiovasc Electrophysiol*. 2004;15:936-941.

117. Shimizu W, Aiba T, Kurita T, Kamakura S. Paradoxic abbreviation of repolarization in epicardium of the right ventricular outflow tract during augmentation of Brugada-type ST segment elevation. *J Cardiovasc Electrophysiol*. 2001;12:1418-1421.
118. Ikeda T, Abe A, Yusu S, Nakamura K, Ishiguro H, Mera H, Yotsukura M, Yoshino H. The full stomach test as a novel diagnostic technique for identifying patients at risk of Brugada syndrome. *J Cardiovasc Electrophysiol*. 2006;17:602-607.
119. Hisamatsu K, Kusano KF, Morita H, Takenaka S, Nagase S, Nakamura K, Emori T, Matsubara H, Mikouchi H, Nishizaki Y, Ohe T. Relationships between depolarization abnormality and repolarization abnormality in patients with Brugada syndrome: using body surface signal-averaged electrocardiography and body surface maps. *J Cardiovasc Electrophysiol*. 2004;15:870-876.
120. Nagase S, Kusano KF, Morita H, Fujimoto Y, Kakishita M, Nakamura K, Emori T, Matsubara H, Ohe T. Epicardial electrogram of the right ventricular outflow tract in patients with the Brugada syndrome: using the epicardial lead. *J Am Coll Cardiol*. 2002;39:1992-1995.
121. Tada H, Aihara N, Ohe T, Yutani C, Hamada S, Miyanuma H, Takamiya M, Kamakura S. Arrhythmogenic right ventricular cardiomyopathy underlies syndrome of right bundle branch block, ST-segment elevation, and sudden death. *Am J Cardiol*. 1998;81:519-522.
122. Takagi M, Aihara N, Kuribayashi S, Taguchi A, Shimizu W, Kurita T, Suyama K, Kamakura S, Hamada S, Takamiya M. Localized right ventricular morphological abnormalities detected by electron-beam computed tomography represent arrhythmogenic substrates in

patients with the Brugada syndrome. *Eur Heart J*. 2001;22:1032-1041.

123. Takagi M, Aihara N, Kuribayashi S, Taguchi A, Kurita T, Suyama K, Kamakura S, Takamiya M. Abnormal response to sodium channel blockers in patients with Brugada syndrome: augmented localised wall motion abnormalities in the right ventricular outflow tract region detected by electron beam computed tomography. *Heart*. 2003;89:169-174.
124. Carlson MD, White RD, Trohman RG, Adler LP, Biblo LA, Merkatz KA, Waldo AL. Right ventricular outflow tract ventricular tachycardia: detection of previously unrecognized anatomic abnormalities using cine magnetic resonance imaging. *J Am Coll Cardiol*. 1994;24:720-727.
125. Papavassiliu T, Wolpert C, Fluchter S, Schimpf R, Neff W, Haase KK, Duber C, Borggrefe M. Magnetic resonance imaging findings in patients with Brugada syndrome. *J Cardiovasc Electrophysiol*. 2004;15:1133-1138.
126. Coronel R, Casini S, Koopmann TT, Wilms-Schopman FJ, Verkerk AO, de Groot JR, Bhuiyan Z, Bezzina CR, Veldkamp MW, Linnenbank AC, van der Wal AC, Tan HL, Brugada P, Wilde AA, de Bakker JM. Right ventricular fibrosis and conduction delay in a patient with clinical signs of Brugada syndrome: a combined electrophysiological, genetic, histopathologic, and computational study. *Circulation*. 2005;112:2769-2777.
127. Royer A, van Veen TA, Le Bouter S, Marionneau C, Griol-Charhbili V, Leoni AL, Steenman M, van Rijen HV, Demolombe S, Goddard CA, Richer C, Escoubet B, Jarry-Guichard T, Colledge WH, Gros D, de Bakker JM, Grace AA, Escande D, Charpentier F. Mouse model of SCN5A-linked hereditary Lenegre's disease: age-related

conduction slowing and myocardial fibrosis. *Circulation*. 2005;111:1738-1746.

128. Akhtar M, Goldschlager NF. Brugada electrocardiographic pattern due to tricyclic antidepressant overdose. *J Electrocardiol*. 2006;39:336-339.
129. Araki T, Konno T, Itoh H, Ino H, Shimizu M. Brugada syndrome with ventricular tachycardia and fibrillation related to hypokalemia. *Circ J*. 2003;67:93-95.
130. Babaliaros VC, Hurst JW. Tricyclic antidepressants and the Brugada syndrome: an example of Brugada waves appearing after the administration of desipramine. *Clin Cardiol*. 2002;25:395-398.
131. Brugada P, Brugada J, Brugada R. Arrhythmia induction by antiarrhythmic drugs. *Pacing Clin Electrophysiol*. 2000;23:291-292.
132. Brugada R, Brugada J, Antzelevitch C, Kirsch GE, Potenza D, Towbin JA, Brugada P. Sodium channel blockers identify risk for sudden death in patients with ST-segment elevation and right bundle branch block but structurally normal hearts. *Circulation*. 2000;101:510-515.
133. Goldgran-Toledano D, Sideris G, Kevorkian JP. Overdose of cyclic antidepressants and the Brugada syndrome. *N Engl J Med*. 2002;346:1591-1592.
134. Nogami A, Nakao M, Kubota S, Sugiyasu A, Doi H, Yokoyama K, Yumoto K, Tamaki T, Kato K, Hosokawa N, Sagai H, Nakamura H, Nitta J, Yamauchi Y, Aonuma K. Enhancement of J-ST-segment elevation by the glucose and insulin test in Brugada syndrome. *Pacing Clin Electrophysiol*. 2003;26:332-337.
135. Ortega-Carnicer J, Bertos-Polo J, Gutierrez-Tirado C. Aborted sudden death, transient Brugada pattern, and wide QRS dysrrhythmias after massive cocaine ingestion. *J Electrocardiol*. 2001;34:345-349.

136. Pastor A, Nunez A, Cantale C, Cosio FG. Asymptomatic brugada syndrome case unmasked during dimenhydrinate infusion. *J Cardiovasc Electrophysiol*. 2001;12:1192-1194.
137. Tada H, Sticherling C, Oral H, Morady F. Brugada syndrome mimicked by tricyclic antidepressant overdose. *J Cardiovasc Electrophysiol*. 2001;12:275.
138. Postema PG, Wolpert C, Amin AS, Probst V, Borggrefe M, Roden DM, Priori SG, Tan HL, Hiraoka M, Brugada J, Wilde AA. Drugs and Brugada syndrome patients: review of the literature, recommendations, and an up-to-date website (www.brugadadrugs.org). *Heart Rhythm*. 2009;6:1335-1341.
139. Nimmannit S, Malasit P, Chaovakul V, Susaengrat W, Vasuvattakul S, Nilwarangkur S. Pathogenesis of sudden unexplained nocturnal death (lai tai) and endemic distal renal tubular acidosis. *Lancet*. 1991;338:930-932.
140. Kum LC, Fung JW, Sanderson JE. Brugada syndrome unmasked by febrile illness. *Pacing Clin Electrophysiol*. 2002;25:1660-1661.
141. Porres JM, Brugada J, Urbistondo V, Garcia F, Reviejo K, Marco P. Fever unmasking the Brugada syndrome. *Pacing Clin Electrophysiol*. 2002;25:1646-1648.
142. Saura D, Garcia-Alberola A, Carrillo P, Pascual D, Martinez-Sanchez J, Valdes M. Brugada-like electrocardiographic pattern induced by fever. *Pacing Clin Electrophysiol*. 2002;25:856-859.
143. Eckardt L. Gender differences in Brugada syndrome. *J Cardiovasc Electrophysiol*. 2007;18:422-424.
144. Shimizu W, Matsuo K, Kokubo Y, Satomi K, Kurita T, Noda T, Nagaya N, Suyama K, Aihara N, Kamakura S, Inamoto N, Akahoshi M, Tomoike H. Sex hormone and gender difference--role of testosterone on male predominance in Brugada syndrome. *J Cardiovasc Electrophysiol*. 2007;18:415-421.

145. Bai CX, Kurokawa J, Tamagawa M, Nakaya H, Furukawa T. Nontranscriptional regulation of cardiac repolarization currents by testosterone. *Circulation*. 2005;112:1701-1710.
146. Song M, Helguera G, Eghbali M, Zhu N, Zarei MM, Olcese R, Toro L, Stefani E. Remodeling of Kv4.3 potassium channel gene expression under the control of sex hormones. *J Biol Chem*. 2001;276:31883-31890.
147. Probst V, Denjoy I, Meregalli PG, Amirault JC, Sacher F, Mansourati J, Babuty D, Villain E, Victor J, Schott JJ, Lupoglazoff JM, Mabo P, Veltmann C, Jesel L, Chevalier P, Clur SA, Haissaguerre M, Wolpert C, Le Marec H, Wilde AA. Clinical aspects and prognosis of Brugada syndrome in children. *Circulation*. 2007;115:2042-2048.
148. Brugada J, Brugada R, Antzelevitch C, Towbin J, Nademanee K, Brugada P. Long-term follow-up of individuals with the electrocardiographic pattern of right bundle-branch block and ST-segment elevation in precordial leads V1 to V3. *Circulation*. 2002;105:73-78.
149. Eckardt L, Probst V, Smits JP, Bahr ES, Wolpert C, Schimpf R, Wichter T, Boisseau P, Heinecke A, Breithardt G, Borggrefe M, LeMarec H, Bocker D, Wilde AA. Long-term prognosis of individuals with right precordial ST-segment-elevation Brugada syndrome. *Circulation*. 2005;111:257-263.
150. Gasparini M, Priori SG, Mantica M, Coltorti F, Napolitano C, Galimberti P, Bloise R, Ceriotti C. Programmed electrical stimulation in Brugada syndrome: how reproducible are the results? *J Cardiovasc Electrophysiol*. 2002;13:880-887.
151. Priori SG, Napolitano C, Gasparini M, Pappone C, Della BP, Giordano U, Bloise R, Giustetto C, De Nardis R, Grillo M, Ronchetti E, Faggiano G, Nastoli J. Natural history of Brugada

syndrome: insights for risk stratification and management. *Circulation*. 2002;105:1342-1347.

152. Kanda M, Shimizu W, Matsuo K, Nagaya N, Taguchi A, Suyama K, Kurita T, Aihara N, Kamakura S. Electrophysiologic characteristics and implications of induced ventricular fibrillation in symptomatic patients with Brugada syndrome. *J Am Coll Cardiol*. 2002;39:1799-1805.
153. Eckardt L, Kirchhof P, Johna R, Haverkamp W, Breithardt G, Borggrefe M. Wolff-Parkinson-White syndrome associated with Brugada syndrome. *Pacing Clin Electrophysiol*. 2001;24:1423-1424.
154. Carlsson J, Erdogan A, Schulte B, Neuzner J, Pitschner HF. Possible role of epicardial left ventricular programmed stimulation in Brugada syndrome. *Pacing Clin Electrophysiol*. 2001;24:247-249.
155. Antzelevitch C. T peak-Tend interval as an index of transmural dispersion of repolarization. *Eur J Clin Invest*. 2001;31:555-557.
156. Antzelevitch C, Shimizu W, Yan GX, Sicouri S, Weissenburger J, Nesterenko VV, Burashnikov A, Di Diego J, Saffitz J, Thomas GP. The M cell: its contribution to the ECG and to normal and abnormal electrical function of the heart. *J Cardiovasc Electrophysiol*. 1999;10:1124-1152.
157. Fish JM, Di Diego JM, Nesterenko V, Antzelevitch C. Epicardial activation of left ventricular wall prolongs QT interval and transmural dispersion of repolarization: implications for biventricular pacing. *Circulation*. 2004;109:2136-2142.
158. Yan GX, Antzelevitch C. Cellular basis for the normal T wave and the electrocardiographic manifestations of the long-QT syndrome. *Circulation*. 1998;98:1928-1936.
159. Emori T, Antzelevitch C. Cellular basis for complex T waves and arrhythmic activity following combined I(Kr) and I(Ks) block. *J Cardiovasc Electrophysiol*. 2001;12:1369-1378.

160. Milberg P, Reinsch N, Wasmer K, Monnig G, Stypmann J, Osada N, Breithardt G, Haverkamp W, Eckardt L. Transmural dispersion of repolarization as a key factor of arrhythmogenicity in a novel intact heart model of LQT3. *Cardiovasc Res*. 2005;65:397-404.
161. Watanabe N, Kobayashi Y, Tanno K, Miyoshi F, Asano T, Kawamura M, Mikami Y, Adachi T, Ryu S, Miyata A, Katagiri T. Transmural dispersion of repolarization and ventricular tachyarrhythmias. *J Electrocardiol*. 2004;37:191-200.
162. Shimizu M, Ino H, Okeie K, Yamaguchi M, Nagata M, Hayashi K, Itoh H, Iwaki T, Oe K, Konno T, Mabuchi H. T-peak to T-end interval may be a better predictor of high-risk patients with hypertrophic cardiomyopathy associated with a cardiac troponin I mutation than QT dispersion. *Clin Cardiol*. 2002;25:335-339.
163. Castro HJ, Antzelevitch C, Tornes BF, Dorantes SM, Dorticos BF, Zayas MR, Quinones Perez MA, Fayad RY. Tpeak-Tend and Tpeak-Tend dispersion as risk factors for ventricular tachycardia/ventricular fibrillation in patients with the Brugada syndrome. *J Am Coll Cardiol*. 2006;47:1828-1834.
164. Bezzina CR, Shimizu W, Yang P, Koopmann TT, Tanck MW, Miyamoto Y, Kamakura S, Roden DM, Wilde AA. Common sodium channel promoter haplotype in asian subjects underlies variability in cardiac conduction. *Circulation*. 2006;113:338-344.
165. Splawski I, Timothy KW, Tateyama M, Clancy CE, Malhotra A, Beggs AH, Cappuccio FP, Sagnella GA, Kass RS, Keating MT. Variant of SCN5A sodium channel implicated in risk of cardiac arrhythmia. *Science*. 2002;297:1333-1336.
166. Chen LY, Ballew JD, Herron KJ, Rodeheffer RJ, Olson TM. A common polymorphism in SCN5A is associated with lone atrial fibrillation. *Clin Pharmacol Ther*. 2007;81:35-41.

167. Gouas L, Nicaud V, Berthet M, Forhan A, Tiret L, Balkau B, Guicheney P. Association of KCNQ1, KCNE1, KCNH2 and SCN5A polymorphisms with QTc interval length in a healthy population. *Eur J Hum Genet*. 2005;13:1213-1222.
168. Chen JZ, Xie XD, Wang XX, Tao M, Shang YP, Guo XG. Single nucleotide polymorphisms of the SCN5A gene in Han Chinese and their relation with Brugada syndrome. *Chin Med J (Engl)*. 2004;117:652-656.
169. Lizotte E, Junttila MJ, Dube MP, Hong K, Benito B, DE Zutter M, Henkens S, Sarkozy A, Huikuri HV, Towbin J, Vatta M, Brugada P, Brugada J, Brugada R. Genetic modulation of brugada syndrome by a common polymorphism. *J Cardiovasc Electrophysiol*. 2009;20:1137-1141.
170. Poelzing S, Forleo C, Samodell M, Dudash L, Sorrentino S, Anaclerio M, Troccoli R, Iacoviello M, Romito R, Guida P, Chahine M, Pitzalis M, Deschenes I. SCN5A polymorphism restores trafficking of a Brugada syndrome mutation on a separate gene. *Circulation*. 2006;114:368-376.
171. Viswanathan PC, Benson DW, Balser JR. A common SCN5A polymorphism modulates the biophysical effects of an SCN5A mutation. *J Clin Invest*. 2003;111:341-346.
172. Ye B, Valdivia CR, Ackerman MJ, Makielski JC. A common human SCN5A polymorphism modifies expression of an arrhythmia causing mutation. *Physiol Genomics*. 2003;12:187-193.
173. Makielski JC, Ye B, Valdivia CR, Pagel MD, Pu J, Tester DJ, Ackerman MJ. A ubiquitous splice variant and a common polymorphism affect heterologous expression of recombinant human SCN5A heart sodium channels. *Circ Res*. 2003;93:821-828.
174. Hong K, Brugada J, Oliva A, Berruezo-Sanchez A, Potenza D, Pollevick GD, Guerchicoff A, Matsuo K, Burashnikov E, Dumaine

R, Towbin JA, Nesterenko V, Brugada P, Antzelevitch C, Brugada R. Value of electrocardiographic parameters and ajmaline test in the diagnosis of Brugada syndrome caused by SCN5A mutations. *Circulation*. 2004;110:3023-3027.

175. Meregalli PG, Ruijter JM, Hofman N, Bezzina CR, Wilde AA, Tan HL. Diagnostic value of flecainide testing in unmasking SCN5A-related Brugada syndrome. *J Cardiovasc Electrophysiol*. 2006;17:857-864.
176. Wolpert C, Echternach C, Veltmann C, Antzelevitch C, Thomas GP, Spehl S, Streitner F, Kuschyk J, Schimpf R, Haase KK, Borggrefe M. Intravenous drug challenge using flecainide and ajmaline in patients with Brugada syndrome. *Heart Rhythm*. 2005;2:254-260.
177. Sangwatanaroj S, Prechawat S, Sunsaneewitayakul B, Sitthisook S, Tosukhowong P, Tungsanga K. New electrocardiographic leads and the procainamide test for the detection of the Brugada sign in sudden unexplained death syndrome survivors and their relatives. *Eur Heart J*. 2001;22:2290-2296.
178. Miyamoto K, Yokokawa M, Tanaka K, Nagai T, Okamura H, Noda T, Satomi K, Suyama K, Kurita T, Aihara N, Kamakura S, Shimizu W. Diagnostic and prognostic value of a type 1 Brugada electrocardiogram at higher (third or second) V1 to V2 recording in men with Brugada syndrome. *Am J Cardiol*. 2007;99:53-57.
179. Paul M, Gerss J, Schulze-Bahr E, Wichter T, Vahlhaus C, Wilde AA, Breithardt G, Eckardt L. Role of programmed ventricular stimulation in patients with Brugada syndrome: a meta-analysis of worldwide published data. *Eur Heart J*. 2007;28:2126-2133.
180. Amin AS, Meregalli PG, Bardai A, Wilde AA, Tan HL. Fever increases the risk for cardiac arrest in the Brugada syndrome. *Ann Intern Med*. 2008;149:216-218.

181. Skinner JR, Chung SK, Nel CA, Shelling AN, Crawford JR, McKenzie N, Pinnock R, French JK, Rees MI. Brugada syndrome masquerading as febrile seizures. *Pediatrics*. 2007;119:e1206-e1211.
182. Antzelevitch C, Brugada P, Borggrefe M, Brugada J, Brugada R, Corrado D, Gussak I, LeMarec H, Nademanee K, Perez Riera AR, Shimizu W, Schulze-Bahr E, Tan H, Wilde A. Brugada syndrome: report of the second consensus conference: endorsed by the Heart Rhythm Society and the European Heart Rhythm Association. *Circulation*. 2005;111:659-670.
183. Sacher F, Probst V, Iesaka Y, Jacon P, Laborderie J, Mizon-Gerard F, Mabo P, Reuter S, Lamaison D, Takahashi Y, O'Neill MD, Garrigue S, Pierre B, Jais P, Pasquie JL, Hocini M, Salvador-Mazenq M, Nogami A, Amiel A, Defaye P, Bordachar P, Boveda S, Maury P, Klug D, Babuty D, Haissaguerre M, Mansourati J, Clementy J, Le Marec H. Outcome after implantation of a cardioverter-defibrillator in patients with Brugada syndrome: a multicenter study. *Circulation*. 2006;114:2317-2324.
184. Sarkozy A, Boussy T, Chierchia GB, Geelen P, Brugada P. An unusual form of bundle branch reentrant tachycardia. *J Cardiovasc Electrophysiol*. 2006;17:902-906.
185. Ohgo T, Okamura H, Noda T, Satomi K, Suyama K, Kurita T, Aihara N, Kamakura S, Ohe T, Shimizu W. Acute and chronic management in patients with Brugada syndrome associated with electrical storm of ventricular fibrillation. *Heart Rhythm*. 2007;4:695-700.
186. Benito B, Brugada R, Brugada J, Brugada P. Brugada syndrome. *Prog Cardiovasc Dis*. 2008;51:1-22.
187. Isom LL, De Jongh KS, Patton DE, Reber BF, Offord J, Charbonneau H, Walsh K, Goldin AL, Catterall WA. Primary

structure and functional expression of the beta 1 subunit of the rat brain sodium channel. *Science*. 1992;256:839-842.

188. Patton DE, Isom LL, Catterall WA, Goldin AL. The adult rat brain beta 1 subunit modifies activation and inactivation gating of multiple sodium channel alpha subunits. *J Biol Chem*. 1994;269:17649-17655.
189. Catterall WA. From ionic currents to molecular mechanisms: the structure and function of voltage-gated sodium channels. *Neuron*. 2000;26:13-25.
190. Hille B. Ionic Channels of Excitable Membranes. 2010. Sinauer Associates.
191. Noda M, Suzuki H, Numa S, Stuhmer W. A single point mutation confers tetrodotoxin and saxitoxin insensitivity on the sodium channel II. *FEBS Lett*. 1989;259:213-216.
192. Terlau H, Heinemann SH, Stuhmer W, Pusch M, Conti F, Imoto K, Numa S. Mapping the site of block by tetrodotoxin and saxitoxin of sodium channel II. *FEBS Lett*. 1991;293:93-96.
193. Heinemann SH, Terlau H, Stuhmer W, Imoto K, Numa S. Calcium channel characteristics conferred on the sodium channel by single mutations. *Nature*. 1992;356:441-443.
194. Schlief T, Schonherr R, Imoto K, Heinemann SH. Pore properties of rat brain II sodium channels mutated in the selectivity filter domain. *Eur Biophys J*. 1996;25:75-91.
195. Sun YM, Favre I, Schild L, Moczydlowski E. On the structural basis for size-selective permeation of organic cations through the voltage-gated sodium channel. Effect of alanine mutations at the DEKA locus on selectivity, inhibition by Ca2+ and H+, and molecular sieving. *J Gen Physiol*. 1997;110:693-715.
196. Kandel E.R., Schwartz J.H., Jessen T.M. Principles of neural science. 2000. McGraw-Hill.

197. Armstrong CM. Sodium channels and gating currents. *Physiol Rev*. 1981;61:644-683.
198. HODGKIN AL, HUXLEY AF. A quantitative description of membrane current and its application to conduction and excitation in nerve. *J Physiol*. 1952;117:500-544.
199. Hirschberg B, Rovner A, Lieberman M, Patlak J. Transfer of twelve charges is needed to open skeletal muscle Na+ channels. *J Gen Physiol*. 1995;106:1053-1068.
200. Guy HR, Seetharamulu P. Molecular model of the action potential sodium channel. *Proc Natl Acad Sci U S A*. 1986;83:508-512.
201. Noda M, Shimizu S, Tanabe T, Takai T, Kayano T, Ikeda T, Takahashi H, Nakayama H, Kanaoka Y, Minamino N, . Primary structure of Electrophorus electricus sodium channel deduced from cDNA sequence. *Nature*. 1984;312:121-127.
202. Yang N, Horn R. Evidence for voltage-dependent S4 movement in sodium channels. *Neuron*. 1995;15:213-218.
203. Yang N, George AL, Jr., Horn R. Molecular basis of charge movement in voltage-gated sodium channels. *Neuron*. 1996;16:113-122.
204. Armstrong CM. Na channel inactivation from open and closed states. *Proc Natl Acad Sci U S A*. 2006;103:17991-17996.
205. Vassilev P, Scheuer T, Catterall WA. Inhibition of inactivation of single sodium channels by a site-directed antibody. *Proc Natl Acad Sci U S A*. 1989;86:8147-8151.
206. Vassilev PM, Scheuer T, Catterall WA. Identification of an intracellular peptide segment involved in sodium channel inactivation. *Science*. 1988;241:1658-1661.
207. West JW, Patton DE, Scheuer T, Wang Y, Goldin AL, Catterall WA. A cluster of hydrophobic amino acid residues required for fast

Na(+)-channel inactivation. *Proc Natl Acad Sci U S A*. 1992;89:10910-10914.

208. Filatov GN, Nguyen TP, Kraner SD, Barchi RL. Inactivation and secondary structure in the D4/S4-5 region of the SkM1 sodium channel. *J Gen Physiol*. 1998;111:703-715.
209. Lerche H, Peter W, Fleischhauer R, Pika-Hartlaub U, Malina T, Mitrovic N, Lehmann-Horn F. Role in fast inactivation of the IV/S4-S5 loop of the human muscle Na+ channel probed by cysteine mutagenesis. *J Physiol*. 1997;505 (Pt 2):345-352.
210. McPhee JC, Ragsdale DS, Scheuer T, Catterall WA. A critical role for transmembrane segment IVS6 of the sodium channel alpha subunit in fast inactivation. *J Biol Chem*. 1995;270:12025-12034.
211. McPhee JC, Ragsdale DS, Scheuer T, Catterall WA. A critical role for the S4-S5 intracellular loop in domain IV of the sodium channel alpha-subunit in fast inactivation. *J Biol Chem*. 1998;273:1121-1129.
212. Smith MR, Goldin AL. Interaction between the sodium channel inactivation linker and domain III S4-S5. *Biophys J*. 1997;73:1885-1895.
213. Tang L, Chehab N, Wieland SJ, Kallen RG. Glutamine substitution at alanine1649 in the S4-S5 cytoplasmic loop of domain 4 removes the voltage sensitivity of fast inactivation in the human heart sodium channel. *J Gen Physiol*. 1998;111:639-652.
214. Armstrong CM, Bezanilla F. Inactivation of the sodium channel. II. Gating current experiments. *J Gen Physiol*. 1977;70:567-590.
215. Bezanilla F, Armstrong CM. Inactivation of the sodium channel. I. Sodium current experiments. *J Gen Physiol*. 1977;70:549-566.
216. Aldrich RW, Stevens CF. Inactivation of open and closed sodium channels determined separately. *Cold Spring Harb Symp Quant Biol*. 1983;48 Pt 1:147-153.

217. Bean BP. Sodium channel inactivation in the crayfish giant axon. Must channels open before inactivating? *Biophys J*. 1981;35:595-614.
218. Vilin YY, Fujimoto E, Ruben PC. A single residue differentiates between human cardiac and skeletal muscle Na+ channel slow inactivation. *Biophys J*. 2001;80:2221-2230.
219. Goldin AL. Mechanisms of sodium channel inactivation. *Curr Opin Neurobiol*. 2003;13:284-290.
220. Ong BH, Tomaselli GF, Balser JR. A structural rearrangement in the sodium channel pore linked to slow inactivation and use dependence. *J Gen Physiol*. 2000;116:653-662.
221. Struyk AF, Cannon SC. Slow inactivation does not block the aqueous accessibility to the outer pore of voltage-gated Na channels. *J Gen Physiol*. 2002;120:509-516.
222. Mitrovic N, George AL, Jr., Horn R. Role of domain 4 in sodium channel slow inactivation. *J Gen Physiol*. 2000;115:707-718.
223. O'Reilly JP, Wang SY, Wang GK. Residue-specific effects on slow inactivation at V787 in D2-S6 of Na(v)1.4 sodium channels. *Biophys J*. 2001;81:2100-2111.
224. Hilber K, Sandtner W, Kudlacek O, Glaaser IW, Weisz E, Kyle JW, French RJ, Fozzard HA, Dudley SC, Todt H. The selectivity filter of the voltage-gated sodium channel is involved in channel activation. *J Biol Chem*. 2001;276:27831-27839.
225. Hilber K, Sandtner W, Kudlacek O, Schreiner B, Glaaser I, Schutz W, Fozzard HA, Dudley SC, Todt H. Interaction between fast and ultra-slow inactivation in the voltage-gated sodium channel. Does the inactivation gate stabilize the channel structure? *J Biol Chem*. 2002;277:37105-37115.

226. Conforti L, Tohse N, Sperelakis N. Tetrodotoxin-sensitive sodium current in rat fetal ventricular myocytes--contribution to the plateau phase of action potential. *J Mol Cell Cardiol*. 1993;25:159-173.
227. Zilberter Y, Starmer CF, Starobin J, Grant AO. Late Na channels in cardiac cells: the physiological role of background Na channels. *Biophys J*. 1994;67:153-160.
228. Zaza A, Belardinelli L, Shryock JC. Pathophysiology and pharmacology of the cardiac "late sodium current.". *Pharmacol Ther*. 2008;119:326-339.
229. Brette F, Orchard CH. No apparent requirement for neuronal sodium channels in excitation-contraction coupling in rat ventricular myocytes. *Circ Res*. 2006;98:667-674.

Chapter 2: A Brugada Syndrome mutation (S216L) and its modulation by H558R polymorphism: standard and dynamic characterization.

Stefano Marangoni, Chiara Di Resta, Lucio Barile, Marcella Rocchetti, Riccardo Rizzetto, Elena Sommariva, Carlo Pappone, Maurizio Ferrari, Sara Benedetti and Antonio Zaza.

*equally contributed to the work

Cardiovascular Research,

Submitted for revision.

Abstract

Aim: The Na^+ channel mutation (p.S216L), previously associated to an LQT3 phenotype, and a common polymorphism (p.H558R) were detected in a patient with an intermittent Brugada Syndrome (BS) ECG pattern. The study aimed to assess p.S216L electrical phenotype, its modulation by p.H558R and to identify abnormalities compatible with a mixed BS-LQT3 phenotype. **Methods and results:** the mutation was expressed alone (S216L channels), or in combination with the polymorphism (S216L-H558R channels), in a mammalian cell line (TSA201). Functional analysis included standard voltage-clamp and dynamic clamp with endo- and epicardial action-potential waveforms. Expression of S216L channels was associated with a 60% reduction in maximum Na^+ current (I_{Na}) density, attributable to protein misfolding (rescued by mexiletine pretreatment), and moderate slowing of inactivation. The persistent component of I_{Na} (I_{NaL}) was unchanged. Under dynamic conditions, mutant I_{Na} displayed a significant "resurgent" component during late repolarization. I_{Na} density partially recovered in S216L-H558R channels, but I_{Na} inactivation and its recovery were further delayed. This was associated with increased I_{Na} density during endocardial (but not epicardial) repolarization and abolition of the resurgent component. **Conclusions:** the BS pattern of p.S216L might result from a decrease in I_{Na} density, which masked gating abnormalities that might otherwise result in a LQT phenotype. The p.H558R polymorphism decreased p.S216L expressivity, partly by lessening p.S216L effects and partly through the induction of further gating abnormalities suitable to blunt p.S216L effects during repolarization.

Introduction

Brugada syndrome (BS) is an inherited autosomal dominant cardiac channelopathy, firstly described in 1992 and characterized by an incomplete penetrance[1]. BS is characterized by cardiogenic syncope in otherwise healthy subjects and a typical electrocardiographic (ECG) pattern with ST-segment elevation in the right precordial leads (V1-V3) and right bundle branch block[2]. In 18-30 % of BS patients, the clinical phenotype is associated with mutations in the *SCN5A* gene, encoding the α subunit of the voltage dependent cardiac sodium channel ($Na_v1.5$)[3]. Also mutations to many other genes have been related to BS[4-9]. In terms of arrhythmogenic mechanisms, BS was initially interpreted as a repolarization disorder[10]; later on, mechanisms based on an impulse propagation disorder were also proposed[11;12]. Moreover, changes in myocardial structure, which may provide a pathological substrate to functional abnormalities, are present in many BS patients[13]. Such a multiplicity of interpretations suggests that BS may be a complex disease, whose pathogenesis is still incompletely understood.

The p.S216L mutation is located in domain I of $Na_v1.5$ channel on the extracellular loop connecting the S3-S4 transmembrane spans. This mutation, detected *post mortem* in a case of sudden infant death syndrome and expressed in TSA201 cells[14], was found to enhanced the persistent component of I_{Na} (I_{NaL}). Accordingly, p.S216L was tentatively identified as a mutation prolonging repolarization by gain of function of Na^+ channels (LQT3)[14].

The *SCN5A* polymorphism p.H558R has been found to segregate differentially in patients subgroups, in relation to the phenotypic expressivity of several coexisting arrhythmogenic mutations[15-19], including those with a BS phenotype[20;21]. Accordingly, this polymorphism is suspected to modulate the expressivity of arrhythmogenic genotypes.

The present work reports of a BS case carrying the p.S216L mutation and the p.H558R polymorphism. Mutant Na^+ channel function, and its modulation by the p.H558R polymorphism, were evaluated by expression in TSA201 cells in the attempt to reconcile its BS phenotype with the LQT3 one previously reported for the same mutant[14]. In keeping with the view that standard voltage-clamp protocols may overlook the functional consequences of subtle gating abnormalities[22], the analysis also included dynamic voltage-clamp experiments. In the following presentation, constructs containing the p.S216L mutation alone, or in combination with the p.H558R polymorphism, are referred to as "S216L channels" and "S216L-H558R channels", respectively.

Methods

Clinical and genetic characterization

The proband and its relatives underwent routine cardiological examination, including standard 12-leads ECG, 24 hours Holter monitoring and echocardiogram. Provocative flecainide test and programmed electrical stimulation were performed in *SCN5A* mutation carriers as detailed in Supplement.

Written informed consent for genetic analysis approved by our Institutional Health Department was signed from all patients. According to national guidelines, approval from the local Ethics Committee is not necessary for diagnostic testing. The investigation conformed with the principles outlined in the Declaration of Helsinki. Genomic DNA was extracted from peripheral blood and *SCN5A* coding sequence was analysed by DHPLC and direct sequencing as detailed in Supplement.

Site-directed mutagenesis and expression system

SCN5A constructs used in functional analysis were obtained by site-directed mutagenesis using the QuickChange Kit XL (Stratagene) on the full-length human hH1 cDNA (ref.seq. M77235)[23], amplified from pSP64T-hH1 plasmid (kindly provided by A.L. George Jr., Vanderbilt University, Nashville, TN) and cloned into the expression vector pcDNA3.1 (Invitrogen). The mutation p.S216L (c.647C>T) was introduced alone and in combination with the p.H558R

polymorphism (c.1673A>G), to obtain p.S216L and p.S216L-p.H558R constructs respectively. All constructs were sequenced to verify the presence of the mutations and rule out spurious substitutions.

TSA201 cells were transfected with Lipofectamine 2000 (Invitrogen) according to manufacturer instructions. The following constructs were co-transfected in equal amounts (0.5 µg/ml): 1) a bicistronic plasmid encoding for green fluorescent protein and the human β1 subunit (pCGI-IRES-hβ1, kindly provided by J.R. Balser, Vanderbilt University, Nashville, TN); 2) wild-type (WT), or p.S216L or p.S216L-p.H558R plasmids. In order to increase I_{Na} density, in dynamic clamp experiments the amount of transfected plasmid was doubled (1 µg/ml) and incubation was maintained overnight.

Functional characterization

Whole-cell patch-clamp experiments were carried out 48 hours after transfection on green fluorescent cells exhibiting peak I_{Na} larger than 1.5 nA, to minimize potential contamination by endogenous currents[24]. Pipettes solution contained (in mmol/L): 10 NaF, 110 CsF, 20 CsCl, 2 EGTA and 10 HEPES (pH 7.35 with CsOH); osmolarity was adjusted with sucrose. Pipette resistance was 0.8-1.4 MΩ. Bath solution contained (in mmol/L): 145 NaCl, 4 KCl, 1.8 $CaCl_2$, 1 $MgCl_2$, 10 HEPES and 10 glucose (pH 7.35 with NaOH). Cells were superfused by a manifold allowing fast solution switch. Temperature, measured at the manifold tip and maintained constant by a

thermostatic circuit, was 26°C in standard voltage-clamp experiments and 37 °C in dynamic ones. Cell membrane capacitance and series resistance were compensated by 85% to 95%; the estimated voltage error was <3 mV in all cases. In standard voltage-clamp experiments squared voltage pulses (steps) were applied at intervals of 5 sec according to protocols specific for the measured parameter, as shown in the relevant figures. I_{NaL} was identified, by digital subtraction, as the current sensitive to tetrodotoxin (TTX, 30 μmol/L). In dynamic voltage-clamp experiments membrane potential was driven at a steady cycle length of 1 s by human endocardial or epicardial action-potential waveforms (EndoAP and EpiAP respectively), generated by a numerical model of human cardiac action potential[25]. I_{Na} was identified as the TTX-sensitive current. For normalization purposes, in each cell, dynamic voltage-clamp was preceded by evaluation of maximal I_{Na} density (I_{max}) by a standard voltage protocol.

To assess whether the changes in I_{Na} were due to protein trafficking/folding abnormalities, immediately after transfection cells were incubated with mexiletine (400 μmol/L), a Na^+ channel blocker previously shown to rescue the phenotype of trafficking-deficient Na^+ channels[26]. Mexiletine was washed out 30 min before recordings.

Data analysis

Current density (pA/pF) was calculated by dividing current amplitude by membrane capacitance. Mean current during a given time-interval was calculated from current (I) recordings as

$$\frac{\int I \bullet dt}{\Delta t}$$

where Δt is the integration interval.

Standard voltage-clamp recordings were analyzed as usual (see on-line supplement), by a dedicated software (Axon pCLAMP 8.0); I_{NaL} was measured as the TTX-sensitive current between 190 and 200 ms after pulse onset. In dynamic voltage-clamp experiments TTX-sensitive current was expressed in terms of absolute density (I_{Na}) and after normalization to I_{max} (I_{Na} = I_{Na} /I_{max}). Normalization aimed to evaluate the functional impact of changes in gating kinetics after removing the effect of changes in absolute current density. I_{Na} and I_{Na} were measured during 4 action potential (AP) phases: the AP upstroke ($I_{Na}P_0$), the AP notch ($I_{Na}P_1$), phase 2 (between AP dome and APD_{50}, $I_{Na}P_2$), during phase 3 (between APD_{50} and APD_{90}, $I_{Na}P_3$) (see Fig. 2.4 and 2.5). Whereas $I_{Na}P_0$ was measured as its peak value, in the other phases I_{Na} was quantified by its mean value; in addition, time to peak (TTP) was measured for $I_{Na}P_0$.

Statistical analysis

Differences between means were compared by the unpaired Student *t* test or ANOVA as appropriate. In text and figures data are presented as mean±SEM; statistical significance was defined as $p<0.05$ (*NS*, not significant).

Results

Case report: clinical and genetic profile

A Caucasian 10-years old male (proband) was referred to the arrhythmology unit for palpitations (at rest, more frequent after meals); his clinical history did not include syncope or other symptoms suggesting hemodynamically significant arrhythmias. ECG at admission showed sinus rhythm at 75 bpm, PR 160 ms, QRS 93ms, right bundle branch block with ST segment elevation of 2 mm in lead V1 and 4.5 mm in lead V2 with negative T-waves in leads V1 and V2, QTc 460 ms. Proband's ECG abnormalities are compatible with the Type 1 BS pattern (Fig. 2.1A). During hospitalization, the BS pattern proved to be intermittent, the ECG periodically reversing to normality without identifiable reasons. Echocardiography showed absence of structural cardiac disease. At the time of programmed electrical stimulation the patient was displaying Type 1 BS pattern. Ventricular fibrillation could not be induced with up to 3 extrastimuli delivered to the right ventricular apex and outflow tract. Proband's mother (age 37 yrs) was healthy and had an entirely normal ECG (sinus rate 62 bpm, PR 138 ms, QRS 93 ms, QTc 430 ms, Fig. 2.1A); she underwent a provocative test with flecainide, which was negative. Proband's father (age 39 yrs) was also healthy and had a normal ECG. Family history was negative for events that could be related to arrhythmias.

Analysis of the coding region of proband's *SCN5A* gene, comprehensive of intron-exon boundaries, identified a heterozygous missense mutation in exon 6. This consisted of a c.647C>T nucleotide

variation (Fig. 2.1B), leading to the replacement of Serine (S) to Leucine (L) at protein residue 216 (p.S216L). Sequence analysis also revealed the presence of the common polymorphism p.H558R in *SCN5A* exon 12, involving a substitution of histidine (H) with arginine (R) at position 558 in the intracellular loop connecting domains I and II of the channel protein. The reported frequency of this variant in the general population is between 19% and 24%[27]. Genetic screening of the family revealed that proband's mother was also a carrier of both the p.S216L mutation and the p.H558R polymorphism.

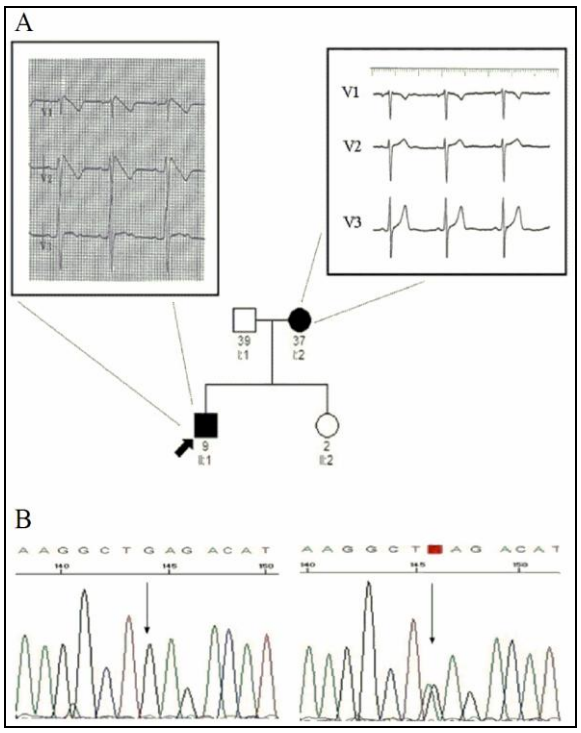

Figure 2.1. ECG phenotype and genotype. **A**, Family pedigree and ECG tracings of the proband (arrow) and of his mother. **B**, Electropherograms of *SCN5A* gene sequence (WT at left); the arrow indicates the c.647C>T substitution leading to the p.S216L mutation.

Functional characterization

To evaluate the electrophysiological consequences of the p.S216L mutation alone, and associated with the p.H558R polymorphism, three TSA201 cells groups were transfected with WT, S216L and S216L-H558R constructs respectively. In the following description, the functional phenotype of mutant channels is expressed relative to that of WT ones.

Standard voltage-clamp analysis

The first set of experiments was devoted to traditional voltage-clamp analysis, whose results are summarized in Table 1. Peak current/voltage (I/V) relationships of S216L channels showed a decrease of I_{Na} density at all membrane potentials to approximately 40% of the WT value. The reduction of I_{Na} density was partially reversed (to approx 60% of WT) in S216L-H558R channels (Fig. 2.2A and B). Density of the persistent component (I_{NaL}) also differed between the three channel types. However, its changes largely mirrored the changes in total I_{Na}; therefore, the I_{NaL}/I_{Na} ratio was roughly similar for the three constructs (Fig. 2.2C); if anything, the I_{NaL}/I_{Na} ratio was slightly decrease in S216L channels. Therefore, the increase in I_{NaL} density previously described[14], was absent in both S216L and S216L-H558R channels.

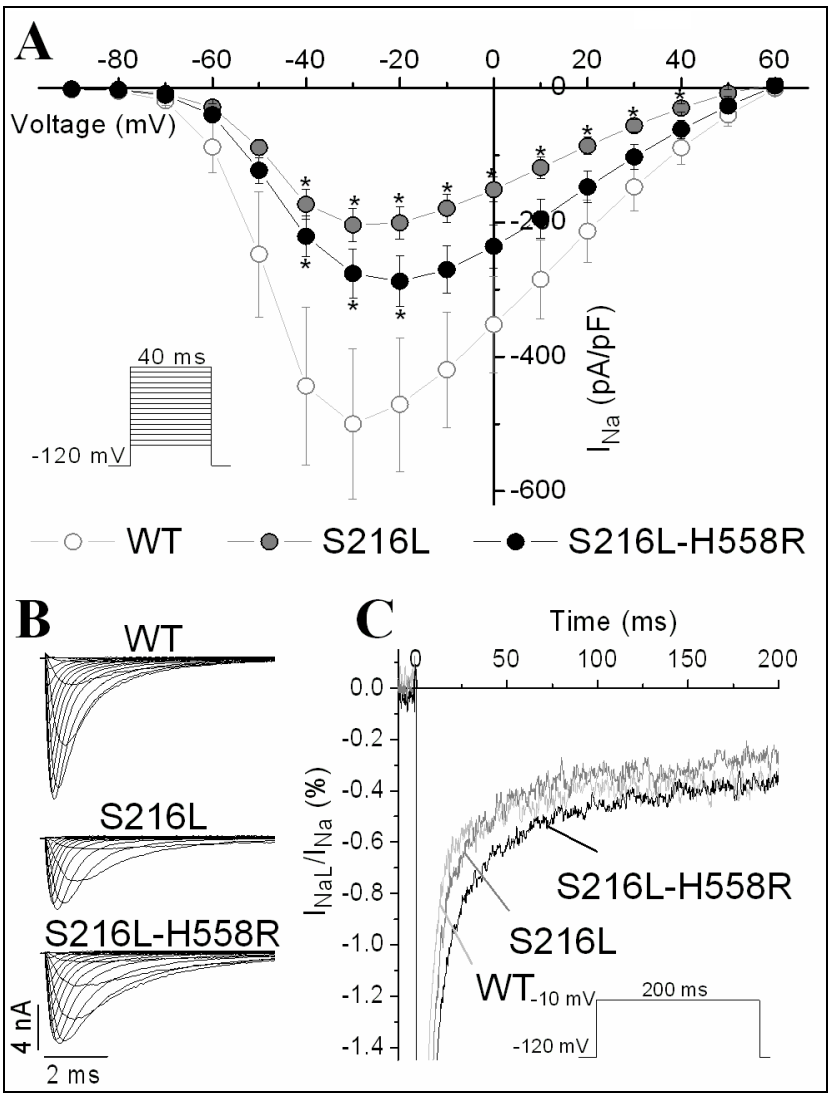

Figure 2.2. Standard voltage-clamp analysis - Peak I_{Na} I/V relations. **A**, Peak I_{Na} I/V relations for WT, S216L and S216L-H558R channels. **B**, Representative I_{Na} recordings for the three channels. **C**, Magnified recordings of TTX-sensitive current showing the persistent component (I_{NaL}) (statistical analysis is reported in Table 1). (*p<0.05 *vs* WT)

The voltage-dependency of steady-state activation (Fig. 2.3A) was normal in S216L channels, but it was slightly shallower in S216L-H558R channels (larger slope factor); no significant changes were observed in mid-activation potential ($V_{1/2}$). The voltage-dependency of steady-state availability was identical in the three channel constructs (Fig. 2.3B). The overlap between activation and availability curves, suitable to support I_{Na} "window" current, was unchanged in S216L channels and slightly diminished in S216L-H558R ones.

Fast inactivation was slightly slower in S216L channels and only at very negative potentials. On the other hand, both inactivation components were significantly delayed in S216L-H558R channels over a wider range of potentials (negative to 0 mV) (Fig. 2.3C). The same pattern was observed for the recovery from inactivation, which was slowest in S216L-H558R channels, with S216L channels displaying intermediate kinetics (Fig. 2.3D).

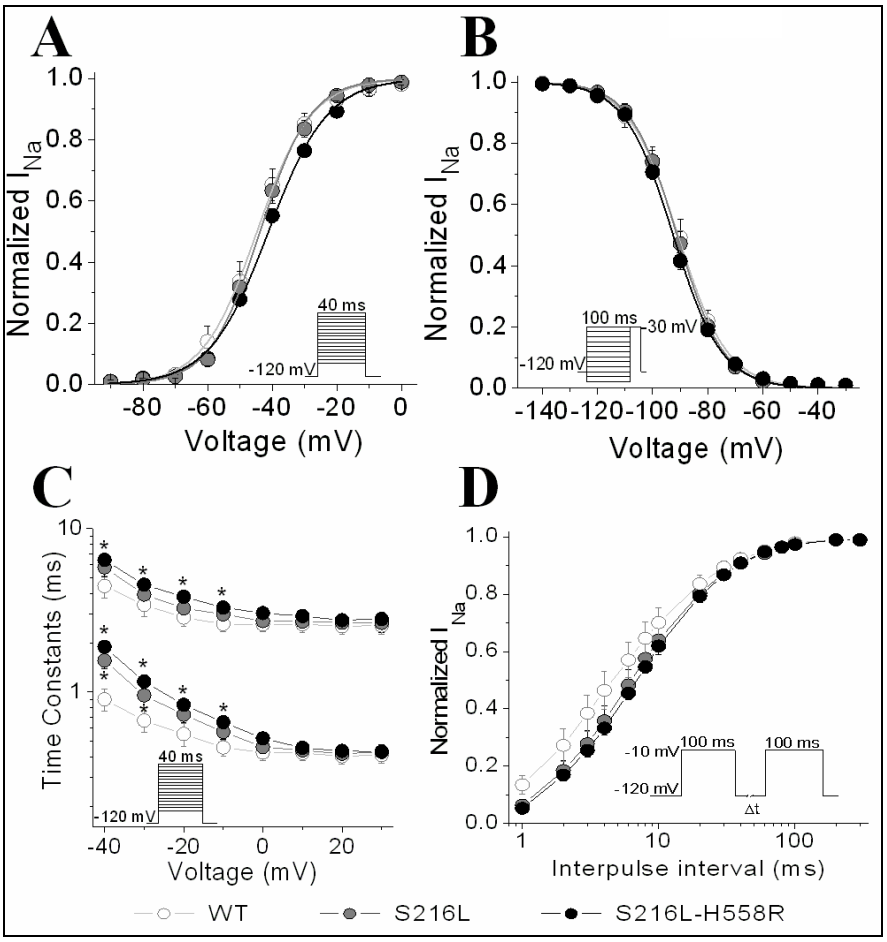

Figure 2.3. Standard Voltage-clamp analysis - I_{Na} gating voltage-dependency. **A**, Steady-state activation. **B**, Steady-state inactivation (availability). In panels A and B data points were fitted with Boltzmann functions (solid lines). **C**, Voltage-dependency of inactivation time constants. Lower and upper curve groups represent fast and slow time constants respectively for the three channel constructs. **D**, Time course of recovery from inactivation. Voltage protocols are shown in the inset of each panel. Statistical analysis is reported in Table 1. (*p<0.05 *vs* WT)

Table 2.1. Standard analysis

	WT	S216L	S216L-H558R
Voltage Dependence of Activation	*n*=16	*n*=16	*n*=46
$V_{1/2}$ (mV)	-44 ± 2	-43 ± 1	-41 ± 1
s (mV)	6.5 ± 0.7	7.2 ± 0.4	8.5 ± 0.2*#
Voltage Dependence of Inactivation	*n*=13	*n*=14	*n*=27
$V_{1/2}$ (mV)	-92 ± 2	-91 ± 1	-92 ± 1
s (mV)	7.6 ± 0.6	7.8 ± 0.4	7.8 ± 0.3
Recovery From Inactivation	*n*=12	*n*=11	*n*=27
τ_f (ms)	4.8 ± 0.8	5.3 ± 0.8	6.4 ± 0.4*
τ_s (ms)	26 ± 4	28 ± 4	40 ± 4*
A_f/A_s (ms)	6 ± 1	2.5 ± 0.6*	3.5 ± 0.5*
Persistent Na^+ Current	*n*=11	*n*=12	*n*=24
I_{NaL}/I_{Na} (%)	0.39 ± 0.08	0.25 ± 0.04	0.42 ± 0.07

*p<0.05 *vs* WT; #p<0.05 *vs* S216L

Dynamic clamp analysis

This set of experiments aimed to evaluate the impact of the mutation on I_{Na} expressed during actual endocardial and epicardial action potentials. In this setting, recordings could be performed at physiological temperature, an important factor in evaluating the effect of changes in gating kinetics. The average of individual records obtained in each experimental group are shown in figure 2.4 for absolute current density (I_{Na}) and figure 2.5 for normalized current (I_{Na}).

In EpiAP, peak I_{Na} during the upstroke was minimal in S216L and intermediate in S216L-H558R channels (Fig. 2.4A); this difference was abolished by normalization (Fig. 2.5A) indicating its consistency with changes in I_{max}. On the other hand, in EndoAP, peak I_{Na} was similar for WT and mutant constructs (Fig. 2.4B); thus, when the normalized current was considered (Fig. 2.5B) the amplitude rank was actually inverted. For both action potential waveforms, TTP was larger in S216L and S216L-H558R channels than in WT ones (Table 2). It should be stressed that changes in TTP measured from individual cells, are not well represented by the average records shown in figures 2.4 and 2.5, whose time-course was slightly altered by the averaging procedure.

In EpiAP, during early repolarization I_{Na} was minimal in S216L and intermediate in S216L-H558R channels (Fig. 2.4A); this difference was abolished by normalization (Fig. 2.5A) as expected from the differences in I_{max}. This was not true in EndoAP, where the

I_{Na} reduction observed for S216L channels was almost entirely rescued in S216L-H558R ones. The impact of changes in gating kinetics during repolarization are highlighted by the analysis of normalized currents (I_{Na}, Fig. 2.5). In both action potential waveforms, S216L I_{Na} was similar to WT during early repolarization but, particularly in the EpiAP, it displayed a "resurgent" I_{Na} during phase 3 (Fig. 2.5, quantified in Table 2 as $I_{Na}P_3/I_{Na}P_2$ ratio). In S216L-H558R channels, I_{Na} was markedly enhanced during early repolarization of EndoAP, but not EpiAP. Independently of the waveform type, the resurgent component observed in S216L channels was completely suppressed in S216L-H558R ones (Fig. 2.5). This qualitative description is substantiated by the quantitative differences in $I_{Na}P_1$, $I_{Na}P_2$ and $I_{Na}P_3$ average values, reported in Table 2.

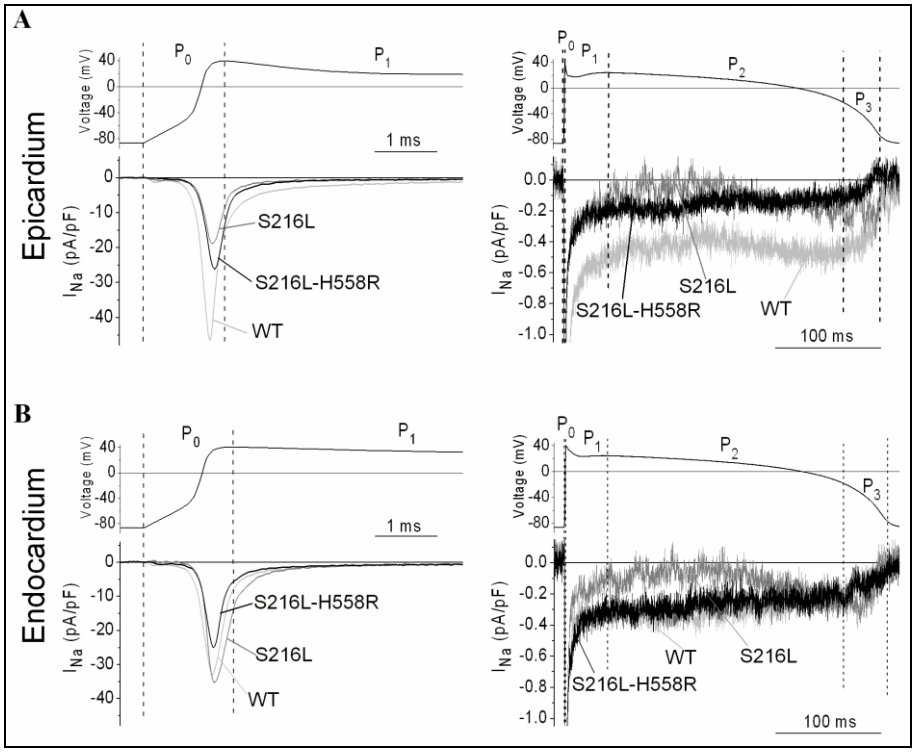

Figure 2.4. Dynamic clamp analysis – Absolute I_{Na} density. Action potential waveforms (upper panel) and average recordings of absolute I_{Na} (TTX-sensitive current) during the action potential upstroke (left) and repolarization (right). **A** and **B**, epicardial action potential. **C** and **D**, endocardial action potential. Dashed lines denote the four action potential phases (P_0-P_3) during which I_{Na} was measured to obtain peak or mean values reported in Table 2.

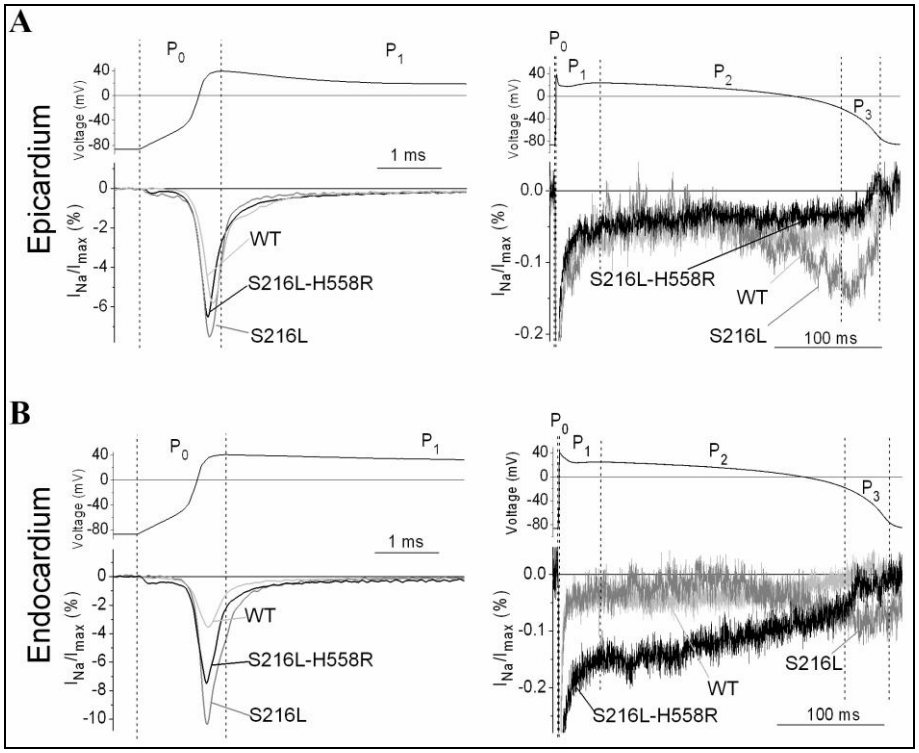

Figure 2.5. Dynamic clamp analysis – Normalized I_{Na} density. I_{Na} was normalized to maximal I_{Na} (I_{max}) obtained within the same cell from the peak I_{Na} I/V relation (not shown). Panels and symbols as in figure 2.4.

Table 2. Dynamic clamp analysis

	WT	S216L	S216L-H558R
Epicardial properties			
TTP (ms)	0.29 ± 0.02	0.32 ± 0.02	0.36 ± 0.02*
Current Density (pA/pF)			
$I_{Na}P_0$	-46 ± 9	-20 ± 4*	-26 ± 9
$I_{Na}P_1$	-0.8 ± 0.2	-0.28 ± 0.07	-0.38 ± 0.08
$I_{Na}P_2$	-0.5 ± 0.1	-0.11 ± 0.05*	-0.15 ± 0.04*
$I_{Na}P_3$	-0.5 ± 0.2	-0.3 ± 0.1	-0.10 ± 0.03
$I_{Na}P_3/I_{Na}P_2$	1.3 ± 0.8	1.8 ± 0.5	0.9 ± 0.2
Normalization to I_{max} (%)			
$I_{Na}P_0$	5 ± 1	8 ± 1	6 ± 1
$I_{Na}P_1$	0.08 ± 0.01	0.14 ± 0.03	0.13 ± 0.03
$I_{Na}P_2$	0.06 ± 0.02	0.09 ± 0.04	0.07 ± 0.02
$I_{Na}P_3$	0.034 ± 0.008	0.10 ± 0.03	0.024 ± 0.007#
$I_{Na}P_3/I_{Na}P_2$	0.6 ± 0.1	1.9 ± 0.5*	0.6 ± 0.2#
n	8	8	9
Endocardial properties			
TTP (ms)	0.29 ± 0.03	0.35 ± 0.03	0.34 ± 0.01
Current Density (pA/pF)			
$I_{Na}P_0$	-33 ± 8	-35 ± 9	-25 ± 5
$I_{Na}P_1$	-0.42 ± 0.08	-0.38 ± 0.09	-0.5 ± 0.1
$I_{Na}P_2$	-0.27 ± 0.09	-0.14 ± 0.06	-0.29 ± 0.07
$I_{Na}P_3$	-0.15 ± 0.06	-0.3 ± 0.1	-0.14 ± 0.04
$I_{Na}P_3/I_{Na}P_2$	0.6 ± 0.2	1.5 ± 0.6	0.5 ± 0.1#
Normalization to I_{max} (%)			
$I_{Na}P_0$	3.4 ± 0.7	9 ± 2*	7 ± 2*
$I_{Na}P_1$	0.06 ± 0.01	0.08 ± 0.01	0.21 ± 0.08*
$I_{Na}P_2$	0.038 ± 0.009	0.030 ± 0.009	0.13 ± 0.04*#
$I_{Na}P_3$	0.02 ± 0.003	0.06 ± 0.03	0.052 ± 0.007*
$I_{Na}P_3/I_{Na}P_2$	1.0 ± 0.4	1.2 ± 0.4	0.7 ± 0.2#
n	8	6	6

*p<0.05 *vs* WT; #p<0.05 *vs* S216L

Rescue of channel expression

This set of experiments tested the hypothesis that protein trafficking or folding abnormalities contributed to the changes in I_{Na} density between the three constructs. I_{Na} density was evaluated by measuring peak I_{Na} I/V relations by the standard voltage-clamp protocol. Incubation with mexiletine did not change maximal I_{Na} density in cells transfected with WT channels, but significantly increased it in both S216L and S216L-H558R transfected cells (Fig. 2.6), thus leading to almost complete rescue of mutation effects.

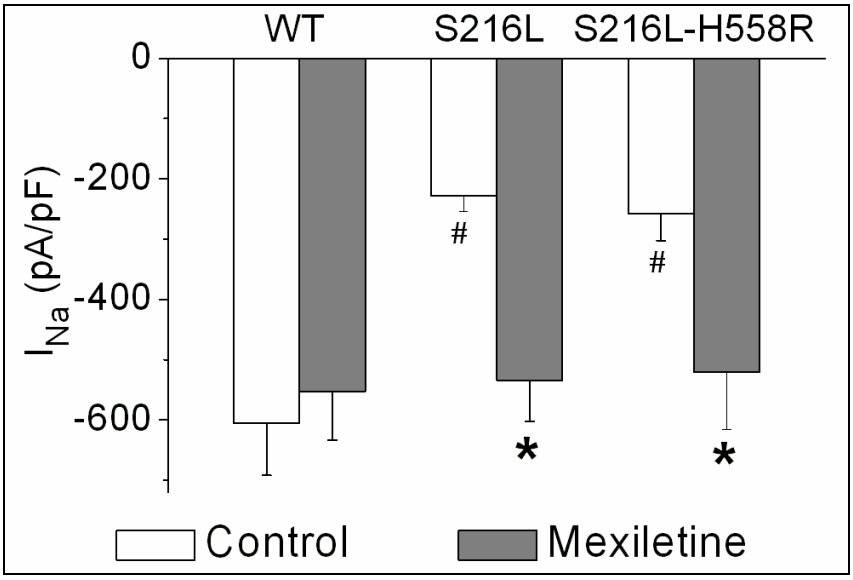

Figure 2.6. Phenotype rescue by mexiletine. Statistics of peak I_{Na} density for the three channel constructs in control cells (white bars) and in cells incubated after transfection with mexiletine 400 µmol/L (grey bars). I_{Na} measurements were performed after mexiletine wash-out (*p<0.05 *vs* control; #p<0.05 *vs* WT; $n \geq 7$).

Discussion

The main effects of the p.S216L mutation, as detected by the standard voltage-clamp approach, included: 1) a substantial decrease in I_{Na} density, a phenotype rescued by incubation with mexiletine; 2) a moderate slowing of I_{Na} inactivation at negative potentials, which did not affect the I_{NaL}/I_{Na} ratio. Coexpression of the p.H558R polymorphism partially reversed the mutation's effects on I_{Na} density, but it delayed inactivation and its recovery. The I_{Na} "window" was unmodified by the p.S216L mutation alone and tended to be reduced by the p.S216L-p.H558R genotype.

Decreased I_{Na} density might result from a change in channel gating properties, or from a decrease in the number of functional channels expressed in the membrane. It has been reported that binding of mexiletine to trafficking-deficient mutant Na^+ channels restores their membrane expression[26], probably through thermodynamic stabilization of the properly folded structure. Thus, the rescue of mutant I_{Na} by incubation with mexiletine, suggests misfolding of the mutant channel as the cause of reduced current density.

Mutation-induced changes in absolute I_{Na} during the action potential (dynamic voltage-clamp experiments) were dominated by the overall decrease in I_{Na} density. The latter was partially compensated by p.H558R coexpression in endocardial action potentials (Fig. 2.4B), but not in epicardial ones (Fig. 2.4A), thus suggesting that gating properties sensitive to action potential contour contributed to the rescuing effect of p.H558R. Compensation of

differences in absolute I_{Na} density by normalization revealed further changes of functional significance in current profile (Fig. 2.5). Notably, these changes might have been overlooked by the standard voltage-clamp approach, which detected gating abnormalities of small magnitude and uncertain functional significance. The relationship between gating features measured with the standard voltage-clamp approach and dynamic I_{Na} profiles deserves to be analyzed.

TTP during the action potential upstroke varied according to inactivation slowing measured by standard voltage-clamp (S216L and S216L-H588R>WT). When the contribution of changes in channel density was eliminated by normalization, peak upstroke current was similarly related to inactivation slowing (S216L and S216L-H588R>WT). Slower inactivation is expected to increase peak current amplitude and prolong TTP; therefore, differences in TTP and peak $I_{Na}P_0$ among the three genotypes might be mechanistically related to those in inactivation rate.

Independently of the action potential type, S216L I_{Na} displayed a distinctive "resurgent" component during terminal repolarization, which was completely suppressed by p.H558R coexpression. If of sufficient magnitude this component would facilitate early afterpotentials, thus supporting an arrhythmogenetic mechanism more commonly associated with LQTS than with BS. A resurgent current behavior during fast repolarization is generally explained as recovery of inactivation of a small proportion of channels and their immediate reactivation[28]. Whereas none of the kinetic features detected by

standard voltage-clamp is apparently suitable to explain why this component was increased in S216L channels, a slower recovery from inactivation might account for its suppression in S216L-H558R ones.

The main peculiarity of S216L-H558R channels was an increase of I_{Na} during early endocardial repolarization (Fig. 2.5B). Analysis of absolute I_{Na} tracings shows that this change compensated the reduction in I_{Na} density caused by the p.S216L mutation, potentially contributing to reduce its expressivity at endocardial level (Fig. 2.4B). When cells were clamped with the epicardial action potential instead, the increase in I_{Na} was not observed. The two action potential waveforms mainly differ by the time course of membrane potential during early repolarization, which may thus account for the differential response to p.H558R coexpression. This observation highlights the sensitivity of the functional expression of gating abnormalities to membrane potential course and underscores the importance of dynamic analysis in assessing the function of mutant channels.

Relationship with the ECG phenotype

In its classical description, the BS ECG pattern consisted of a repolarization abnormality, with substantially preserved impulse propagation. The I_{Na} abnormality found to be associated with BS and best suited to account for this pattern, was an acceleration of fast inactivation, without major changes in peak I_{Na} density[10;29].

Nevertheless, the BS ECG pattern has also been found in association with mutations affecting mainly peak I_{Na} density and interpreted by numerical simulations as a large delay in transmural propagation[11].

The p.S216L mutant was characterized by a significant reduction of I_{Na} density and its gating features do not predict selective I_{Na} reduction during early repolarization; thus, the observed p.S216L phenotype is more likely to cause BS through conduction slowing than by altering repolarization. The absence of overt conduction disturbance in proband's ECG (normal PQ and QRS intervals) might result from 1) partial recovery of peak I_{Na} amplitude because of inactivation slowing and/or 2) partial rescue of I_{Na} density and the additional gating modifications afforded by the p.H558R polymorphism. Furthermore, inconsistency or absence of ECG signs of conduction slowing could be a manifestation of the large functional redundancy of I_{Na} expression. When the decrease in I_{Na} density was compensated by normalization, S216L channels revealed the tendency to generate a significant resurgent component. This property suggests that, if I_{Na} density were restored by recovery of channel trafficking, the p.S216L mutation might be associated to perturbations of terminal repolarization, an abnormality typical of long QT (LQT) phenotypes. Mixed BS-LQT3 phenotypes have been described for several *SCN5A* mutations[30-32]; however, these mutations invariably caused enhancement of the persistent I_{Na} component (I_{NaL}). The present findings suggest that gating abnormalities related to BS might also affect late repolarization, independently of I_{NaL} enhancement.

Proband's genotype included the p.H558R polymorphism which, in principle, might have contributed to the ECG abnormality. Our observations indicate that p.H558R coexpression may partially compensate the effect of the p.S216L mutation by simultaneously increasing I_{Na} density and causing subtle changes in gating, which tend to offset mutation-induced I_{Na} abnormalities under dynamic conditions. Thus, p.H558R coexpression may limit p.S216L expressivity, which was indeed mild in the proband (intermittent BS pattern) and null in his mother. The observation that p.H588R coexpression further delayed recovery from inactivation (Fig. 2.3D and Table 1), an apparent phenotype aggravation, might look at odd with this interpretation. However, under dynamic conditions delayed recovery might be responsible for eliminating the I_{Na} resurgent component, a potentially arrhythmogenic feature of p.S216L.

Comparison with previous studies

The electrophysiological profile of the p.S216L mutation, as detected by standard voltage-clamp measurements, sharply differs from that previously reported[14]. Whereas in the previous report the observation of a marked I_{NaL} enhancement led to postulate a LQT3 phenotype, in the present experiments the mutation proportionally reduced I_{NaL} and peak I_{Na} densities, as expected by defective channel expression. This discrepancy could not be attributed to differences in the expression system, vectors and recording conditions, which were

similar between the two studies. Consistent with a lack of significant I_{NaL} enhancement, proband's QTc was normal in the present case; the ECG was unfortunately unavailable in the previous report, which concerned a case of sudden death in a newborn[14]. In the attempt to resolve the discrepancy, we postulated that the present experimental conditions might be somehow inadequate to disclose I_{NaL} enhancement. However, when tested in the same experimental setting, the LQT3 prototype mutation pK1505_Q1507del (ΔKPQ), produced the expected I_{NaL} enhancement (supplementary results).

Previous studies have postulated a role of the p.H558R polymorphism in the modulation of the phenotype of several SCN5A arrhythmogenic mutations. The common observation of a higher p.H558R prevalence in SCN5A mutation carriers has been variably interpreted. Whereas some authors interpreted p.H558R as a risk factor[18;20;21], others viewed it as a protective factor, maintained by positive selection in a high risk population[19]. The present findings are consistent with previous ones in which p.H558R expression was found to rescue gating and trafficking abnormalities induced by various mutations[15-17]. This supports the view that p.H558R polymorphism has been evolutionarily selected for its protective effect.

The observation that a single genetic variant (p.H558R) may compensate diverse gating abnormalities, caused by different mutations, is puzzling and the underlying mechanism is unknown. In the present case, the p.S216L mutation and p.H558R polymorphism affected the same allele, as in previous instances of rescue of gating

abnormalities[15]. Rescue of channel trafficking, also observed in the present study, has been previously reported to occur also when mutation and polymorphism affected different alleles[17]. Therefore, both cis and trans modulation mechanisms may be involved in the protective effect of p.H558R.

Study limitations

Under physiological conditions membrane current and potential mutually interact in a closed feed-back loop. Under dynamic clamp conditions changes in current cannot feed-back to determine potential course, which is fixed (open loop). Therefore, prediction of action potential changes (i.e. the electrical phenotype) from the mutation-induced changes in I_{Na} is somewhat arbitrary. Nevertheless, this technique allows to analyze the actual I_{Na} behavior during dynamic changes in membrane potential at physiological temperature. As neither of these conditions apply to standard Voltage-clamp, dynamic-clamp can help in disclosing features of mutant currents of potential importance in cardiac electrical activity. Also, caution should be used when translating data obtained from *in vitro* functional studies to the clinical phenotype, since these do not take into account all possible differences in the genetic background. Moreover only α- and β1-subunits were expressed in TSA201 cells, whereas additional factors which could modulate I_{Na} may be present in native myocytes[33].

Conclusions

The association between the p.S216L mutation and the BS phenotype may be primarily accounted for by a decrease in I_{Na} density, which leads to postulate the "conduction abnormality"[34] as the most likely interpretative model. The decrease in I_{Na} density masks gating abnormalities, other than I_{NaL} enhancement, that might otherwise result in a LQT phenotype.

Coexpression of the p.H558R polymorphism is likely to decrease p.S216L expressivity: this occurs partly through reversal of p.S216L effects and partly because of the induction of further abnormalities suitable to blunt p.S216L effects during repolarization (dynamic conditions).

The same gating abnormalities may differentially affect the I_{Na} profile during epicardial and endocardial action potentials.

Funding: This work was supported by PRIN 2007 [to Dr. A. Zaza], and grants from Medtronic Italy [to Dr. M. Ferrari] and the Italian Istituto Superiore di Sanità [ISS-526D/55 to Dr. C. Pappone].

Acknowledgements: We thank Dr. Pasquale Vergara for help with clinical data collection and interpretation. We are indebted to Dr. A.L. George and Dr. J.R. Balser for pSP64T and hb/pirGFP constructs.

Conflict of Interest: None.

Supplement Material

Methods

Clinical and Genetic characterization

The proband and its relatives underwent routine cardiological examination, including standard 12-leads ECG, 24 hours Holter monitoring and echocardiogram. Provocative flecainide test and programmed electrical stimulation were performed in *SCN5A* mutation carriers. Programmed electrical stimulation was performed to evaluate sinus- and atrio-ventricular node function and atrial and ventricular inducibility by premature electrical stimulation. The latter included one to three extrastimuli at right ventricular apex and outflow tract, applied during pacing at cycle lengths of 500 and 400 ms. Patients were considered as "inducible" when presenting one the following: i. nonsustained but syncopal ventricular tachycardia; ii. sustained ventricular tachycardia (≥ 30 s or requiring electric interruption for hemodynamic instability); iii. ventricular fibrillation.

Written informed consent for genetic analysis approved by our Institutional Health Department was signed from all patients. According to national guidelines, approval from the local Ethics Committee is not necessary for diagnostic testing. The investigation conformed with the principles outlined in the Declaration of Helsinki. Genomic DNA was extracted from peripheral blood and *SCN5A*

coding sequence was analysed by Denaturing High Performance Liquid Chromatography and direct sequencing. Genomic DNA was extracted with the Maxwell®16 System (Promega) and all *SCN5A*-coding exons were amplified with primers in the intronic flanking region by polymerase chain reaction (PCR). Primers and PCR conditions are available on request. Mutation analysis has been performed using DHPLC (Wave system 4500 HT [Transgenomic]) and direct automated DNA sequencing with the ABI 3730 automatic DNA Sequencer (Applied Biosystems).

Site-Directed Mutagenesis and expression system

SCN5A constructs to be used in functional analysis were obtained by site-directed mutagenesis. The latter was performed by the QuickChange XL (Stratagene) kit on the full-length human hH1 cDNA (ref.seq. M77235)[23], amplified from pSP64T-hH1 plasmid (kindly provided by A.L. George Jr. Vanderbilt University, Nashville, TN) and cloned into the expression vector pcDNA3.1 (Invitrogen). The mutation p.S216L (c.647 C>T) was introduced alone and in combination with the p.H558R polymorphism (c.1673A>G), to obtain p.S216L and p.S216L+p.H558R constructs respectively. All constructs were sequenced to verify the presence of the mutations and rule out spurious substitutions.

The mammalian cell line TSA201 was transfected by using Lipofectamine 2000 (Invitrogen) in accordance with producer guidelines and incubated with the transfection medium for 8 hours.

The following constructs were co-transfected in equal amounts (0.5 µg/ml): 1) a bicistronic plasmid encoding for green fluorescent protein and the human β1 subunit (pCGI-IRES-hβ1); 2) wild-type (WT) or S216L or S216L-H558R plasmids. I_{Na} amplitude during repolarization (dynamic clamp) was expected to approach the limit of measurement resolution. Thus, in these experiments the amount of transfected plasmid was doubled (1 µg/ml) and incubation was maintained overnight to increase current density. I_{Na} recordings were performed 48 hours after transfection in all cases.

Functional characterization

Whole-cell patch-clamp experiments were carried out on green fluorescent cells exhibiting peak I_{Na} larger than 1.5 nA, in order to minimize potential contamination by endogenous TTX-sensitive currents[24]. Pipettes were filled with a solution containing (in mmol/L): 10 NaF, 110 CsF, 20 CsCl, 2 EGTA and 10 HEPES (pH 7.35 with CsOH); osmolarity was adjusted with sucrose. Pipette resistance ranged from 0.8 to 1.4 MΩ in Tyrode solution. Bath solution contained (in mmol/L): 145 NaCl, 4 KCl, 1.8 $CaCl_2$, 1 $MgCl_2$, 10 HEPES and 10 glucose (pH 7.35 with NaOH). Superfusion was applied through an electrically switched manifold, allowing fast solution changes; temperature was measured at the manifold tip and maintained constant by a thermostatic circuit.

Cell membrane capacitance and series resistance were compensated by 85% to 95%; the estimated voltage error was <3 mV

in all cases. Current signals were acquired by a MultiClamp 700A amplifier (Axon Instruments) at 50 kHz, filtered at 4 kHz (Axon Digidata 1200) and analyzed with a dedicated software (pCLAMP 8.0).

Experiments were performed by standard voltage-clamp (voltage steps) and dynamic voltage-clamp (action-potential waveforms). In standard voltage-clamp experiments voltage steps were applied at intervals of 5 s (protocols were shown in figures), to improve voltage control and resolution of current time-course, these experiments were performed at 26°C. In dynamic voltage-clamp experiments membrane potential was driven at a steady cycle length of 1 s by human endocardial or epicardial action-potential waveforms (EndoAP and EpiAP respectively), generated *in-silico* at the same cycle length by a numerical model[25]. In order to approximate physiological channel gating rates, dynamic clamp experiments were performed at 37°C. For normalization purposes, in each cell, dynamic voltage-clamp was preceded by evaluation of maximal I_{Na} density (I_{max}) by a standard voltage protocol. I_{Na} during dynamic voltage-clamp and the sustained component of I_{Na} (I_{Na}) in standard voltage-clamp protocols were identified by digital subtraction, as current sensitive to tetrodotoxin (TTX, 30 µmol/L).

To assess whether the changes in I_{Na} were due to protein trafficking/folding abnormalities, I_{Na} recordings were performed after incubation of transfected cells with mexiletine (400 µmol/L), added to culture medium immediately after transfection and washed out 30

minutes before recordings. Mexiletine is a Na^+ channel blocker previously shown to rescue the phenotype of trafficking-deficient Na^+ channels[26].

Data analysis

Current density (pA/pF) was calculated by dividing current amplitude by membrane capacitance. Mean current during a given time-interval was calculated from current (I) recordings as

$$\frac{\int I \bullet dt}{\Delta t}$$

where Δt is the integration interval.

Standard voltage-clamp analysis addressed the transient (I_{NaT}) and late (I_{NaL}) components of I_{Na} separately. I_{NaT} analysis included: 1) peak I_{Na} (I_{NaT}) current/voltage (I/V) relationship (holding potential -120 mV); maximal conductance (G_{max}) was estimated from its linear portion ; 2) voltage dependency of activation and inactivation (availability); mid-potentials ($V_{1/2}$) and slope factor (s in mV) were estimated by Boltzmann fitting of normalized (I/Imax) curves; 3) kinetics of inactivation and recovery from inactivation, measured by bi-exponential fitting of current decay and restitution curves of peak I_{Na} respectively. In both cases kinetics were quantified by time constants (τ_f and τ_s) and their respective weights (A_f and A_s). I_{NaL} was measured as the mean TTX-sensitive current between 190 and 200 ms of a depolarization pulse to –10 mV (holding potential –120 mV).

In dynamic voltage-clamp experiments TTX-sensitive current was expressed in terms of absolute density (I_{Na}) and after normalization to I_{max} (I_{Na} = I_{Na} /I_{max}). Normalization aimed to evaluate the functional impact of changes in gating kinetics after removing the effect of changes in absolute current density. I_{Na} and I_{Na} were measured during 4 AP phases: the AP upstroke ($I_{Na}P_0$), the AP notch ($I_{Na}P_1$), phase 2 (between AP dome and APD_{50}, $I_{Na}P_2$), during phase 3 (between APD_{50} and APD_{90}, $I_{Na}P_3$) (see figures 2.4 and 2.5). Whereas $I_{Na}P_0$ was measured as its peak value, in the other phases I_{Na} was quantified by its mean value; in addition, time to peak (TTP) was measured for $I_{Na}P_0$.

Statistical analysis

Differences between means were compared by the unpaired Student *t* test or ANOVA as appropriate. In text and figures data are presented as mean±SEM; statistical significance was defined as $p < 0.05$ (*NS*, not significant).

Supplementary figure 2.I

To assess the ability of the present experimental conditions to disclose persistent sodium current, control recordings were carried with a p.K1505_Q1507del (ΔKPQ) mutated channel. Such a mutation has been widely associated with an enhancement of persistent current[35-37]. ΔKPQ construct has been kindly provided by A.L. George Jr. (Vanderbilt University, Nashville, TN).

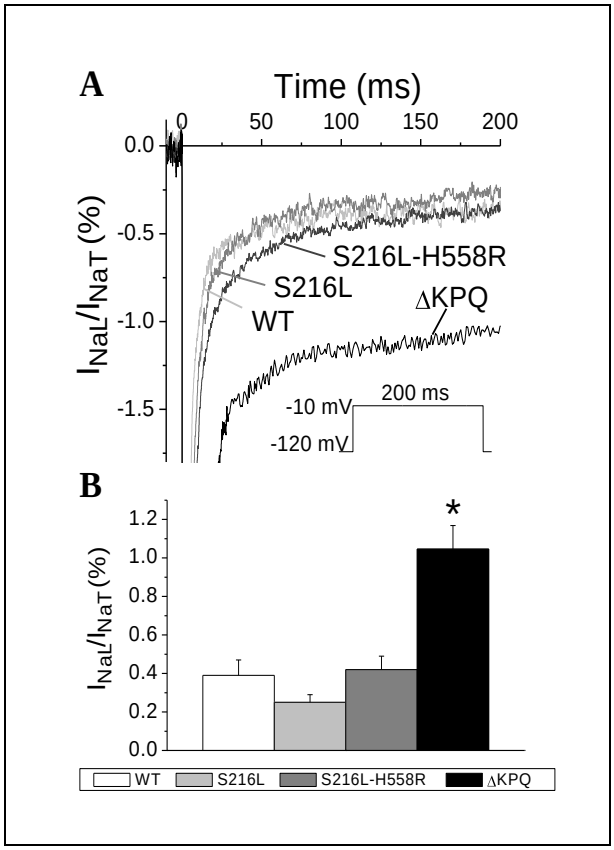

A, Representative current traces of tetrodotoxin-sensitive persistent sodium current flowing through WT, S216L, S216L-H558R and the positive control ΔKPQ channels. Voltage protocol is depicted in the inset. **B**, Barr graph representing mean±SE values of persistent/transient sodium current ratio (**p* < 0.05 *vs* WT; *n*≥7).

Results obtained demonstrated the ability of preset experimental conditions to detect, if present, an enhancement of persistent component of the sodium current.

Reference List of Chapter 2

1. Brugada P, Brugada J. Right bundle branch block, persistent ST segment elevation and sudden cardiac death: a distinct clinical and electrocardiographic syndrome. A multicenter report. *J Am Coll Cardiol*. 1992;20:1391-1396.
2. Brugada J, Brugada R, Brugada P. Right bundle-branch block and ST-segment elevation in leads V-1 through V-3 - A marker for sudden death in patients without demonstrable structural heart disease. *Circulation*. 1998;97:457-460.
3. Antzelevitch C. Brugada syndrome, report of the Second Consensus Conference (vol 2, pg 429, 2005). *Heart Rhythm*. 2005;2:905.
4. Watanabe H, Koopmann TT, Le Scouarnec S, Yang T, Ingram CR, Schott JJ, Demolombe S, Probst V, Anselme F, Escande D, Wiesfeld AC, Pfeufer A, Kaab S, Wichmann HE, Hasdemir C, Aizawa Y, Wilde AA, Roden DM, Bezzina CR. Sodium channel beta1 subunit mutations associated with Brugada syndrome and cardiac conduction disease in humans. *J Clin Invest*. 2008;118:2260-2268.
5. Hu D, Barajas-Martinez H, Burashnikov E, Springer M, Wu Y, Varro A, Pfeiffer R, Koopmann TT, Cordeiro JM, Guerchicoff A, Pollevick GD, Antzelevitch C. A mutation in the beta 3 subunit of the cardiac sodium channel associated with Brugada ECG phenotype. *Circ Cardiovasc Genet*. 2009;2:270-278.
6. Delpon E, Cordeiro JM, Nunez L, Thomsen PE, Guerchicoff A, Pollevick GD, Wu Y, Kanters JK, Larsen CT, Hofman-Bang J, Burashnikov E, Christiansen M, Antzelevitch C. Functional effects

of KCNE3 mutation and its role in the development of Brugada syndrome. *Circ Arrhythm Electrophysiol*. 2008;1:209-218.

7. Antzelevitch C, Pollevick GD, Cordeiro JM, Casis O, Sanguinetti MC, Aizawa Y, Guerchicoff A, Pfeiffer R, Oliva A, Wollnik B, Gelber P, Bonaros EP, Jr., Burashnikov E, Wu Y, Sargent JD, Schickel S, Oberheiden R, Bhatia A, Hsu LF, Haissaguerre M, Schimpf R, Borggrefe M, Wolpert C. Loss-of-function mutations in the cardiac calcium channel underlie a new clinical entity characterized by ST-segment elevation, short QT intervals, and sudden cardiac death. *Circulation*. 2007;115:442-449.
8. London B, Michalec M, Mehdi H, Zhu X, Kerchner L, Sanyal S, Viswanathan PC, Pfahnl AE, Shang LL, Madhusudanan M, Baty CJ, Lagana S, Aleong R, Gutmann R, Ackerman MJ, McNamara DM, Weiss R, Dudley SC, Jr. Mutation in glycerol-3-phosphate dehydrogenase 1 like gene (GPD1-L) decreases cardiac Na+ current and causes inherited arrhythmias. *Circulation*. 2007;116:2260-2268.
9. Burashnikov E, Pfeiffer R, Barajas-Martinez H, Delpon E, Hu D, Desai M, Borggrefe M, Haissaguerre M, Kanter R, Pollevick GD, Guerchicoff A, Laino R, Marieb M, Nademanee K, Nam GB, Robles R, Schimpf R, Stapleton DH, Viskin S, Winters S, Wolpert C, Zimmern S, Veltmann C, Antzelevitch C. Mutations in the Cardiac L-Type Calcium Channel Associated with Inherited J Wave Syndromes and Sudden Cardiac Death. *Heart Rhythm*. 2010.
10. Yan GX, Antzelevitch C. Cellular basis for the Brugada syndrome and other mechanisms of arrhythmogenesis associated with ST-segment elevation. *Circulation*. 1999;100:1660-1666.
11. Bebarova M, O'Hara T, Geelen JL, Jongbloed RJ, Timmermans C, Arens YH, Rodriguez LM, Rudy Y, Volders PG. Subepicardial

phase 0 block and discontinuous transmural conduction underlie right precordial ST-segment elevation by a SCN5A loss-of-function mutation. *Am J Physiol Heart Circ Physiol*. 2008;295:H48-H58.

12. Meregalli PG, Wilde AA, Tan HL. Pathophysiological mechanisms of Brugada syndrome: depolarization disorder, repolarization disorder, or more? *Cardiovasc Res*. 2005;67:367-378.
13. Hoogendijk MG, Opthof T, Postema PG, Wilde AA, de Bakker JM, Coronel R. The Brugada ECG pattern: a marker of channelopathy, structural heart disease, or neither? Toward a unifying mechanism of the Brugada syndrome. *Circ Arrhythm Electrophysiol*. 2010;3:283-290.
14. Wang DW, Desai RR, Crotti L, Arnestad M, Insolia R, Pedrazzini M, Ferrandi C, Vege A, Rognum T, Schwartz PJ, George AL, Jr. Cardiac sodium channel dysfunction in sudden infant death syndrome. *Circulation*. 2007;115:368-376.
15. Viswanathan PC, Benson DW, Balser JR. A common SCN5A polymorphism modulates the biophysical effects of an SCN5A mutation. *J Clin Invest*. 2003;111:341-346.
16. Ye B, Valdivia CR, Ackerman MJ, Makielski JC. A common human SCN5A polymorphism modifies expression of an arrhythmia causing mutation. *Physiol Genomics*. 2003;12:187-193.
17. Poelzing S, Forleo C, Samodell M, Dudash L, Sorrentino S, Anaclerio M, Troccoli R, Iacoviello M, Romito R, Guida P, Chahine M, Pitzalis M, Deschenes I. SCN5A polymorphism restores trafficking of a Brugada syndrome mutation on a separate gene. *Circulation*. 2006;114:368-376.
18. Chen JZ, Xie XD, Wang XX, Tao M, Shang YP, Guo XG. Single nucleotide polymorphisms of the SCN5A gene in Han Chinese and

their relation with Brugada syndrome. *Chin Med J (Engl)*. 2004;117:652-656.

19. Lizotte E, Junttila MJ, Dube MP, Hong K, Benito B, DE Zutter M, Henkens S, Sarkozy A, Huikuri HV, Towbin J, Vatta M, Brugada P, Brugada J, Brugada R. Genetic modulation of brugada syndrome by a common polymorphism. *J Cardiovasc Electrophysiol*. 2009;20:1137-1141.
20. Gouas L, Nicaud V, Berthet M, Forhan A, Tiret L, Balkau B, Guicheney P. Association of KCNQ1, KCNE1, KCNH2 and SCN5A polymorphisms with QTc interval length in a healthy population. *Eur J Hum Genet*. 2005;13:1213-1222.
21. Chen LY, Ballew JD, Herron KJ, Rodeheffer RJ, Olson TM. A common polymorphism in SCN5A is associated with lone atrial fibrillation. *Clin Pharmacol Ther*. 2007;81:35-41.
22. Zaza A. Control of the cardiac action potential: The role of repolarization dynamics. *J Mol Cell Cardiol*. 2010;48:106-111.
23. Gellens ME, George AL, Jr., Chen LQ, Chahine M, Horn R, Barchi RL, Kallen RG. Primary structure and functional expression of the human cardiac tetrodotoxin-insensitive voltage-dependent sodium channel. *Proc Natl Acad Sci U S A*. 1992;89:554-558.
24. He B, Soderlund DM. Human embryonic kidney (HEK293) cells express endogenous voltage-gated sodium currents and Na v 1.7 sodium channels. *Neurosci Lett*. 2010;469:268-272.
25. Grandi E, Pasqualini FS, Pes C, Corsi C, Zaza A, Severi S. Theoretical investigation of action potential duration dependence on extracellular Ca2+ in human cardiomyocytes. *J Mol Cell Cardiol*. 2009;46:332-342.

26. Cordeiro JM, Barajas-Martinez H, Hong K, Burashnikov E, Pfeiffer R, Orsino AM, Wu YS, Hu D, Brugada J, Brugada P, Antzelevitch C, Dumaine R, Brugada R. Compound heterozygous mutations P336L and I1660V in the human cardiac sodium channel associated with the Brugada syndrome. *Circulation*. 2006;114:2026-2033.
27. Yang P, Kanki H, Drolet B, Yang T, Wei J, Viswanathan PC, Hohnloser SH, Shimizu W, Schwartz PJ, Stanton M, Murray KT, Norris K, George AL, Jr., Roden DM. Allelic variants in long-QT disease genes in patients with drug-associated torsades de pointes. *Circulation*. 2002;105:1943-1948.
28. Raman IM, Bean BP. Inactivation and recovery of sodium currents in cerebellar Purkinje neurons: evidence for two mechanisms. *Biophys J*. 2001;80:729-737.
29. Dumaine R, Towbin JA, Brugada P, Vatta M, Nesterenko DV, Nesterenko VV, Brugada J, Brugada R, Antzelevitch C. Ionic mechanisms responsible for the electrocardiographic phenotype of the Brugada syndrome are temperature dependent. *Circ Res*. 1999;85:803-809.
30. Bezzina C, Veldkamp MW, van den Berg MP, Postma AV, Rook MB, Viersma JW, Van Langen IM, Tan-Sindhunata G, Bink-Boelkens MT, Der Hout AH, Mannens MM, Wilde AA. A single Na(+) channel mutation causing both long-QT and Brugada syndromes. *Circ Res*. 1999;85:1206-1213.
31. Veldkamp MW, Viswanathan PC, Bezzina C, Baartscheer A, Wilde AA, Balser JR. Two distinct congenital arrhythmias evoked by a multidysfunctional Na(+) channel. *Circ Res*. 2000;86:E91-E97.
32. Grant AO, Carboni MP, Neplioueva V, Starmer CF, Memmi M, Napolitano C, Priori S. Long QT syndrome, Brugada syndrome, and

conduction system disease are linked to a single sodium channel mutation. *J Clin Invest*. 2002;110:1201-1209.

33. Meadows LS, Isom LL. Sodium channels as macromolecular complexes: implications for inherited arrhythmia syndromes. *Cardiovasc Res*. 2005;67:448-458.
34. Zimmer T, Surber R. SCN5A channelopathies--an update on mutations and mechanisms. *Prog Biophys Mol Biol*. 2008;98:120-136.
35. Dumaine R, Wang Q, Keating MT, Hartmann HA, Schwartz PJ, Brown AM, Kirsch GE. Multiple mechanisms of Na+ channel--linked long-QT syndrome. *Circ Res*. 1996;78:916-924.
36. Bennett PB, Yazawa K, Makita N, George AL, Jr. Molecular mechanism for an inherited cardiac arrhythmia. *Nature*. 1995;376:683-685.
37. Nagatomo T, Fan Z, Ye B, Tonkovich GS, January CT, Kyle JW, Makielski JC. Temperature dependence of early and late currents in human cardiac wild-type and long Q-T DeltaKPQ Na+ channels. *Am J Physiol*. 1998;275:H2016-H2024.

Chapter 3: Conclusion

Summary

Introduction

Brugada syndrome is an arrhythmogenic pathology, leading to sudden death, mainly associated with a loss-of-function of the cardiac sodium channel. Although some pharmacological treatments have been proposed[1], a non-invasive, effective treatment of the syndrome, as well as a widely accepted risk stratification, is still lacking[2;3]. This occurs partially because of the large variability of mechanisms which potentially underlie the syndrome onset[4]. Thus, although it implies to spend many time and money, the only present way to establish the actual pathological mechanism of a proband is the *in vitro* electrophysiological characterization. Moreover, this kind of analysis is useful to enrich the general insight, in order to provide new ideas and knowledge for the syndrome treatment.

S216L mutation has been previously described *post mortem* in a case of sudden death, without clinical features available, and associated with a sodium channel gain-of-function (i.e. an abnormally large persistent sodium current, I_{NaL}) and consequently to the long-QT syndrome[5]. By contrast, the same mutation, in addition with the H558R polymorphism, has been observed in the case of a boy with clinically overt Brugada syndrome (spontaneously intermittent Type 1 pattern). To the aim of clarify this discrepancy and to elucidate the actual mechanism underling the syndrome in the proband, the present

study investigated the electrophysiological effects of the S216L mutation and their modulation by the presence on the same allele (in *cis*) of the H558R polymorphism.

Original results

Standard voltage-clamp characterization of mammalian cells (TSA201) transfected with the S216L mutant sodium channel (S216L channel) revealed a huge reduction of sodium current (I_{Na}) as compared to wild-type one (WT channel). This reduction seems to be partially rescued by the presence of the polymorphism H558R (S216L-H558R channel). To explain the mechanism underling this conductance reduction, a comparison among gating properties of the three channels have been carried out, finding no differences in neither activation nor inactivation voltage-dependency (except for a slight reduction of the slope of the S216L-H558R channel activation curve). Even the persistent component of I_{Na} was unchanged among the three channel forms. The latter result strongly contrasted previous data[5], nevertheless, positive control investigation confirmed its accuracy. By contrast with I_{Na} reduction, abnormalities in inactivation rate seem to account for a gain-of-function phenotype, as it is slower in S216L channel in comparison with WT one at negative membrane potentials and H558R presence exacerbates this feature.

Taken together, even considering the finding of a slight delay in recovery from inactivation in S216L and S216L-H558R channel, these results seem not to be suitable to account for the observed conductance reduction. Therefore, to explain the I_{Na} reduction, folding/trafficking defects have been hypothesized and demonstrated

by pretreatment with mexiletine, proposed to thermodynamically stabilize the properly folded structure[6], and the consequent complete rescue of I_{Na}.

Although I_{Na} reduction was likely the main cause of proband's phenotype while gating differences (especially between S216L and S216L-H558R channels) were negligible under standard square-wave voltage-clamp conditions, their actual relevance under physiological conditions was extremely uncertain, due to a mix of loss- (I_{Na} density, activation curve slope, recovery from inactivation) and gain-of-function one (inactivation rate). To clarify this issue, a quantitative action-potential clamp analysis has been carried out at 37 °C to fully account for physiological kinetic differences; furthermore, both epi- and endocardial action-potential (AP) waveforms were applied to investigate specific transmural behavior. In addition to many qualitative observations, the major findings of this analysis have been 1) the delay in the time to peak of transient I_{Na}, in S216L and S216L-H558R channels, during AP phase 0; 2) the surprisingly presence of a large "resurgent" current, during AP phase 3, expressed by S216L channel, especially in the epicardium and 3) the unexpected complete rescue of I_{Na} density by the presence of H558R polymorphism in endocardium.

Discussion

The channel misfolding is a known mechanism of current reduction[6] which can explain a Brugada phenotype[7]. The observed partial rescue of channel expression and the slight electrophysiological

positive modulation due to H558R presence agree with many previous works[8-14].

Some findings of action-potential clamp experiments are quite easy to relate with standard voltage-clamp results, such as the delayed time to peak is likely due to slower inactivation rate. By contrast, some others require a high level of speculation, including suitable differences in kinetics, persistent current component and voltage-dependency, such as the opposite behavior of S216L and S216L-H558R channels during AP plateau and late repolarization. Although hard to interpret, these observations highlight the sensitivity of gating abnormalities to membrane potential course and underscore the importance of dynamic analysis in assessing the function of mutant channels.

Conclusions

S216L mutation – Repolarization vs depolarization hypothesis

Repolarization hypothesis (RH) is based on a proposed outward imbalance of transmembrane current during AP early repolarization and plateau in the epicardium[15] whereas depolarization hypothesis (DH) is focused on a conduction delay particularly regarding the right ventricular outflow tract (RVOT) and possibly some mild structural defects[16] (see also Chapter 1). On one hand, dynamic clamp analysis of both S216L and S216L-H558R channel electrophysiological phenotype revealed a delayed time to peak which, in addition with strong reduction of I_{Na} and negligible gating changes, supports the DH. Nevertheless, the absence of signs of conduction delay in the proband ECG argues against this hypothesis, suggesting that the delay in time to peak could be only an effect of inactivation slowing; however, a conduction delay localized in the RVOT can not be discarded. On the other hand, the small currents recorded during epicardial AP early repolarization and plateau and the concomitant presence of a current similar to WT one in endocardium could account for a transmural dispersion, in the proband's heart, which would support RH. Moreover, the concave course of the S216L current, which is very small during plateau and then strongly "resurge" during late repolarization, could lead to the idea of a strong spike-and-dome AP shape which would determine the Type 1 ECG pattern from the RH point of view. Nevertheless, since the proband carries both S216L and H558R, the latter consideration is a mere speculation.

Neither DH nor RH can be demonstrated nor rejected, thus it seems likely that both events take part to the arrhythmogenic mechanism in the proband,which is indeed further complicated by its intermittence. This fact highlighted the trouble in finding an univocal suitable treatment for the syndrome.

H558R polymorphism - Risk stratification

It is hard to believe that a single amminoacidic change can, at list partially, rescue loss-of-function phenotype by a number of different ways, including both *cis* or *trans* chaperon-like effect and electrophysiological modulation. Nevertheless, these properties have been well documented[12-14] and confirmed by the present study. Thus the presence of H558R seems to be considered as a protective factor to hold in regard for risk stratification of Brugada syndrome patients. Notably, its presence has also been reported as a risk factor for other arrhythmogenic disease[9] including long-QT[10] syndrome, characterized by a sodium channel gain-of-function. A speculative mechanism accounting for these features could be a excess in thermodynamic stabilization of the protein; from this point of view, the chaperon-like activity, at list in *cis*, is quite easy to explain. Furthermore this hypothesis can easily allow to the idea that thermodynamic changes could increase stability of the conductive state, thus resulting in a gain-of-function phenotype.

Dynamic-clamp – Patient treatment

Dynamic voltage-clamp analysis has been able to point out some behaviors of the channels under physiological conditions of great interest for patient treatment. When the decrease in I_{Na} density was compensated by normalization, S216L channels revealed the tendency to generate a significant resurgent current. This property suggests that in a patient carrying only S216L mutation, a treatment aimed to restore I_{Na} density by recovering channel trafficking, might be associated with perturbations of terminal repolarization, an abnormality which would lead to an acquired long-QT syndrome. Since the gating properties of S216L-H558R channel largely compensate I_{Na} reduction in endocardium, the same therapeutic approach could determine similar side effects also in the proband.

These considerations demonstrate the importance of dynamic-clamp in assessing the actual electrophysiological phenotype of a patient. Since in the present case large and completely unexpected features have been revealed by this experimental technique, it is likely that similar surprisingly behaviors could be revealed in many other cases previously described only through standard voltage analysis.

Epicardial and endocardial waveforms used in the present study were very similar, nevertheless strong differences were observed in channel behaviors. This finding demonstrates that every perturbation of the AP course, even physiological or pathological or therapeutic, could greatly affect the expression of all ionic currents involved. Thus, even channel-selective drug treatments could indirectly modulate

other currents and produce potentially harmful side effects almost unpredictable by standard voltage analysis.

On the base of the possible role of “hidden” current features in establishing a therapeutic treatment and considering that it is the only experimental tool to predict side effects of a drug therapy caused by AP perturbation, dynamic-clamp (i.e. AP clamp) analysis deserves to acquire, from a translational point of view, a relevant position in the analysis of all arrhythmogenic diseases.

Future perspectives

The full comprehension of Brugada syndrome is far to be reached and it still requires a lot of work, from both a genetic- or population-based and a mechanistic point of view.

As demonstrated, dynamic-clamp would be very useful for mechanism comprehension and disease treatment, nevertheless its use as a standard technique is extremely unlikely. This is mostly because of its high cost in terms of time and because it is strictly mutation-specific. A solution to these problems is partially given by *in silico* modeling; a mathematical model would be extremely useful because, moving from standard voltage observations, it would be able to reproduce the actual current features during AP. Once this model would be perfected, it would be used to investigate the effects of the hundreds arrhythmia-inducing mutations previously described only from a standard point of view; moreover, it would easily predict the effects of AP waveform changes on every current.

In order to create this useful tool to assist clinicians in establishing patient therapy, some work has been already carried out and some preliminary data have been obtained. A mathematical model[17] has been implemented with current density, voltage-dependence and kinetic features of WT and S216L-H558R currents, in order to reproduce empirical results in simulated experiments (Fig. 3.1).

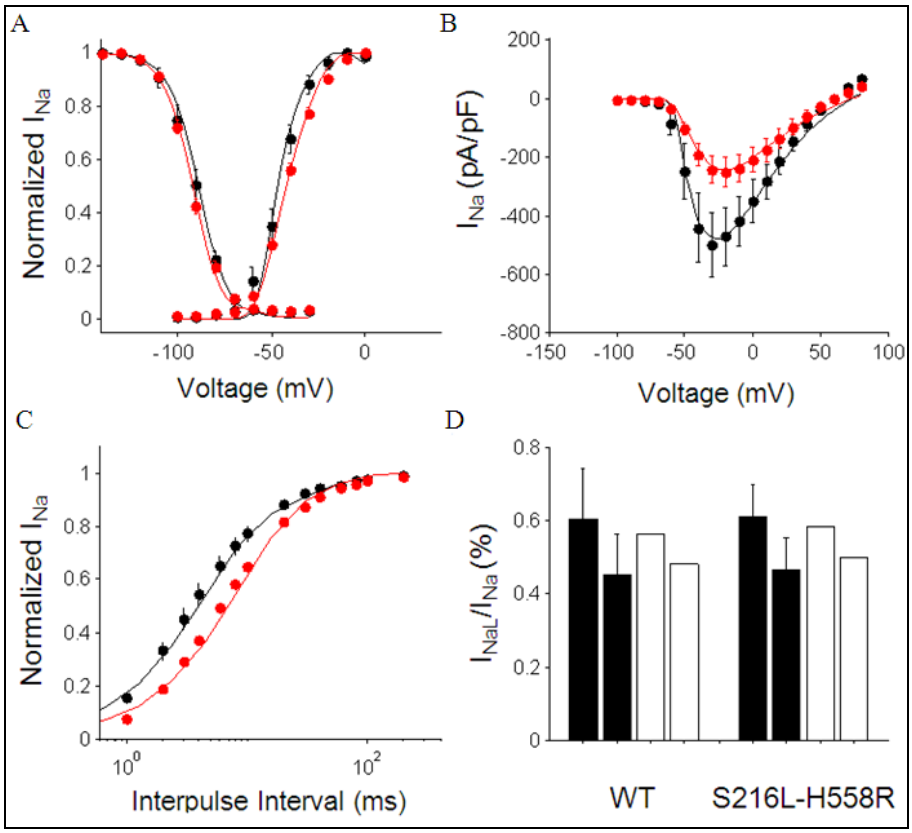

Figure 3.1. Implementation of *in silico* model. **A)** activation and inactivation voltage-dependency; **B)** Current/voltage relation; **C)** Recovery from inactivation; **D)** persistent current component. In **A**, **B** and **C**, black dots and curves represent WT channel experimental points and their fitting by the implemented model, respectively; the same for S216L-H558R channel in red. In **D**, black bars represent experimental data of persistent current component (%) at 100 and 200 ms of depolarization, open bars represent model fitting.

The implemented model obtained has been run to simulate AP clamp experiments (Fig. 3.2 and 3.3). Many experimental behaviors are well reproduced by the model, whereas some others are not. Abbreviations and methods are the same of chapter 2. Accordingly with experimental findings time to peak is delayed in S216L-H558R

current and the inversion of peak amplitude by considering normalized currents suggests that slower inactivation rate partially rescues an otherwise smaller current. Similarly, the *in silico* experiment partially reproduces the differences in "resurgent" current, by predicting a slightly smaller one in S216L-H558R channel. Nevertheless, some features underling current differences during plateau and epi- or endocardial specific behavior are completely absent, such as sustained current during AP plateau.

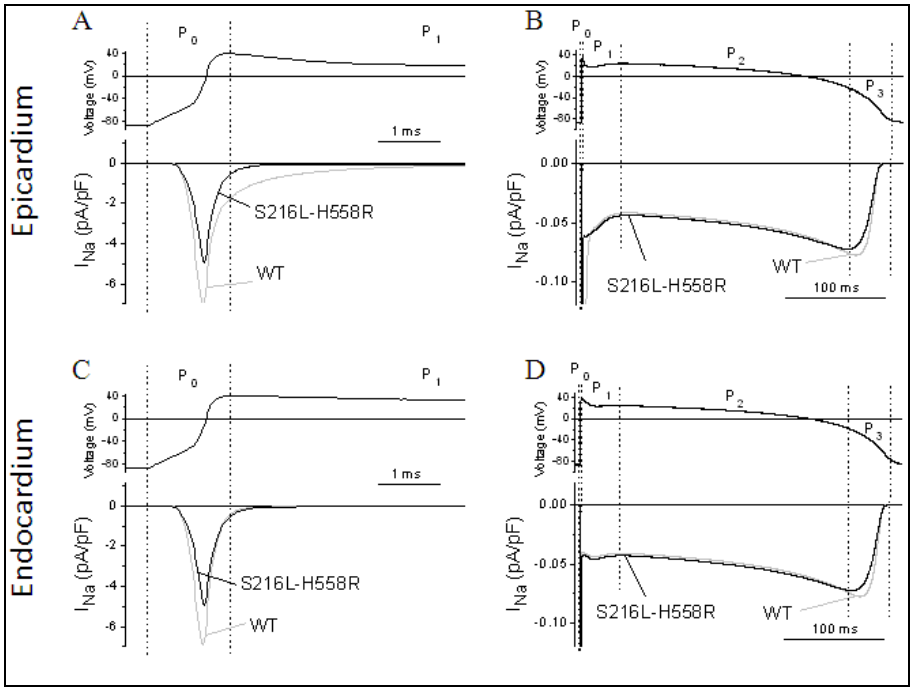

Figure 3.2. Dynamic clamp analysis – Absolute I_{Na} density. AP waveforms (upper panels) and simulated absolute I_{Na} density during the action potential upstroke (left) and repolarization (right) (cell capacitance was arbitrarily assumed as 100 pF). **A** and **B**, epicardial AP. **C** and **D**, endocardial AP. Dashed lines denote the four AP phases (P_0-P_3) during which I_{Na} was evaluated in chapter 2.

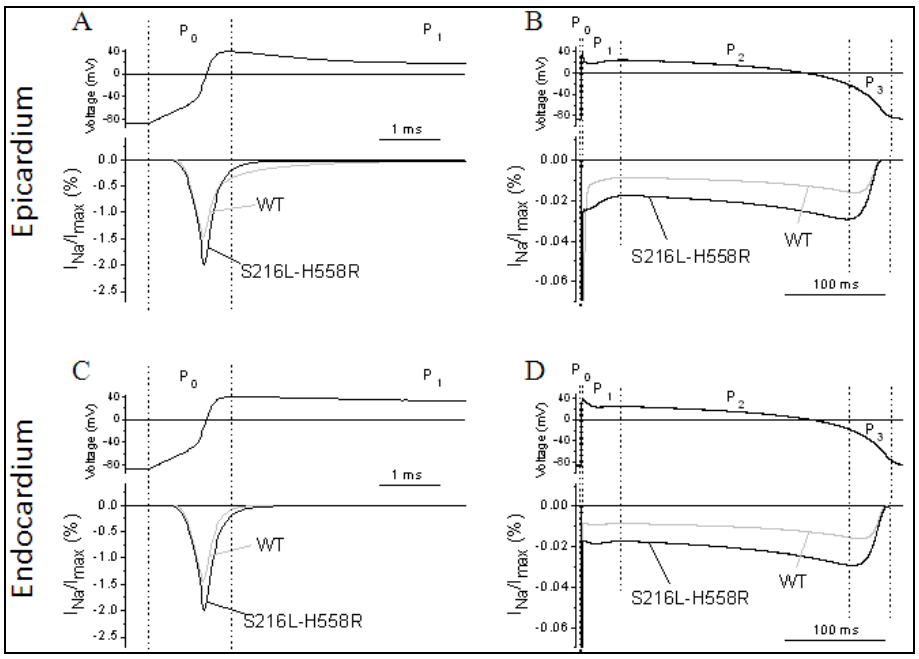

Figure 3.3. Dynamic clamp analysis – Normalized I_{Na} density. Simulated I_{Na} was normalized to maximal I_{Na} (I_{max}) obtained whit a simulated I/V relation. Panels and symbols as in figure 3.2.

The deep analysis of the mechanism driving the model is still in progress. Since the mathematical algorithm used is based on the Hodgkin-Huxley model[18] (see also Chapter 1), some discrepancy with experimental data are likely easily solvable by a little implementation of the model; nevertheless, others, as the absence of transmural specificity, seem to require a completely different approach and the use of a markovian model. Despite this, on the base of the potential benefits, the further work which is required to perfect this tool absolutely deserves to be completed.

Reference List of Chapter 3

1. Postema PG, Wolpert C, Amin AS, Probst V, Borggrefe M, Roden DM, Priori SG, Tan HL, Hiraoka M, Brugada J, Wilde AA. Drugs and Brugada syndrome patients: review of the literature, recommendations, and an up-to-date website (www.brugadadrugs.org). *Heart Rhythm*. 2009;6:1335-1341.
2. Benito B, Brugada J, Brugada R, Brugada P. Brugada syndrome. *Rev Esp Cardiol*. 2009;62:1297-1315.
3. Morita H, Zipes DP, Wu J. Brugada syndrome: insights of ST elevation, arrhythmogenicity, and risk stratification from experimental observations. *Heart Rhythm*. 2009;6:S34-S43.
4. Wilde AA, Postema PG, Di Diego JM, Viskin S, Morita H, Fish JM, Antzelevitch C. The pathophysiological mechanism underlying Brugada syndrome: depolarization versus repolarization. *J Mol Cell Cardiol*. 2010;49:543-553.
5. Wang DW, Desai RR, Crotti L, Arnestad M, Insolia R, Pedrazzini M, Ferrandi C, Vege A, Rognum T, Schwartz PJ, George AL, Jr. Cardiac sodium channel dysfunction in sudden infant death syndrome. *Circulation*. 2007;115:368-376.
6. Cordeiro JM, Barajas-Martinez H, Hong K, Burashnikov E, Pfeiffer R, Orsino AM, Wu YS, Hu D, Brugada J, Brugada P, Antzelevitch C, Dumaine R, Brugada R. Compound heterozygous mutations P336L and I1660V in the human cardiac sodium channel associated with the Brugada syndrome. *Circulation*. 2006;114:2026-2033.
7. Bebarova M, O'Hara T, Geelen JL, Jongbloed RJ, Timmermans C, Arens YH, Rodriguez LM, Rudy Y, Volders PG. Subepicardial phase 0 block and discontinuous transmural conduction underlie

right precordial ST-segment elevation by a SCN5A loss-of-function mutation. *Am J Physiol Heart Circ Physiol*. 2008;295:H48-H58.

8. Chen JZ, Xie XD, Wang XX, Tao M, Shang YP, Guo XG. Single nucleotide polymorphisms of the SCN5A gene in Han Chinese and their relation with Brugada syndrome. *Chin Med J (Engl)*. 2004;117:652-656.
9. Chen LY, Ballew JD, Herron KJ, Rodeheffer RJ, Olson TM. A common polymorphism in SCN5A is associated with lone atrial fibrillation. *Clin Pharmacol Ther*. 2007;81:35-41.
10. Gouas L, Nicaud V, Berthet M, Forhan A, Tiret L, Balkau B, Guicheney P. Association of KCNQ1, KCNE1, KCNH2 and SCN5A polymorphisms with QTc interval length in a healthy population. *Eur J Hum Genet*. 2005;13:1213-1222.
11. Lizotte E, Junttila MJ, Dube MP, Hong K, Benito B, DE Zutter M, Henkens S, Sarkozy A, Huikuri HV, Towbin J, Vatta M, Brugada P, Brugada J, Brugada R. Genetic modulation of brugada syndrome by a common polymorphism. *J Cardiovasc Electrophysiol*. 2009;20:1137-1141.
12. Poelzing S, Forleo C, Samodell M, Dudash L, Sorrentino S, Anaclerio M, Troccoli R, Iacoviello M, Romito R, Guida P, Chahine M, Pitzalis M, Deschenes I. SCN5A polymorphism restores trafficking of a Brugada syndrome mutation on a separate gene. *Circulation*. 2006;114:368-376.
13. Viswanathan PC, Benson DW, Balser JR. A common SCN5A polymorphism modulates the biophysical effects of an SCN5A mutation. *J Clin Invest*. 2003;111:341-346.
14. Ye B, Valdivia CR, Ackerman MJ, Makielski JC. A common human SCN5A polymorphism modifies expression of an arrhythmia causing mutation. *Physiol Genomics*. 2003;12:187-193.

15. Yan GX, Antzelevitch C. Cellular basis for the Brugada syndrome and other mechanisms of arrhythmogenesis associated with ST-segment elevation. *Circulation*. 1999;100:1660-1666.
16. Meregalli PG, Wilde AA, Tan HL. Pathophysiological mechanisms of Brugada syndrome: depolarization disorder, repolarization disorder, or more? *Cardiovasc Res*. 2005;67:367-378.
17. Grandi E, Pasqualini FS, Pes C, Corsi C, Zaza A, Severi S. Theoretical investigation of action potential duration dependence on extracellular Ca2+ in human cardiomyocytes. *J Mol Cell Cardiol*. 2009;46:332-342.
18. HODGKIN AL, HUXLEY AF. A quantitative description of membrane current and its application to conduction and excitation in nerve. *J Physiol*. 1952;117:500-544.

Appendix: List of Academic Contributions

Peer-reviewed Articles

Marangoni S., Di Resta C., Barile L., Rocchetti M., Rizzetto R., Sommariva E., Pappone C., Ferrari M., Benedetti S., Zaza A. A Brugada syndrome mutation (S216L) and its modulation by H558R polymorphism: standard and dynamic characterization. *Cardiovascular Research.* CVR-2010-1222. Submitted.

Altomare C., Barile L., Marangoni S., Rocchetti M., Alemanni M., Mostacciuolo G., Giacomello A., Messina E., Zaza A. Caffeine-induced Ca2+ signalling as an index of cardiac progenitor cells differentiation. *Basic Research in Cardiology.* 2010;105(6):737-49.

Tamás B., Horváth B., Virág L., Szabó G., Szentandrássy N., Harmati G., Magyar J., Marangoni S., Zaza A., Varró A., Nánási P.P. Reverse rate dependency is an intrinsic property of canine cardiac preparations. *Cardiovascular Research.* 2009;84(2):237-44.

Proceedings

Rocchetti M., Marangoni S., Mostacciuolo G., Zaza A. Differential effects of chronic hypoxia on the sodium current in right and left ventricles. *European Journal of Heart Failure Supplements.* 2009; Vol. 8(2).

Rocchetti M., Marangoni S., Mostacciuolo G., Zaza A. Chamber-specific effects of chronic hypoxia on the late Na+ current and repolarization. *European Journal of Heart Failure Supplements.* 2009; Vol. 8(2).

Altomare C., Barile L., Marangoni S., Rocchetti M., Mostacciuolo G., Giacomello A., Messina E., Zaza A. (2008). Cardiac-type Calcium Release Mechanism in Cardiac Precursor Cells. *Abstract 338: Circulation*. 2008; 118: S_287.

Altomare C., Barile L., Marangoni S., M. Rocchetti M., Mostacciuolo G., Giacomello A., Messina E., Zaza A. Differentiation of cardiac-type calcium release mechanism in cardiac precursor cells. *European Heart Journal*. (2008) 29 (Abstract Supplement), 527.

Oral Communication

Marangoni S., Altomare C., Barile L., Rocchetti M., Giacomello A., Messina E., Zaza A. Differentiation of cardiac type calcium release mechanism in cardiac progenitor cells. 32nd EWGCCE Annual Meeting, Madrid, Spain, September 18-20, 2008.

Posters

Marangoni S., Rizzetto R., Di Resta C., Rocchetti M., Benedetti S., Ferrari M., Zaza A. Can the S216L mutation of the cardiac sodium channel lead to a Brugada phenotype? III Biosimposio del Dipartimento di Biotecnologie e Bioscienze dell'Università degli Studi di Milano-Bicocca. Milano, Italia, 11 Dicembre, 2009.

Di Resta C., Marangoni S., Sommariva E., Redaelli C., Sacco F.M., Sala S., Ferrari M., Zaza A., Benedetti S., Pappone C. Can the S216L mutation of the cardiac sodium channel lead to a Brugada phenotype? XII Congresso della Società Italiana di Genetica Umana (SIGU). Torino, Italia, 8-10 Novembre, 2009.

Altomare C., Barile L., Marangoni S., Rocchetti M., Sampaolesi M., Giacomello A., Zaza A. Caffeine-induced Ca^{2+} signaling as an index of cardiac differentiation. XIX World Congress of the International Society for Heart Research (ISHR). Bologna, Italy, June 22-25, 2007.